T.C

UNIVERSITY OF YEDİTEPE

INSTITUTE OF HEALTH SCIENCES

DEPARTMENT OF DENTOMAXILLOFACIAL RADIOLOGY

A CONE BEAM COMPUTED TOMOGRAPHY IMAGE ANALYSIS METHODE TO EVALUATE THE INFERIOR ALVEOLAR NERVE CANAL WITH ITS ASSOCIATED ANATOMICAL STRUCTURES AND VARIATIONS:

A RETROSPECTIVE STUDY

DOCTOR OF PHILOSOPHY THESIS

Dt. MERVET EL-ZUKI

ISTANBUL 2018

THESIS APPROVAL FORM

Institute : Yeditepe University- Institute of Health Sciences.

Programme : PhD programme in Dentomaxillofacial Radiology Department.

Title of the Thesis: A Cone Beam Computed Tomography Image Analysis Method To Evaluate The Inferior Alveolar Nerve Canal With Its Associated Anatomical Structures And Variations: A Retrospective Study.

Owner of the Thesis : Mervet EL- ZUKI

Examination Date : 19.01.2018

This study has been approved as a Doctorate Thesis in regard to content and quality by the Jury.

Chair of the Jury: Prof. Dr. Dilhan İLGÜY
(Yeditepe University)

Supervisor: Assoc. Prof. Dr. Erdoğan FIŞEKÇIOĞLU
(Yeditepe University)

Examiner: Prof. Dr. Jale TANALP
(Yeditepe University)

Examiner: Prof. Dr. İlknur ÖZCAN
(Istanbul University)

Examiner: Prof. Dr. Tamer Lütfi ERDEM
(Okan University)

APPROVAL

This thesis has been deemed by the jury in accordance with the relevant articles of Yeditepe University Graduate Education and Examinations Regulation and has been approved by Administrative Board of Institute with decision dated 25..01..2018.. and numbered 2018/02-15

Prof. Dr. Bayram YILMAZ
Director of Institute of Health Sciences.

ii

DECLARATION

I hereby declare that this thesis is my own work and that, to the best of my knowledge and belief, it contains no material previously published or written by another person nor material which has been accepted for the award of any other degree except where due acknowledgment has been made in the text.

19.01.2018

…………….

Mervert EL-ZUKI

DEDICATION

"In Contribution to My Present, Past, and Future:

I Dedicate This Work to My Dearly loved Parents, Grandparents, and Children".

AKNOWLEDGMENTS

TABLE OF CONTENTS

LIST OF TABLES

LIST OF FIGURES

LIST OF SYMBOLS AND ABBREVIATIONS

CBCT   Cone Beam Computed Tomography

FOV   Field-of –View

MPR   Multi-planar Reformation

FPDs   Flat Panel Detectors

CNV   Trigeminal Nerve

CNV1   Ophthalmic Nerve Branch

CNV2   Maxillary Nerve Branch

CNV3   Mandibular Nerve Branch

IAN   Inferior Alveolar Nerve

IANC   Inferior Alveolar Nerve Canal

MaFN   Mandibular Foramen Number

MaCN   Mandibular Canal Number

BMC   Bifid Mandibular Canal

RMC   Retromolar Canal

TMC   Trifid Mandibular Canal

MeFN   Mental Foramen Number

MeCLe   Mental Canal Length

ALL   Anterior Loop length

MeCl   Mental Canal location

MeCO   Mental Canal Orientation

MeCA   Mental Canal Angulation

MIC   Mandibular Incisive Canal

LLVCsN   Lateral Lingual Vascular Canals Number

LLVCsLe   Lateral Lingual Vascular Canals Length

LLVCsO   Lateral Lingual Vascular Canals Orientation

LLVCsr   Lateral Lingual Vascular Canals range between teeth

LLVCsH   Lateral Lingual Vascular Canals Height

LLVCA   Lateral Lingual Vascular Canals Aspect

NCsN   Nutrient Canals Number

NCsR   Nutrient Canals Range

LCN   Lingual Canal Number

LCA   Lingual Canal Aspect

LCl   Lingual Canal location

LCGT   Lingual Canal in relation to Genial Tubercles

LCfig   Lingual Canal resembling allocated figures

LFN   Lingual Foramen Number

LFA   Lingual Foramen Aspect

LFl   Lingual Foramen location

LC Class   Lingual Canal Class

ABSTRACT

Objective: The aim of this study was to produce a systematic method of CBCT image analysis to investigate the Inferior Alveolar Nerve Canal (IANC) trajectory along with its associations and variations, and to provide evidence that the visibility of the IANC and its prolongation on CBCT imaging can be detected as a one continuous component, starting from the Mandibular Foramen (MaF) through the Mental Foramen (MeF), and ending as the Mandibular Incisive Canal (MIC) at the midline region.

Materials and Methods: This study was a retrospective, cross-sectional review of CBCT images from 200 patients. Sagittal, coronal, axial, and multi-planar reformatted images were evaluated by two Dentomaxillofacial radiologists in a specific, identical method to investigate the following image parameters: Mandibular Foramen (MaF), types of Mandibular Canals (MaC), Mental Foramen (MeF), types of Mental Canals including: length, symmetry and angulations, visibility of Mandibular Incisive Canal (MIC), types of Lateral Lingual Vascular Canals (LLVCs); including length, height, orientation, location, and opening aspect, Nutrient Canals (NCs) number and range between teeth, as well as types of Lingual Foramen (LF) and their associated canals (LC); according to number, orientation, location in relation to the genial tubercles and opening aspect.

Results: The visibility of the MIC was detected in the 200 (100%) images. In regards to gender, and amongst all the measured image parameters, the right and left MeC length, the LLVCs range on the right side, and the LC location in relation to genial tubercles are statistically significant; 0.000, 0.006, 0.002 and 0.020 respectively. There was a strong positive correlation between the LLVCs orientation and the LLVCs height at the measurement site. There was a moderate positive correlation between the MeC orientations on the right side with that on the left side, and between the MeC lengths on right and left sides.There was a weak positive correlation between the LLVCs number and length on the right side and the LLVCs number and length on the left, between the right LLVCs orientation and the left LLVCs orientation when there was one canal, between the number of the MaC on the right and left sides, and between the number of the MaC on the left side and the number of MeF on the same side.

Conclusion: To avoid the potential of any unexpected risks, prior to surgical insertion of dental implants in the vicinity of the IANC, and in consideration to the variable values, and anatomical variation and associations at that vicinity; the inclusion of a "Systematic Method of CBCT Image Analysis" evaluation in the "Radiology Report" is essential.

Key words: CBCT, Image Analysis Method, Inferior Alveolar Nerve Canal, Mandibular Canal, Retromolar Canal, Accessory Mental Foramina, Mental Canal, Anterior loop, Mandibular Incisive Canal, Lateral Lingual Vascular Canals, Nutrient Canals, Lingual Canals, Lingual Foramen.

İNFERIOR ALVEOLAR KANALIN ANATOMIK YAPISININ VE VARIYASYONLARININ KONIK IŞINLI BILGISAYARLI TOMOGRAFI ILE METODOLOJIK ANALIZI: RETROSPEKTIF ÇALIŞMA

ÖZET

Amaç: Bu çalışmanın amacı, İnferior Alveolar Sinir Kanalının (İASK) bağlantı ve variyasyonlarının Konik Işıklı Bilgisayarlı Tomografi (KIBT) ile sistematik bir metod oluşturmak ve Mandibular Foramenden (MaF) başlayıp Mental Foramen (MeF) ile devamedip Mandibular Insiziv Kanalının (MİK) orta hat bölgesine kadar olan İnferior Alveolar Sinir Kanalının ve uzantısının KIBT ile gözlene bilen ve devam eden bir kanal olduğunu kanıtlamaktır.

Materyal Method: Bu çalışma, 200 hastanın KIBT görüntülerini retrospektif ve kesitsel olarak çeşitli parmetreler kullanılarak iki Ağız-Diş-Çene Radyolojisi uzmanı tarafından değerlendirildi. Parametreler: Mandibular Foramen (MaF), Mandibular Kanalların Tipleri (MaK), Mental Foramen (MeF) , Mental Kanal türleri dahilinde: uzunluk, simetri ve açısallıkları, Mandibular İnsiziv Kanal (MİK) görünürlüğü, Lateral Lingual Vascular Kanalların türleri (LLVK); Uzunluk, yükseklik, yönlendirme, konum ve açılma açısı, Besleyen Kanal (BK) sayıları ve diş aralığı ve aynı zamanda Lingual Foramen (LF) ve Lingual Foramenin bağlantılı kanal (LFBK) türleridir. Bunlar sayıya, yönlendirmeye, genial tüberküllere ve açılma açısı ve konuma göre değişir.

Bulgular: MİK'in görünürlüğü 200 (%100) görüntüde tespit edildi. Cinsiyet ve ölçülen tüm görüntü parametreleri arasında, sağ ve sol MaK uzunluğu, sağ LLVK aralığı ve genial tüberküloz ile ilişkili LC konumu istatistiksel olarak anlamlıdır; sırasıyla 0.000, 0.006, 0.002 ve 0.020'dir. LLVK'lerin yönleri ile ölçüm alanındaki LLVK'lerin yüksekliği arasında güçlü bir pozitif korelasyon vardır. Sağ taraftaki MeK yönleri ile sol taraftaki MeK yönleri arasında, sağ ve sol MeK uzunlukları arasında ise orta derecede pozitif bir korelasyon vardır. LLVK sayısı ile sağ taraf arasındaki uzunluk ile solda taraftaki LLVK sayısı ve uzunluğu arasında, bir kanal olduğu zaman sağ LLVK'lerin yönü ile sol LLVK'lerin yönleri arasında, MaK sayısı arasında- sağ ve sol taraftaki MaK sayıları ile tek başına sol taraftaki MaK sayıları aynı taraftaki MeF sayıları arasında zayıf bir pozitif korelasyon vardır.

Sonuç: Diş implantlarının AASK çevresinde cerrahi olarak yerleştirilmesinden önce, beklenmedik risklerin ortaya çıkma potansiyelinden kaçınmak için o çevredeki değişken değerler ve anatomik varyasyonları da dikkate alarak "Radyoloji Raporu" değerlendirmesine 'KIBT Görüntü Analizi Sistematik Yöntemi'nin de dahil edilmesi gerekmektedir.

Anahtar Kelimeler: KIBT, görüntü analiz yöntemi, Alt Alveolar Sinir Kanalı, Mandibular Kanal, Retromolar Kanal, Aksesuar Mental Foramen, Ön Loop, Mandibular İnsiziv Kanal, Yan Lingual Damar Kanalı, Nütrisyonel Kanallar, Lingual Kanallar, Lingual Foramen.

1. INTRODUCTION AND AIM

1.1. Introduction:

In the mandible, the Inferior Alveolar Nerve (IAN) is a very important anatomical structure to consider while planning endosseous dental implant procedures, as there is a surgical risk to damage it (1, 2). Although many studies explain this nerve at the posterior mandible, only few histological and radiographic studies are available regarding this anatomical structure at the anterior mandible (3-9). These recent studies illustrate the presence of the Mandibular Incisive Canal (MIC) and the Lingual Foramen (LF) with the accessory foramina (10-14). The MIC is described as the terminal prolongation of the Mandibular Canal (MaC) with its neurovascular content after giving a branch at the level of the Mental Foramen (MeF), and the anterior area between the two mental foramina is named as the interforaminal region (1, 2, 10). However, the exact anatomy of the interforaminal region, with its potential clinical implications, is still controversial, and some researchers even disregard its existence (2). Diagnostic imaging is an essential part in the detection of these vital anatomic structures prior to endosseous implant placement as it reduces the risk of complications (15). With the advancement in imaging modalities, Cone Beam Computed Tomography (CBCT) provides a great value in the visualization of osseeous architecture, and a reliable 3-Diamentions (3-D) localization of the Inferior Alveolar Nerve Canal (IANC), which houses the IAN in 3-D (15, 16). Correlated literature reveals unaccompanied studies, using 3-D imaging modalities either concerning the assessment of the IANC and its variations pending to the level of the MeF, or concerning the interforaminal region with related anatomical associations and variations as separate components (5, 11, 14, 15, 17-25).

1.2. Aim and Objectives:

The aim of this study is to provide evidence that the visibility of the IANC and its prolongation on CBCT imaging system can be detected as a one continuous component, starting from the Mandibular Foramen (MaF) through the MeF into the interforaminal region, and finally

ending as the MIC at the midline region. Accordingly, the **Hypothesis** is: On CBCT images, the visibility of the IAC and its prolongation can be detected as a continuous component. The **Null Hypothesis** is: On CBCT images, the visibility of the IANC and its prolongation cannot be detected as a continuous component. This can be achieved through the following objectives:

(1) To identify and develop a consistent method of CBCT image analysis to be utilized for visibility detection and evaluation of the IANC course with its associated anatomical structures, and variations on both right and left sides for the same patient.

(2) To apply this image analysis method, retrospectively, to a set of pre-existing CBCT images.

2. LITERATURE REVIEW

2.1. Background of CBCT:

Multi-planar imaging presents a distinctive diagnostic approach as it provides the facility to generate different sections of images at different flat and curved planes. Since a volume of data can be acquired, stored and reformatted in any form of images that the diagnostician requires, a perspective image assessment can be obtained, eliminating the superimposition of the investigated area with adjacent structures. This concept of volumetric type of data is inherent in conventional Computed Tomography (CT), CBCT, and Magnetic Resonance Imaging (MRI) (26).

CBCT is the most significant advanced multi-planar imaging modality, widely used in the maxillofacial region over the last decade. In the early 1980s, CBCT was primarily developed for angiography. Then, in the late 1990s, four technologic advances congregated, facilitating the production of reasonably priced CBCT units that are, unlike conventional CT unites, small enough to be employed in the dental office for maxillofacial imaging; namely: X-ray detectors capable of rapid multiple image acquisition, high-output X-ray generators, suitable image acquisition and integration algorithms, and affordable computers powerful enough to process the vast quantity of acquired image data (27-29).

The radiation source in CBCT unites emit an X-ray beam shaped like a cone, hence the name Cone Beam CT, which covers the entire field of interest, rather than a fan as in conventional CT unites; only one pass or less of the X-ray source is necessary for acquiring images, and accordingly less ionizing radiation is utilized in regards to conventional CT unites (27, 30, 31).

2.2. Image Acquisition:

CBCT machines utilize a source of ionizing radiation and two-Dimentional (2-D) panel detector attached to a revolving gantry to give several sequential transmission images known as "Basis images". These are similar to lateral cephalometric radiographic images that are slightly

offset from each other, and are incorporated directly to generate a 3-D volumetric data set that can be used to provide primary reconstruction images in three orthogonal planes: axial, sagittal, and coronal. Image acquisition is constituted of four main components (27, 28):

1. X-ray Generation.
2. Image Detection System.
3. Image Reconstruction.
4. Image Display.

2.2.1. X-ray Generation:
2.2.1.1. CBCT Imaging Hardware:
2.2.1.1.1. X-ray Tube:

As a basic principle, X-rays are generated in a vacuumed tube called: the X-ray tube. This tube contains an electrical circuit with two oppositly charged electrodes named as cathode and anode. When an electric current is applied, the cathode, which is composed of a tungsten filament, is heated, releasing electrons through an effect known as "Thermoionic emission". Since the voltage or the potential difference between the cathod and anode is high, these released electrons are accelerated towards the anode, colliding with it at high velocities at a point sized target made of tungsten known as "the focal spot". A typical focal spot size in a CBCT X-ray tube is 0.5mm wide, and the size of this focal spot determines the image sharpness. Sharpness or spatial resolution refers to the ability to differentiate small structures in an image. The energy generated through this collision is mostly lost in the form of heat; nevertheless, a small part of this energy is converted into X-rays through two main effects known as "Bremsstrahlung or Braking Radiation", and "Characteristic Radiation". At the anode, X-rays are emitted in all directions, but only a divergent beam is allowed to emerge through the exit window of the X-ray tube. The anode surface is slightly tilted at a certain angle in order to maximize the outgoing of this X-ray beam (29) (Figure 2.1).
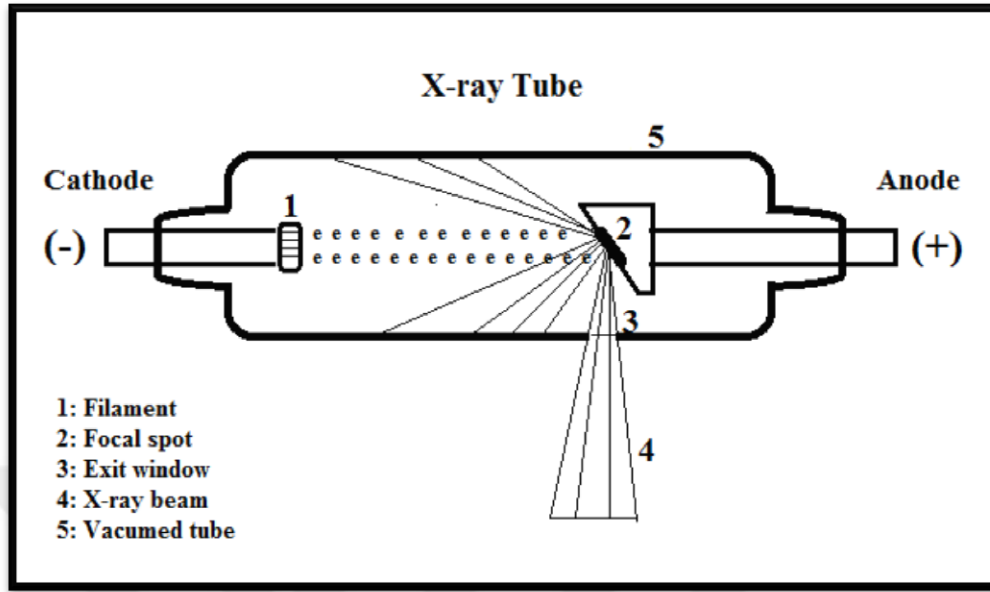
Figure 2.1. Schematic illustration of an X-ray tube in CBCT (Illustration by: E-Z M).

The X-ray beam is attenuated by both internal (inherent) and external (added) filtration. In the internal filtration, X-rays photons interact with the tube housing before exiting the X-ray tube. In this interaction, mainly low-energy X-ray photons are absorbed. Low-energy photons have a high probability of being absorbed within the patient's tissues, as they contribute to the patient's radiation dose, but not to the radiographic image. Additional filtration, on the other hand, is obtained by adding metallic sheets, usually made of aluminum or copper with an aluminum equivalent thickness ranging between 2.5 and 10 mm, placed at the exit window to absorb the majority of low-energy photons while exiting the X-ray tube. Unlike the tube voltage (kV), tube current (mA) and exposure time are in direct proportion to the amount of X-ray photons exiting the tube, and accordingly to the radiation dose (27, 29).

In order to limit the patient's exposed area to that required for data acquisition, the beam size is restricted or collimated by blocking the X-rays that are not passing through the scanned volume. In other terms, collimation reduces radiation dose exposure. Collimation is conducted by using a lead-alloy collimator that has a rectangular opening for X-rays to pass through. The

majority of CBCT systems have multible pre-defined Field-of-View (FOV) sizes; therefore a collimator will have many pre-defined openings according to the FOV size (29).

2.2.1.1.2. Gantry:

Most CBCT systems use a setup of X-ray tube and detector connected by a fixed gantry or a C-shaped arm, which usually rotates in the horizontal plane, allowing for seated and\or standing patient positioning, or rotates in the vertical plane, allowing for supine patient position (27, 29).

2.2.2. Image Detection System:
2.2.2.1. Detector:

X-ray detectors convert the received X-ray photons to an electrical signal and are consequently a critical component of the imaging procedure. The efficiency and speed at which the conversion is carried out are crucial characteristics of X-ray detectors. In CBCT imaging, different types of detectors are used. Recently, differet types of Flat Panel Detectors (FPDs) are used, as these detectors are distortion free, have higher dose efficiency, a wider dynamic range, and can be produced with either a smaller or larger FOV. Most CBCT systems use indirect FPDs where a layer of scintillator material, is used to convert X-ray photons to light photons, which in turn are converted into electrical signals. Modern scintillators have high image quality and dose efficiency, as their columnar structure reduces the light spread between the scintillators. Different componenets and technologies can be used for signal read-out in FPDs. These technologies differ in regards to detector size, voxel size, noise level, sensitivity and read-out speed, and they have varying cost efficiency depending on the total size of the detector (29).

2.2.3. Image Reconstruction:
2.2.3.1.Basic Principles:

During CBCT imaging, as previously mentioned, the X-ray tube and detector rotate a single 360^0 rotation along a circular course at a fixed distance. Even though faster and slower scan protocols exist, normal rotation times range between 10 and 40 seconds. During this rotation, a

cone-shaped X-ray beam results in several hundred 2-D X-ray projections, each with more than million pixels. These projections of raw data are received on the detector and then can be reconstructed into a 3-D representation of the scanned object (27-29).

2.2.3.2. Pre-processing of Raw Data:

Prior to image reconstruction, the raw data may follow a number of pre-processing steps. These steps are usually implemented in order to remove irregularities associated with variations in detector dark current gain and pixel defects. Common pre-processing tools are offset and gain corrections that compensate for sensitivity differences among detectors and among pixels of a detector. Moreover, an after glow correction can be performed to remove the latent image of the preceding projection. This is particularly important when a long sequence of projections per second is obtained (29).

2.2.3.3. Reconstruction:

It is essential to process the projection of raw data, which are named, as previously mentioned, basis images or basis projection frames to produce the volumetric data set. This process is called "Primary Reconstruction". Although a single cone-beam rotation may last for less than 30 seconds, it generates around 100-600 basis projection frames, each with more than million pixels with 12 to 16 bits of data assigned to each pixel. The reconstruction of these data is a complex procedure. In order to facilitate data handling, data are frequently obtained by one personal computer called "Acquisition Computer", and transferred by an Ethernet connection to another personal processing computer called "Workstation Computer". Unlike conventional CT, CBCT data reconstruction is executed by personal computer-based workstation, rather than workstation platforms (28, 29).

2.2.3.4. Reconstruction Algorithms:

Image reconstruction is a procedure in which an image is reconstructed from multiple 2-D projections. The scanned object is reconstructed as a 3-D matrix of voxels with each voxel being

assigned a grey value depending on the attenuation of the material constituting the scanned object. Projection data are a summation of linear attenuation coefficients along the X-ray path. This is, mainly, the inverse or back projection process of the weighted and filtered projections, in which the value for each pixel in the projection image is assigned to each voxel along the path of the X-ray.

As this is achieved for every projection, an image of the scanned object is reconstructed. The filter, on the other hand, consists of two parts: 1) Ramp filter to correct the intrinsic blur of the projection, and 2) Smoothing filter to reduce high-frequency noise that is amplified by the ramp filter. Smoothing filter can significantly affect image quality by reducing noise on the expense of spatial resolution. The cut-off frequency of such filters is freely adjustable; the higher the cut-off frequency, the sharper, yet noisier the reconstructed imsge. For a particular imaging task, some kinds of software allow the adjustment of reconstruction parameters as desired. Once an initial reconstruction is acquired, the imsge is adjusted according to what the projection data arising from the current reconstruction estimate would be. These are compared with the actual projection data, after which a new corrected reconstruction is acquired. This process continues until a specified level of acceptability is accomplished (29).

2.2.4. Image Display:
2.2.4.1. Display:

For most CBCT procedures, the volumetric data set is a collection of all available voxels, and this set is presented to the radiologist on a monitor as standard reconstructed images in orthogonal planes, generally, at a thickness defaulted to the subject resolution. CBCT reconstruction is a process that creates a 3-D matrix that can be viewed as a series of 2-D cross sectional views in: axial, sagittal and coronal planes. Axial planes are sequences of 2-D slices from superior to inferior, sagittal planes are sequences of 2-D slices from right to left, and coronal planes are sequences of 2-D slices from anterior to posterior aspects (28) (Figure 2. 2).
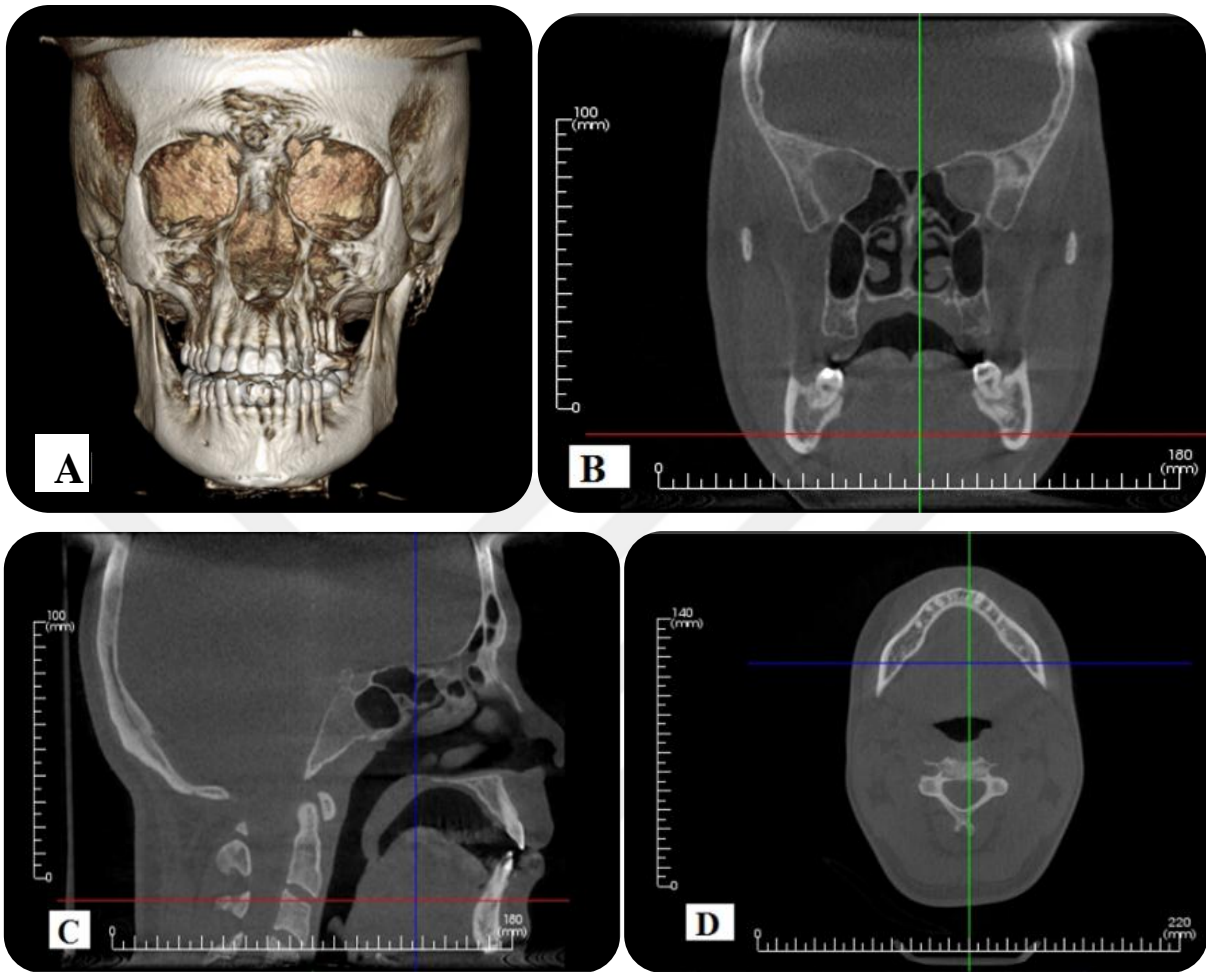
Figure 2.2. Standard Display Modes of CBCT. **A**: Volumetric 3-D representation of hard tissue. **B**: Representative coronal image. **C**: Representative sagittal image. D: Representative axial image (Images obtained with i-CAT® Model 17-19; CBCT Imaging Unit: InVivoDental5 Version 5.2 Anatomage, software): Dentomaxillofacial Radiology Department; Faculty of Dentistry- University of Yeditepe.

The optimal visualization of these images depends on the adjustment of window level, window width to protract bone, and on specific filter applications (28).Therefore, in digital imaging, a display monitor is required. For CBCT images, the main criteria are related to size and resolution of the monitor, as images should be displayed at their occupant resolution, either 1:1 ratio between the display pixel and the image pixel, or multiple display pixels for every pixel image for maximum image sharpness. In addition, contrast ratio and luminance should also be at an adequate level. For example, imaging a 60x60 mm CBCT image with a voxel size of $0.1mm^3$;

every slice in this image will be 600x600 pixels. When visualizing this image, using a multi-planar reformatting, a monitor will require a minimum resolution of 1200x1200 pixels to illustrate each slice at a 1:1 ratio. Consequently, optimal visualization of these images depends on large-size, high resolution monitors, zooming tools, specific filter applications, and adjustment of window level and window width to protract bone whenever applicable (28, 29).

2.2.4.1. Multi-planar Reformatting:

In a Multi-planar Reformation (MPR) window, the three orthogonal planar views are related through intersection lines, allowing for straight forward orientation and rotation. After reconstruction, besides MPR, oblique and curved reformatting can be performed. Oblique and curved reformatting allows the user to cut through the FOV at any angle. Manipulation of the oblique reformation can be performed by rotating the intersection lines, as well as drawing new lines. Moreover, CBCT images can be manipulated in different ways to optimize the visualization of anatomical structures, pathological lesions, and to isolate certain segments of the image (29) (Figure 2.3).
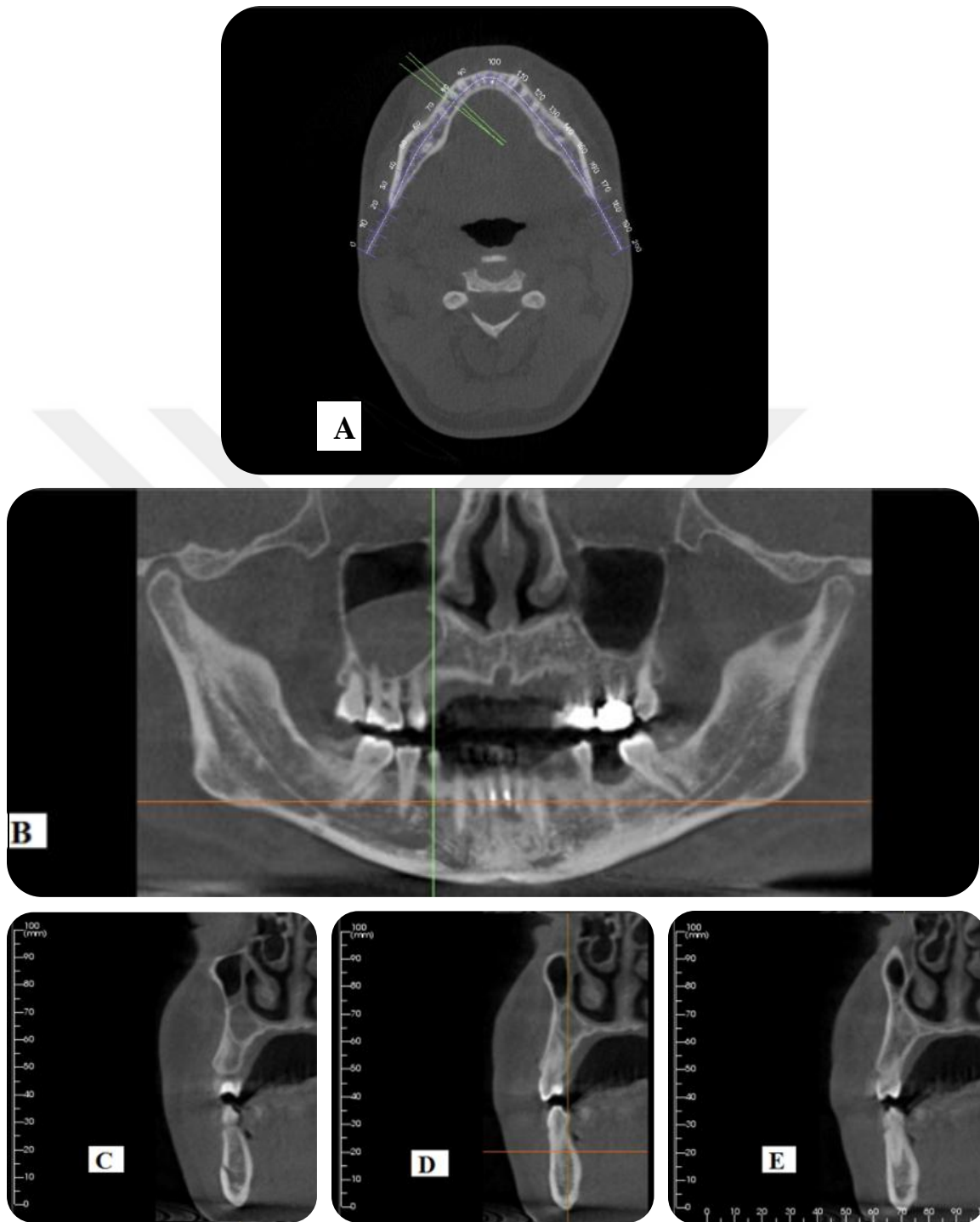
Figure 2.3. Multi-planar Reformation Arch Section. **A**: an axial image with sites of cross-sections on the right side. **B**: a reformatted panoramic view and serial cross-section 2 mm-interval sites. **C, D** and **E**: the cross- sectional images presented at the cross-section sites on the right side, which are shown on the axial and panoramic images. The axial and panoramic images are used as reference images to show the location of the cross-sectional images (Images obtained with i-CAT® Model 17-19; CBCT Imaging Unit: InVivoDental5 Version 5.2 Anatomage, software): Dentomaxillofacial Radiology Department; Faculty of Dentistry- University of Yeditepe.

2.3. Clinical Considerations of CBCT:

CBCT imaging represents a fundamental change for dental and maxillofacial radiology, facilitating the transition of dental diagnosis from 2-D to 3-D images and expanding its task from diagnosis to image guidance in interventional procedures by means of software applications (31, 32). This 3-D information tends to offer the potential of improved diagnosis, treatment planning, surgery execution, and evaluation of healing stages. Therefore, it provides a broad spectrum of variable clinical dental applications and indications. Perhaps the greatest application of CBCT is the planning of endosseous dental implants placement in the jaws (29-31, 33, 34).

Dental implants are metal devices surgically placed in jawbone to replace missing teeth. There are many types of dental implants; nevertheless this study is only concerned with the root form type of dental implants. This type is usually made of titanium, and is cylindrical or tapered in shape. It can be smooth, serrated, or with holes, and it is surgically placed in the alveolar process of the maxilla or the mandible. Subsequent to a successful implant placement, a period of osseointegration occurs and then a crown can be placed over the metal device (34). For implant site assessment, CBCT imaging provides cross-sectional views of the alveolar bone height, width, and angulations as well as precise views of vital structures, such as: the IANC and the maxillary sinus. In many cases, a diagnostic stent is made with radiographic markers and inserted at the time of the scan. This stent presents an exact reference of the location of the proposed implant (27).

Other CBCT imaging applications may include: 1) complicated endodontic treatments and complex endodontic surgeries, 2) diagnosis and evaluation of bony invasion of the jaws by oral carcinoma, 3) evaluation of osseous degenerative changes in the Tempromandibular joint, 4) assessment of maxillofacial fractures for surgery management, and 5) assessment of facial structures, impacted teeth, cleft palate and cases of complex skeletal abnormality for orthodontic treatment, planning, management and orthodontic surgery (29-31, 33-35).

However, it is important to highlight the fact that CBCT can be indicated as an alternative imaging modality to conventional CT where radiation dose is revealed to be lower and soft tissue detail is not a requirement (35). In addition, the common use of CBCT, recently, has resulted in many concerns regarding radiation protection involving: justification, optimization, as well as quality standards and quality assurance of CBCT units (29, 36).

According to Radiation Protection No.172: CBCT for Dental and Maxillofacial Radiology Evidence Based Guidelines by the SEDENTEXCT project; not only the CBCT assessments must be justified on individual basis by illustrating that the potential benefits to the patients outweigh the potential risks, but also CBCT assessments should potentially add new information to aid the patient's management. Consequently, a record of this justification process must be preserved for each patient subsequent to a systematic clinical evaluation in the form of a "Radiological Report" of the complete image dataset. Moreover, justification and referral criteria should be obtained for CBCT applications and indications in regards to the same guidelines. For example, CBCT is indicated for cross-sectional imaging prior to implant placement (35).

Furthermore, a quality assurance programme must be established and implemented for each CBCT unit; including: equipment, technique, and quality control procedures. As regarding quality standards and quality assurance, published equipment performance criteria should be regularly reviewed and revised in testing dental CBCT units. This testing procedure should follow published recommendations, and a specially trained maxillofacial radiologist should be involved. Also, assessment of the clinical quality of images should constitute an essential part of a quality assurance programme for each CBCT system (35).

2.4. CBCT in Regards to Conventional CT:

2.4.1. Strengths of CBCT in Regards to Conventional CT:

CBCT imaging is a modification of conventional CT imaging allocated for dentistry and related disciplines. They both provide reliable 3-D data in all three planes. The main difference, however, between CBCT and conventional CT is that the CBCT utilizes a divergent cone-shaped X-ray beam rather than a fan-shaped beam, and the CBCT utilizes a flat panel X-ray detector as an alternative of one or several rows of detectors. Therefore, the CBCT unit is smaller in size, less in price and only a single rotation of a faster image acquisition time is required to assemble the data necessary to construct the examined volume in all anatomical planes, 3-D reconstructions, and multi-planar views, allowing the examiner to apply interactive image analysis and to scroll through the sub-millimeter image slices with a high resolution up to $0.075mm^3$ voxel size (37, 38). Thus, decreasing patient radiation dose in relation to conventional CT, and consequently; replacing its role in dentistry (27, 39). For example, in CBCT, the

radiation required to produce a medium FOV ranges from 69 to 560 microSieverts (mSv); whereas in conventional CT, a similar FOV size produces 860 mSv. Additional strengths of CBCT also include: high levels of image accuracy, uniform magnification, ideal assessment of multiple sites and full mouth implant planning, easy access to varied software types for image analysis, and special display modes exclusive to maxillofacial imaging that can aid in treatment planning through implant simulation and 3-D reformation (34, 37, 40). Furthermore, many studies reported that CBCT scans are very precise in dimensional accuracy and measurements, in regards to other radiographic techniques, are accurate within 1 mm (34, 38, 41-45). As a result, they exemplify a high degree of reproducibility and reliability (16-18, 37, 46-48).
.

2.4.2. Limitations of CBCT in Regards to Conventional CT:

In general, the high cost of CBCT units and the demand of expert personal involvement limit its availability. Accordingly, the image expense is reasonably high. Moreover, CBCT radiation dose is higher, when compared to conventional 2-D radiographic techniques; besides there is a probability of developing image artifacts (16, 34, 38, 41, 49).

In CBCT imaging, an artifact is the inconsistency between the reconstructed visual image and the original object. This can be induced by discrepancies between the physical setting of the CBCT setup, and position of the investigated object (50, 51). As an X-ray beam passes through an object, lower energy photons are absorbed in preference to higher energy photons. This phenomenon is called "Beam Hardening", and it results in two kinds of artifacts: 1) image distortion, 2) white streaks and dark bands that can appear between two dense objects (28) (Figure 2.4). This means; the gray scale values in the image do not accurately reflect the attenuation values of the object, and the accuracy of the image in relation to the true characteristics of the investigated object is distorted. Image artifacts misrepresent the region of interest, causing significant image degradation, and consequently alter diagnostic information (50, 51). Furthermore, metal streaking and image distortion artifacts can, in particular, disturb bone assessment around existing dental implants (34).
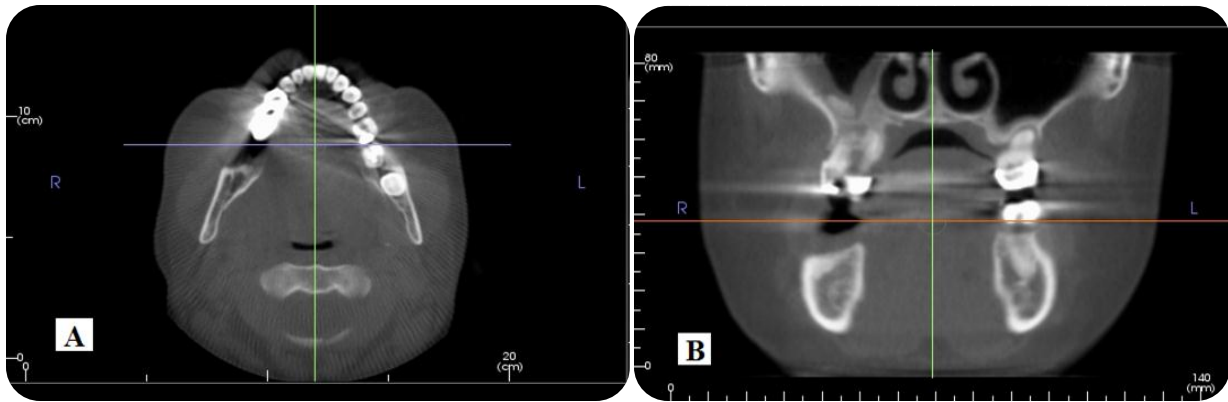
Figure 2.4.CBCT Artifacts. **A** and **B**: Axial and coronal views of the same section, showing black bands of beam hardening, white streaks due to scatter, and image distortion artifacts (Images obtained with i-CAT® Model 17-19; CBCT Imaging Unit: InVivoDental5 Version 5.2 Anatomage, software): Dentomaxillofacial Radiology Department; Faculty of Dentistry- University of Yeditepe.

Perhaps the two main limitations of CBCT images, compared with conventional CT, are image noise and poor soft tissue contrast. The increased divergence of the X-ray beam and the CBCT projection acquisition results in a large volume irradiation by X-ray photons. These photons undergo: Compton scattering interactions, producing scattered radiation. This radiation, scatters in all directions and can be recorded by pixels on the CBCT area detector. As a result, the number of photons detected, at each pixel, dose not reproduce the acutual attenuation of the object. This additional recorded X-ray detection is called "Noise" and it contributes to image degradation. Scattered radiation also reduces object contrast resolution, which is the ability of an image to reveal subtle differences in image density according to differential tissue attenuation, by adding background signals that are not representative of the anatomy, producing images of poor soft tissue contrast. Therefore, CBCT images are of less soft tissue contrast than that of conventional CT (27).

2.5. Anatomy:

In general, basic anatomy information can be derived from literature that is based on anatomy studies, histology studies, radiology studies, and different combinations of these three kinds of studies. Radiography studies, specifically, include those based on 2-D radiography, namely: panoramic radiographs, panoramic radiographs in association with other 2-D

radiological investigations; such as periapical radiographs, as well as 3-D volumetric imaging (52). The fundamental anatomy information in this section is derived from literature that is based on anatomy studies and radiology studies.

2.5.1. General Considerations:

Prior to surgical procedures in the mandible, it is a matter of a great importance for the clinician to determine and identify the location of the Mandibular Canal (MaC) and any related anatomical variations. Failure to identify these variations can result in surgical complications, leading to serious adverse consequences. The presence of anatomical variations in the mandible are usually ignored and received with little attention in many anatomy textbooks. Nevertheless, many reports in relevant literature do consider this presence. The most accurate method to diagnose the presence of anatomic variations is by visual inspection of dry mandible dissections. In clinical practice, paradoxically, the identification of these anatomical variations during patient management can be only obtained by radiography (53).

Since it has multiple applications in "Dentomaxillofacial Diagnosis", CBCT imaging has become widely used over the last decade. It is an advanced imaging modality that presents excellent visualization of the dental hard tissues; reliable localization of IANC, and osseous structures in 3-D (16, 27). Nevertheless, it is important to highlight that CBCT imaging does not validate the IAN itself, but it only illustrates the bony canal, including the MaC, and the diagnostic accuracy for imaging MaC is higher for CBCT than for other imaging modalities (16, 39, 54, 55). In this context, although some authors claim that there are no differences between conventional CT and CBCT concerning the diagnosis of anatomical variations of the MaC (56), a recent meta- analysis review suggests that CBCT is the modality of choice for this application (22), owing to the fact that CBCT offers an increased image quality level of the bone tissue than that of conventional CT (22, 57).

In the same context, and in regards to dental implants; Radiation Protection No.172: CBCT for Dental and Maxillofacial Radiology Evidence Based Guidelines stated that: CBCT is indicated for cross-sectional imaging prior to implant placement as an alternative to existing cross-sectional techniques where the radiation dose of CBCT is shown to be lower; as for cross-

sectional imaging prior to implant placement, the advantage of CBCT with adjustable FOV compared with conventional CT, becomes greater where the region of interest is a localized part of the jaws, as a similar sized FOV can be used (35, 36).

2.5.2. Image Anatomy of the "Extra-cranial Segment" of the Trigeminal Nerve:

The Trigeminal nerve or the 5th cranial nerve (CN5, or CNV) is a mixed nerve that comprises a large sensory cranial nerve of head and face, and a motor nerve for muscles of mastication. As regarding the image anatomy, the CN5 is composed of 4 segments: 1. Intra-axial, 2. Cisternal or preganglionic, 3. Interdural, and 4. Extra-cranial or postganglionic (34).

It is beyond the scope of this study to discuss the image anatomy of the first 3 segments; the extra-cranial segment, on the other hand, contains 3 branches: the ophthalmic nerve branch (CNV1), the maxillary nerve branch (CNV2), and the mandibular nerve (CNV3), which is the largest trigeminal branch (21, 34).

This work is only concerned with the third division; the mandibular nerve branch. In general, the mandibular nerve exits directly through Meckel cave, passing in an inferior direction through foramen oval into masticator space. This nerve subdivides, providing three groups of branches; branches from stem of the CNV3, branches from the anterior division of CNV3, and branches from the posterior division of CNV3. Branches from stem provide motor supply to medial pterygoid, tensor tympani, and tensor veli palatine muscles. Branches to masseter, temporalis and lateral pterygoid muscles are derived from anterior division of CNV3. From the posterior division of CNV3, the mylohyoid nerve branches to supply motor innervations to anterior belly of digastrics and mylohyoid muscles. Main sensory branches from the posterior division include inferior alveolar, lingual, and auriculotemporal nerves. The lingual nerve is sensory to anterior tongue, floor of the mouth, and lingual gingiva. It also carries afferent taste fibers from anterior two thirds of tongue via chorda tympani from the 7th cranial nerve. Branch of lingual nerve and blood vessels from lingual artery and vein enter lingual foramen (LF) at the midline on the lingual surface of the mandible between the Genial Tubercles (GT), which are small bony projections that give attachment to genioglossus and geniohyoid muscles. The anatomy of the LF is highly variable in regards to number, and location; as it can be superior or

inferior to GT. The radiographic appearance shows it as a round radiolucent area surrounded by a densely corticated border (34, 58) (Figure 2.5).
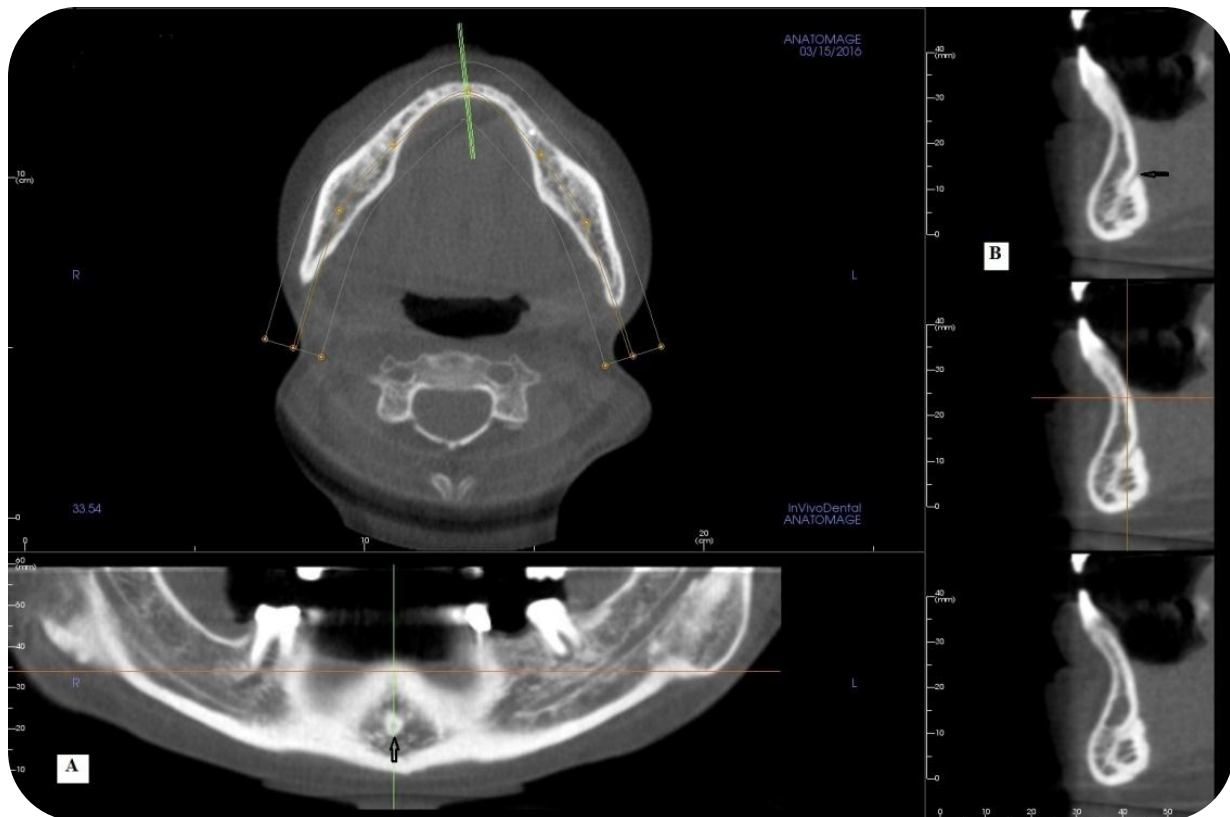
Figure 2.5. Multiplanar Reformation Arch Section. **A**: a reformatted panoramic view showing the lingual foramen at the midline; radiolucent dot surrounded with a radioopaque ring (black arrow). **B**: a cross-section, showing the lingual foramen (black arrow) and the lingual canal emerging through it denoted as a radiolucent line (Images obtained with i-CAT® Model 17-19; CBCT Imaging Unit: InVivoDental5 Version 5.2 Anatomage, software): Dentomaxillofacial Radiology Department; Faculty of Dentistry- University of Yeditepe.

2.5.3. The Inferior Alveolar Nerve:

The IAN enters the Mandibular Foramen (MaF), which is located on medial mid ramus of the mandible. It runs through MaC, below the apices of lower posterior teeth, and innervates ipsilateral premolars and molars. It divides into mental and incisive branches (34). The MaC is

usually a single channel enclosed by bone, forming an upward concave curve (52). The path of the MaC is traced through the mandible, running obliquely downward and forward, extending from the MaF at the lingula on the lingual aspect of the mandible to the MeF in a horizontal direction. It contains a bundle that is comprised of the inferior alveolar nerve, artery and vein which are responsible for the somato-sensory sensation and blood innervations of the lower teeth, inter-dental papilla, periodontal and alveolar bone tissues (4, 19, 22-25, 27, 59, 60). In CBCT cross-sections, the MaC appears as a round or oval radiolucent area surrounded by a corticated radiopaque border. This corticated border is, occasionally, thin or barely visible (27) (Figure 2.6). In coronal and reconstructed panoramic sections it can be described as a radiolucent band between two white lines (52). The relationship between the MaC and teeth roots is variable, especially at the molar region, ranging from close to the root apices to adjacent to the lower border of the mandible (27).

At the level of the periapical area of premolar teeth, the MaC extends anterior to the MeF before it loops in a posterior direction as the Mental Canal (MeC) or Anterior Loop (AL), and then it exits through the MeF on the buccal surface of the mandible. The AL is an important anatomic variation to detect while placing dental implants in this region. The mental nerve is the anterior extraosseous branch of IAN that provides sensory innervations to skin and mucosa of lower lip, anterior labial gingival, and chin (27, 34). The MeF is a bilateral structure that is presented with an oblique orientation in a postero-superior direction. Radiographically, it appears as a single round non- corticated radiolucent structure (21) (Figure 2.7). The size, shape, and location of this foramen are, significantly, variable, and the incidence of an accessory mental foramen has been accounted (27).
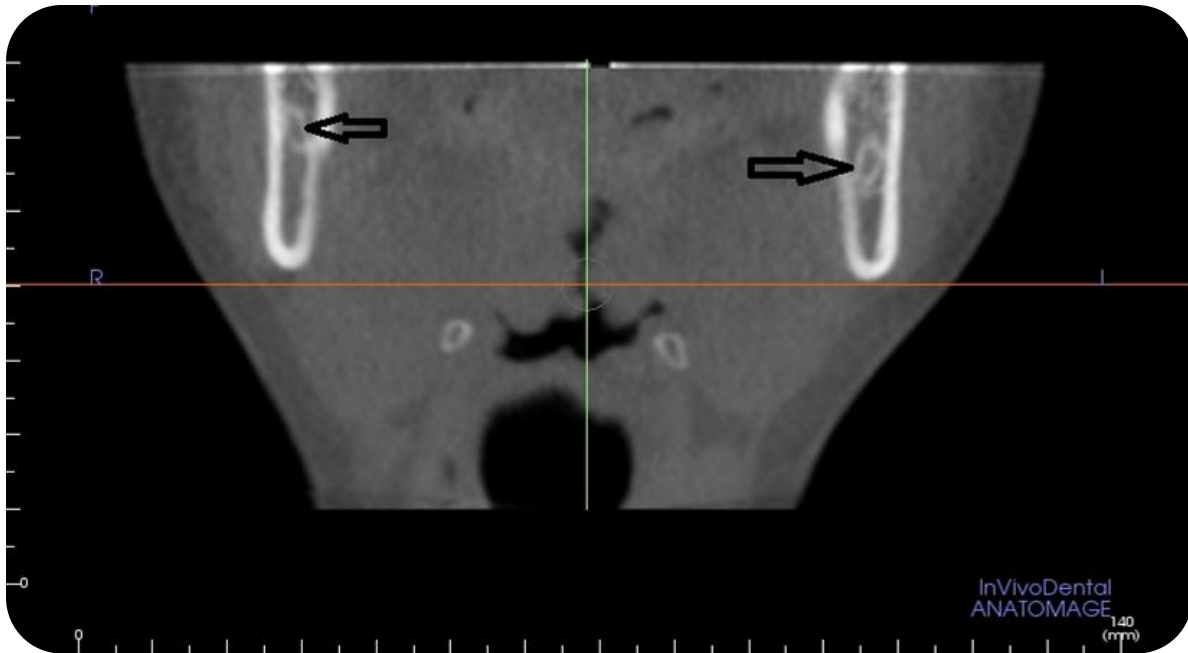
Figure 2.6.A coronal section of the mandible at the ramus level, showing the cross-sections of the right and left Mandibular Canals (black arrows) on right and left sides (Images obtained with i-CAT® Model 17-19; CBCT Imaging Unit: InVivoDental5 Version 5.2 Anatomage, software): Dentomaxillofacial Radiology Department; Faculty of Dentistry- University of Yeditepe.

Figure 2.7. Sections of the mandible at the mental foramen area. **A**: Axial section of the mandible showing symmetrical mental foramina on right and left sides (black arrows). **B**: coronal section of the same case, showing the mental foramina on right and left sides (black arrows) with the anterior loops emerging through them denoted by the radiolucent lines opening in a superior direction. (Images obtained with i-CAT® Model 17-19; CBCT Imaging Unit: InVivoDental5 Version 5.2 Anatomage, software): Dentomaxillofacial Radiology Department; Faculty of Dentistry-University of Yeditepe.

Anterior to the MeF, the IAN becomes the MIN (34). Olivier (61) described the MIN as the anterior intra-osseous terminal branch of the IAN that prolongs its pathway into the mandibular anterior area, innervating the mandibular canines and incisor teeth in the interforaminal part, and may provide cross-innervations if it reaches the midline; as it may connect with the Lingual Canal (LC) (6, 9, 14, 17, 34, 61). These innervations may be obtained through small neurovascular bundles called Nutrient Canals (NCs) that appear in periapical radiographs as radiolucent lines running vertically from the IANC directly to apices of teeth, or between teeth through the interdental spaces. NCs are more commonly detected in images of patients with hypertension, diabetes mellitus, periodontal diseases, or in black patients, or male patients, or in elderly and edentulous patients. NCs are visible in around 5-40% of the cases, indicating a thin ridge. This clue is useful in dental implant assessment around the midline area (27).

At the midline, the LF conducts the terminal branch of the MIN through the emerging of the LC, which in sagittal CBCT sections appears as a narrow radiolucent passage with a wide range of variation in number, orientation, and location being superior or inferior to the GT (34) (Figures 2.5 and 2.8). Moreover, assessment of the micro-anatomical dissections showed a clear neurovascular bundle in both superior and inferior lingual foramina and their bony canals. Branches of the lingual artery, vein, and lingual nerve comprised the contents of the superior lingual canal, whereas branches of the submental and\or sublingual, and mylohyoid nerve comprised the contents of the inferior canals (62).

A number of authors presume that the MIN runs through the intramedullary spaces, and is not contained by a bony canal, thus, it is not commonly detected by conventional 2-D radiography (6, 10, 17, 63). However, anatomical studies using advanced imaging modalities have revealed strong evidence supporting the existence of MIC (6, 10, 17, 38, 46, 63) placed on the mesial side of the MeF, with a smaller diameter and less corticated borders than that of the MaC (9, 11, 13, 14, 17, 64). Furthermore, the intra-osseous course of a well-corticated MIC, usually, extends from the MeF to the lateral incisor level, and then it becomes indefinite at the central incisor level, where it terminates, and the neurovascular plexus conquests, allowing cross-innervation at the mandibular midline level (11). On cross-sectional CBCT scans, MIC

appears as a round radiolucent area surrounded by a radiopaque border, contained in the mandibular trabecular bone (11, 17, 38) (Figure 2.9).
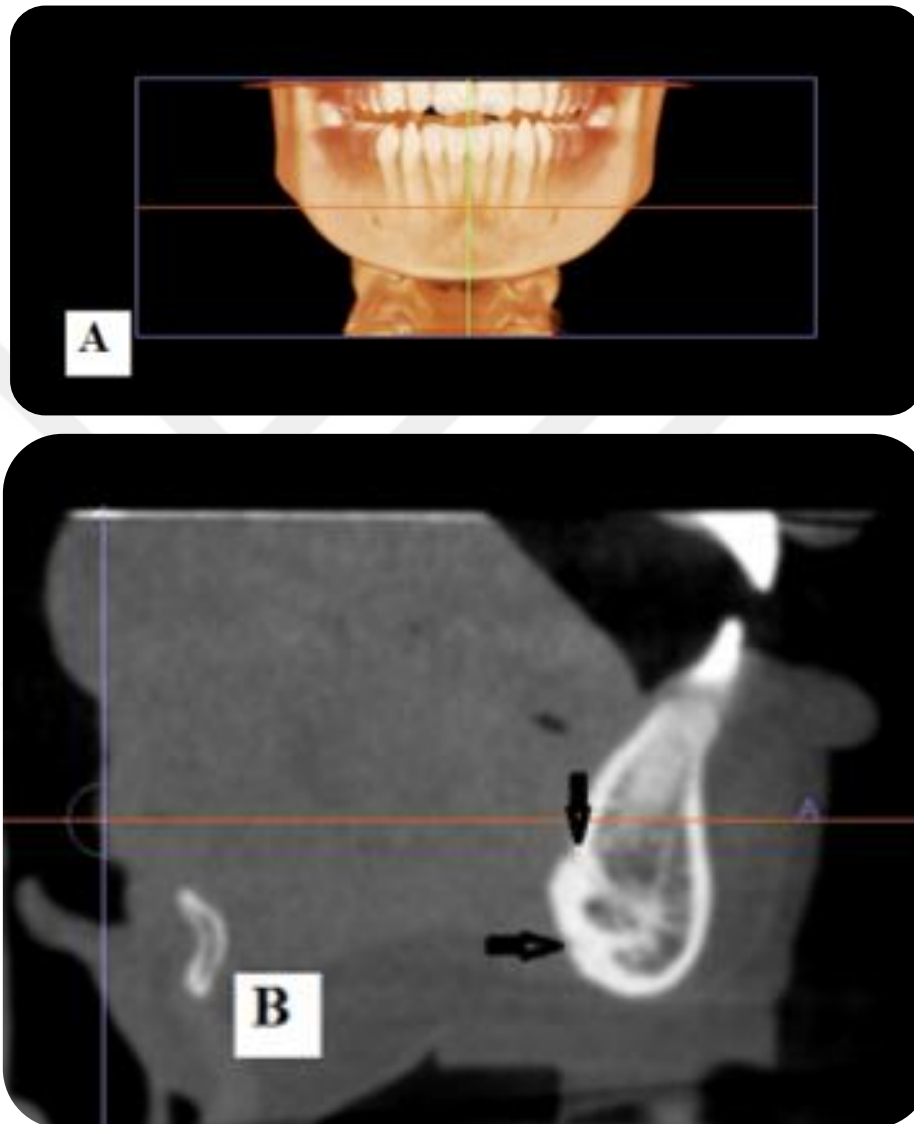
Figure 2.8. Sections at the midline. **A**: Volumetric 3-D representation of the mandible showing the level of the sagittal section at the midline. **B**: the cross- section of the same case at the midline, showing two lingual canals; one above the genial tubercle (radiopaque protrusion), opening in a superior direction (vertical black arrow), and the other canal below the genial tubercle opening in an inferior direction (horizontal black arrow) (Images obtained with i-CAT® Model 17-19; CBCT Imaging Unit: InVivoDental5 Version 5.2 Anatomage, software): Dentomaxillofacial Radiology Department; Faculty of Dentistry- University of Yeditepe.
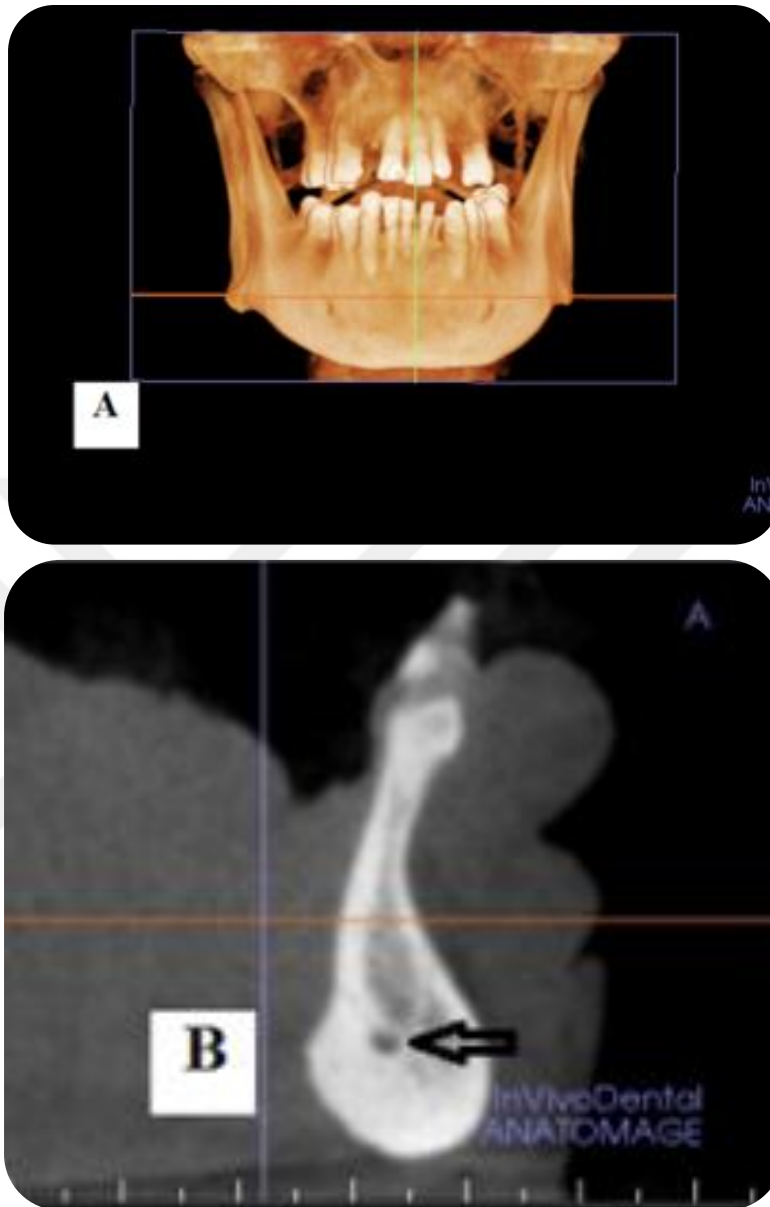
Figure 2.9.A: Volumetric 3-D representation of the mandible showing the level of the sagittal section slightly lateral to the midline. **B**: the cross- section of the same case lateral to the midline, showing the mandibular incisive canal (black arrow) denoted as a round radiolucent area surrounded by a corticated area (Images obtained with i-CAT® Model 17-19; CBCT Imaging Unit: InVivoDental5 Version 5.2 Anatomage, software): Dentomaxillofacial Radiology Department; Faculty of Dentistry-University of Yeditepe.

Therefore, the presence of the MIC, containing the neurovascular bundle should not be underestimated at the time of pre-surgical planning in the interforaminal area or the "safe zone", as it has been reported that transient or long term postoperative sensory disturbances, edema, hematoma, lack of implant osseo-integration, and pulp sensitivity changes, may occur (9, 10, 17, 18, 47, 65-67).

Knowledge of the normal morphology of human mandible and its possible variations have attracted special interests in the recent years, and meticulous detection of the MaC position and its associations is essential in surgical procedures involving the mandible, such as third molar extractions, dental implant placement, and sagittal split ramus osteotomy (19, 20). Anatomical variations of the MaC, such as Bifid Mandibular Canals (BMC) or Trifid Mandibular Canals (TMC) have been reported in the literature, using panoramic radiography (20, 23, 60, 68-73), conventional CT (20, 52, 74, 75), and CBCT (19, 20, 66, 76-82). However,only 3-D modalities that provide high-resolution images; namely conventional CT and CBCT are considered superior in displaying the MaC and its variations, such as BMC and TMC (20, 66, 78).

The origin of the BMC or TMC can be attributed to the theory that suggests that the IAN most probably occurs in the mandible as three individual nerve paths, originating at different stages of development. It is hypothesized that the pattern of tooth agenesis within the three mandibular teeth groups, namely; incisors, primary molars, and permanent molars is related to the three separate paths of innervations of the dentition. As through the remodeling stage of the embryological development, these three divisions of the IAN, innervating the three different mandibular teeth groups fuse, incompletely, due to rapid prenatal growth and intra-membranous ossification in the mandibular ramus region, resulting in gradual coalescence of the canal entrances, and consequently the occurrence of BMC, or TMC (83, 84).

As regarding BMC, the term bifid is derived from the Latin word meaning clefting or branching into two divisions (74). The bifid canals branch from the MaF and may each contain a neurovascular bundle (74). Based on cadavers and radiographic images, the previous research reported different types and classifications of the mandibular canal according to anatomical position and pattern with both conventional and advanced imaging techniques (19, 56, 60, 68,

69, 74, 82, 85). Carter and keen (69) examined dissected human mandibles and described three types of IAN patterns; Type 1: The nerve is a single large structure lying in a bony canal and the tips of the molar roots projecting into the canal as the branches supplying these roots are short and direct, Type 2: The nerve is located considerably in a lower level than that of type 1, and the dental branches to the molar roots are given off more posteriorly, and are therefore longer and obliquely oriented, and Type 3: The Nerve divides into two branches posteriorly, which together can be considered as equivalent to an alveolar branch (69, 74).

Nortje (60) examined panoramic radiographs and described three main types of BMC (74). Langlais (68) examined panoramic radiographs and developed a four type classification system for BMC (74). Furthermore, the following classification was adapted from Naitoh et al. (19, 56), Orhan et al. (82, 85), and Muinelo-Lorenzo et al. (86). They classified BMC into five types: Type I: Retromolar Canal (RMC) (87- 89), Type II: Dental Canal, Type III: Forward Canal, Type IV: Bucco-lingual Canal, and Type V: Superior Canal (86) (Table 2.1).

Table 2.1. The classification of Bifid Mandibular Canals, adapted from: Naitoh et al., Orhan et al., and Muinelo-Lorenzo et al.

Type	Name	Description
I	**Retromolar Canal**	The canal bifurcates from the IANC in the mandibular ramus region and travels in a recurrent path anterosuperiorly, or posterosupriorly, reaching the retromolar fossa behind the third molar.
II	**Dental Canal**	The canal runs forward and ends in the periapical area of the second or third molars.
III	**Forward Canal**	The canal courses towards the front with or without joining the inferior alveolar canal.
IV	**Bucco-lingual Canal**	The canal sprouts in a buccal or lingual direction from its origin.
V	**Superior canal**	The canal follows a superior direction and does not meet the classification criteria of any other group.

The RMC is an anatomical variant in the posterior mandible that houses and transmits neurovascular component in and to the retromolar fossa, providing additional innervation to the mandibular molars and the buccal area (88, 90, 91). This anatomical variant is usually neglected in anatomical text books, and is usually associated with considerable population diversity with a frequency ranging from 1.7% to 72% (92, 93).

In 1986 and 1987, Ossenberg (94) put forth one of the first few descriptions of RMC (87). Based on anatomical studies on dry mandibles and according to the course of RMC branching from the MaC, Ossenberg (94) classified RMC into 3 types: Type 1: RMC with a vertical course, Type 2: RMC with a horizontal course, and Type 3: RMC with a separate foramen in the mandibular ramus (11, 94, 95). The third type is also referred to as: Temporal Crest Canal (TCC) and has been rarely noted (87, 94). Moreover, Ossenberg (94) reported a peak incidence of the Retromolar Foramen (RMF) in adolescents, as she speculated that this fact might reflect the increased neurovascular requirements related to the adolescent growth spurt and eruption of the third molars (89). In 2011, based on panoramic radiographs and sagittal CBCT images, Von Arx et al. (89) classified RMC according to course and morphology, into 5 types: Type A1: RMC with a vertical course, Type A2: RMC with a vertical course and an additional horizontal branch, Type B1: RMC with a curved course, Type B2: RMC with a curved course and an additional horizontal branch, and Type C: RMC with a horizontal course (89) (Figures 2.10 and 2.11).

In the posterior mandible, the presence of the mandibular canal and foramina variations and associations is frequently ignored, unnoticed, or misdiagnosed (21). Unrecognized anatomical variations of the MaC may lead to complications during dental surgical procedures, such as somato-sensory impairment, traumatic neuroma, bleeding and bruising signs (22, 53, 72, 74, 80, 96-98). Moreover, the presence of anatomical variations, such as RMC, can be associated with difficulties in performing alveolar mandibular nerve block, or even failure of local anesthesia and consequential pain and discomfort, especially, in surgical removal of impacted third molars, bone harvesting for bone graft surgery, sagittal split ramus osteotomy, and dental implant placement (22, 69,72, 74, 92-94, 96, 99-105). It can also be a reason of anxiety for inexperienced practitioners (88).
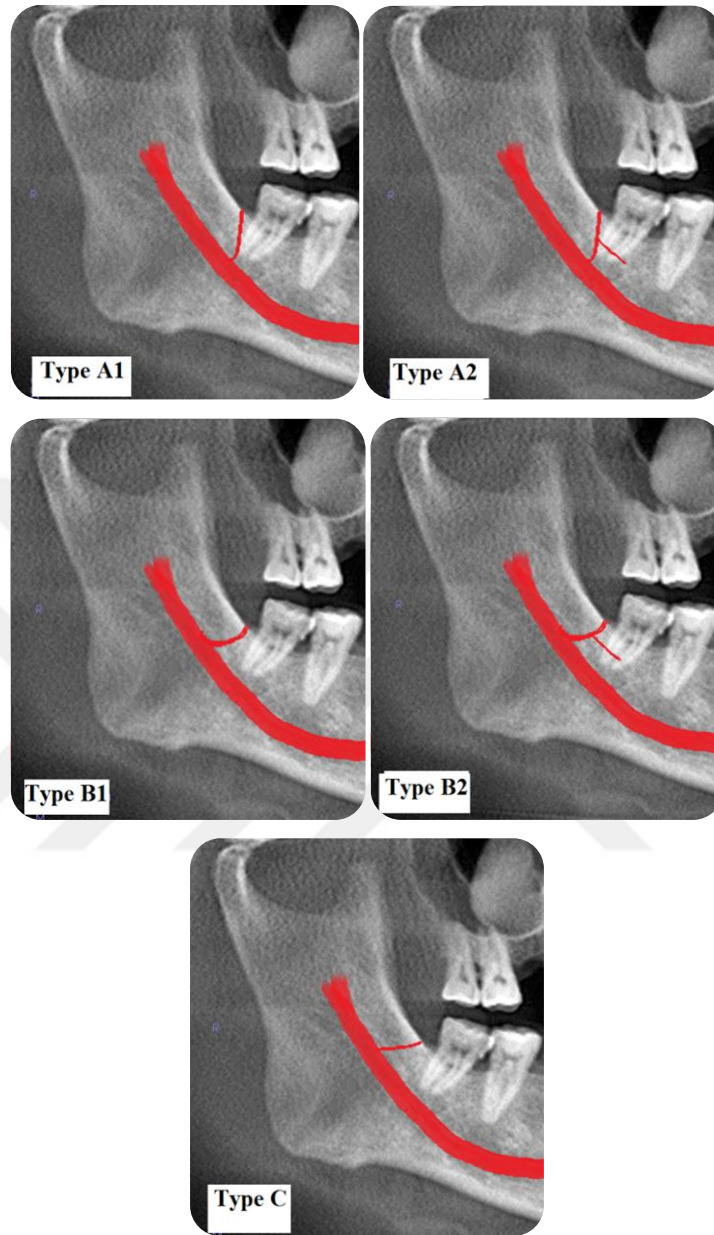
Figure 2.10. Cropped reformatted panoramic view of the mandible, showing a schematic illustration of the Retromolar canal types applied on the same cropped panoramic view; Classification by Von Arx et al., and illustrations by E-Z M (Images obtained with i-CAT® Model 17-19; CBCT Imaging Unit: InVivoDental5 Version 5.2 Anatomage, software): Dentomaxillofacial Radiology Department; Faculty of Dentistry- University of Yeditepe.
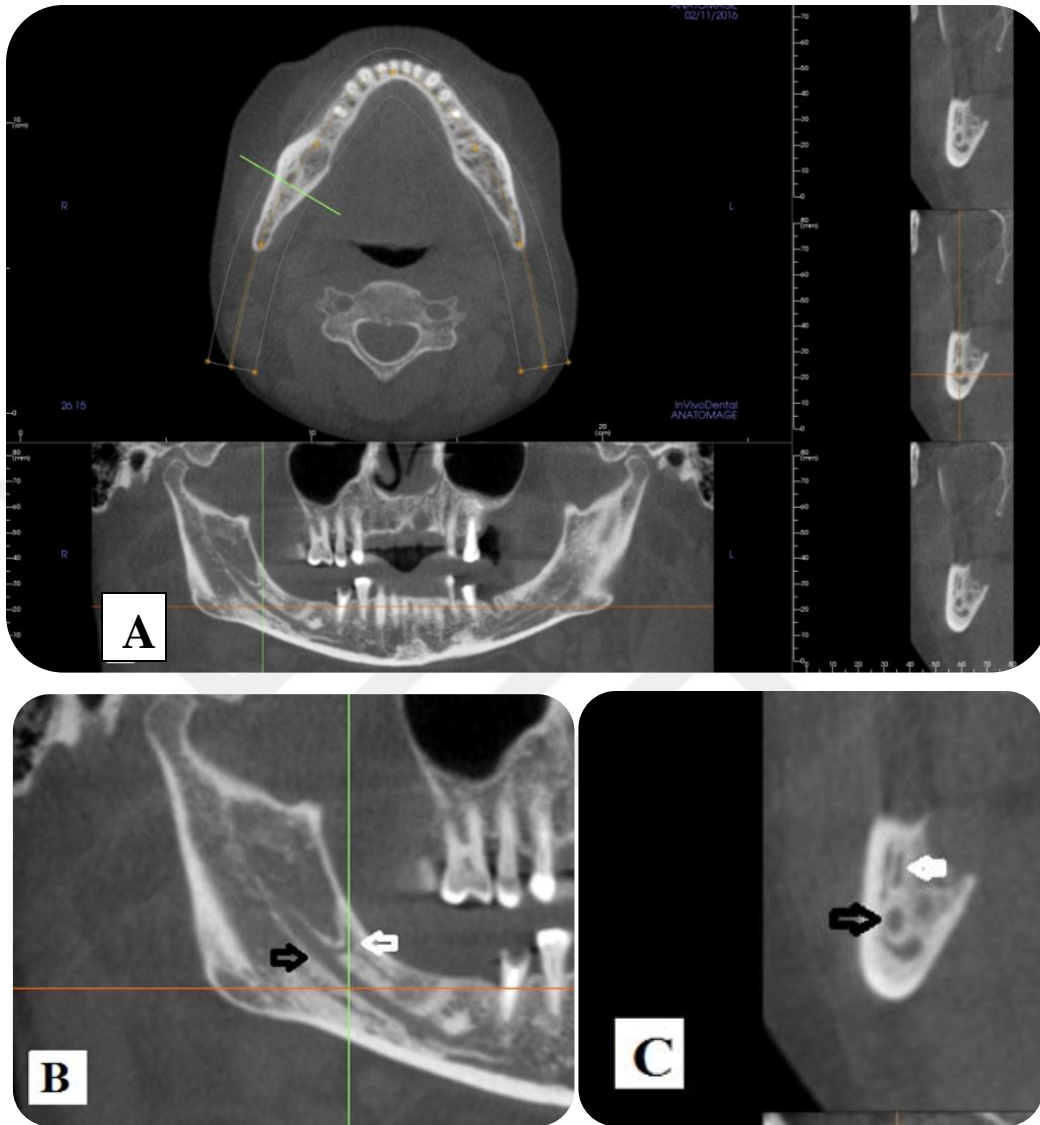
Figure 2.11. Multi-planar Reformation Arch Section. **A**: a reformatted panoramic view, showing a curved retromolar canal with a horizontal branch (Type B2) at the right side of the mandible, and serial cross-sections; 0.125mm-interval slices. B: cropped magnified image from the same section; black arrow denoting the mandibular canal at the level of RMC, and white arrow denoting the RMC at the level of the horizontal branch. **C**: a cross-section of the RMC; black arrow denoting the mandibular canal and white arrow denoting the RMC with the horizontal branch (Images obtained with i-CAT® Model 17-19; CBCT Imaging Unit: InVivoDental5 Version 5.2 Anatomage, software): Dentomaxillofacial Radiology Department; Faculty of Dentistry-University of Yeditepe.

The inherent limitations of 2-D conventional radiographic techniques (22, 84, 106, 107), as well as higher radiation dose and more cost of conventional CT (22, 106, 107) indicate that CBCT can be the most appropriate imaging modality to assess the IANC, as it provides enhanced visualization of anatomical structures, in terms of location, shape, and association to adjacent structures (16, 21, 22, 108).

As regarding anatomical variations in the anterior mandible, similar complications have been reported during or after surgical procedures for the same reasons of ignorance (37, 109-112), that can be due to the inadequate information about the region's significance, the controversy surrounding its precise anatomy, presence of anatomical variations, and intra-osseous content of accessory canals (10). Furthermore, the fact that the common failure of conventional radiography to detect the presence of the MIC, for example, cannot be justified by technical limitations of the image only, but it can be attributed to the observer limitations as well (11). An observer needs to be knowledgeable, skillful, and experienced to be able to recognize anatomical landmarks such as the LF and MIC (11, 113). The fact that these anatomical landmarks are described in radiology textbooks (114-117) and not in anatomy textbooks (118-122) may indicate that these anatomical structures are not perceived by observers relying on anatomy textbooks only (11). Nevertheless, the prevalent use of CBCT recently, especially prior to dental implant surgery, increased the interest in anatomical features and anatomical variations in the human mandible and jaw bone in general (123-125).

Reports illustrated the presence of accessory foramina and canals, mainly on the lingual side of the mandible (124, 126). Accessory foramina on the lingual side can bedivided according to their location into two main groups: medial and lateral lingual foramina (124, 127). The canal structures of these foramina are called "vascular canals", because of their arterial content, which includes either different arterial branches, or anastomosis of the arteries (128, 129). However, Sutton (126) illustrated the structures associated with the LF as a neurovascular bundle. In the literature, medial lingual vascular canals or LC, as mentioned earlier, are common (129, 130), whereas lateral lingual vascular canals (LLVCs) are rare (129, 131, 132). However, it is essential to consider CBCT imaging of LLVCs in the premolar and the interforaminal regions before

surgical procedures, particularly implant insertions, as the risk of hemorrhage exists (37, 127, 129, 131, 132).

On CBCT cross-section images, LLVCs appear as thin radiolucent canals, connected with the IANC, or the MIC (37) (Figure 2.12). It is acknowledged that the connection of LLVCs with either the IANC or the MIC supports collateral neural and vascular supply (128, 130). Examinations of LLVCs demonstrated that canals originating from the premolar area mainly connect with the MIC, whereas canals originating from the molar area connect with the IANC or with the apices of adjacent teeth (130).
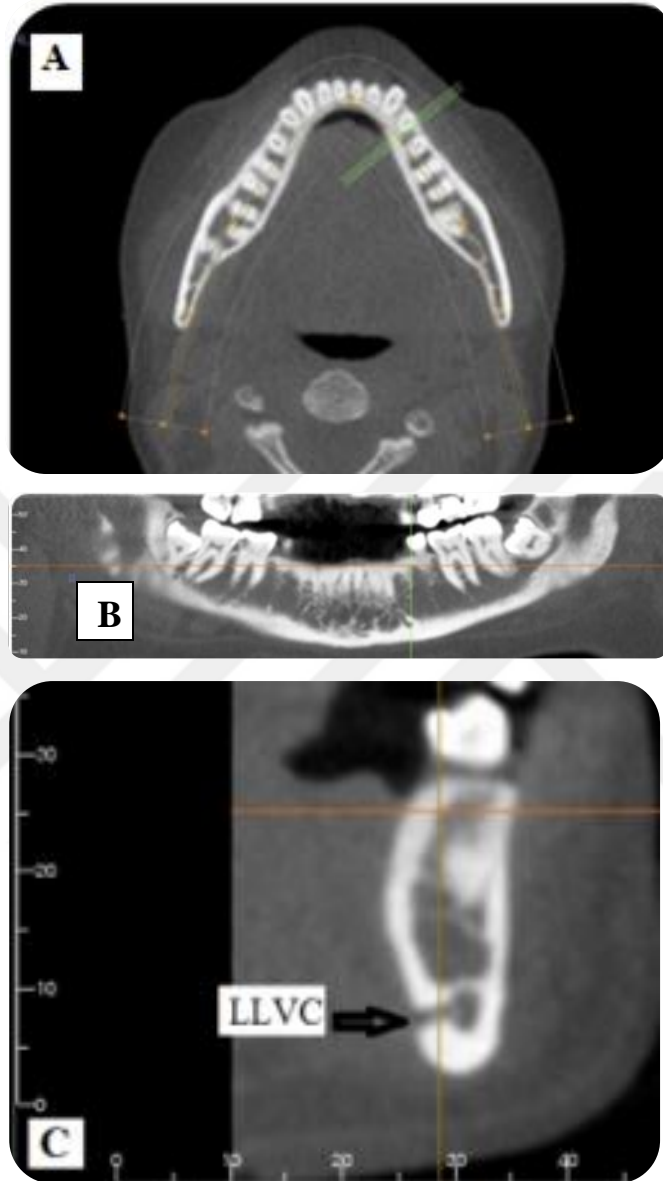
Figure 2.12. Multiplanar Reformation Arch Section. A: an axial image (cropped) with sites of cross-sections on the left side distal to the first premolar tooth. B: a reformatted panoramic view and serial cross-section 1mm-interval sites. C: a cross-sectional image, showing a lateral lingual vascular canal (LLVC) (black arrow) denoted as a radiolucent line (Images obtained with i-CAT® Model 17-19; CBCT Imaging Unit: InVivoDental5 Version 5.2 Anatomage, software): Dentomaxillofacial Radiology Department; Faculty of Dentistry- University of Yeditepe.

2.5.4. Summary:

The mandibular canal travels at the lower one- third of the mandibular body in approximation to the lingual cortical plate. Eventually, it divides into the mental and incisive canals (34, 133- 135).The mental canal curves in a posterior, superior, and lateral direction to exit through the mental foramen and the incisive canal prolongs forward to the incisor teeth (34, 133, 136). During this course, the mental foramen is located posterior to this division, and the mandibular canal   usually forms the anterior loop and then returns back to the mental canal in the interforaminal area (4, 34, 133, 137). The incisive canal has partly corticated boundaries, and is consequently difficult to differentiate from the surrounding structures on radiographic imaging (6, 18, 133). Nevertheless, the presence of the mandibular canal variations and\or associations is frequently ignored, overlooked, or misdiagnosed (21).

The success of dental management is directly related with the detection of anatomical variations and associations, which should be thoroughly evaluated prior to invasive dental procedures to avoid serious complications (138). The intrinsic limitations of conventional radiographic techniques (22, 32, 84, 106, 107), higher radiation dose and expensive conventional CT (16, 22,32, 106, 107), the facility of precise localization in CBCT (139), capability of its software, measurement accuracy and the fact that,   unlike conventional CT, there is no magnification in its linear measurements (57,140-145); all indicate that CBCT can mainly be the appropriate imaging modality to evaluate the IANC, as an anatomical structure with its associations and variations (16, 21, 22, 108).

Consequently, the aim of this study is to develop a reliable and consistent method of CBCT image analysis to assess the IANC, starting from the mandibular foramen at one side to the lingual foramen at the midline to involve the whole IANC structure and to accommodate all of its anatomical associations and anatomical variations in this method.

3. MATERIALS AND METHODS

3.1. Radiographic Material:

This study is a "Retrospective Cross-Sectional" study. The sample consists of 510 consecutive patients' images from which pre-operative CBCT imaging was obtained in the period from 2014 to 2016. These images were indicated for various clinical reasons; mainly for planning implants at the Department of Dentomaxillofacial Radiology, Faculty of Dentistry and Dental Hospital at the University of Yeditepe. Prior to the imaging procedure, all patients approved the written informed consents for the use of images in scientific research, (Appendix 1). For the retrieved CBCT images, a list with codes and corresponding names was created in an encrypted file for patient confidentiality and protection reasons. This study followed the ethical principles of "The Declaration of Helsinki 1964" and its later amendments on human research ethics. All procedures were performed in accordance with the standards of the Ethic Committee of Clinical Research at the University of Yeditepe; Ethic Committee Approval Ref.: 2017\701 and the Ministry of Health Clinical Research Committee in Turkey.

The sample was subjected to inclusion and exclusion criteria. The inclusion criteria are:

1. The presence of the mandible in the field of view; adequate FOV.
2. Complete database of Turkish patients.
3. Complete patient database with age more than 14 and less than 80 years.
4. Dentate patients.

Whereas the exclusion criteria are:

1. The presence of fractures or evidence of surgical intervention in the mandible.
2. The presence of pathological lesions in the mandible, such as odontogenic tumors or odontogenic cysts.
3. The presence of sever bone resorption due to metabolic or bone disease.
4. The presence of artifacts or distortion affecting the image quality.

From the original sample size (510), a final sample of 200 CBCT images (400 IANCs) was selected (Figure 3.1).

<div align="center">

Original sample size: 510 images

</div>

4 images : fractured mandible.	**56 images : patient less then 14 years old.**
28 images: odontogenic lesions.	**21 images : bone atrophy.**
7 images : mandibular hypertrophy.	**128 images : small FOV***
7 images: impacted teeth obstructing the visiability of IANC.**	**4 images: bone necrosis.**
	10 images : surgical intervension in the mandible.
6 images: implants obstructing the visiability of IANC.**	**39 images: artifacts.**

<div align="center">

Final sample size: 200 images

</div>

Figure 3.1. Algorithm showing sample size subjected to inclusion and exclusion criteria.

*FOV: Field Of View.   **IANC: Inferior Alveolar Nerve Canal.

3.2. Imaging System:

CBCT images were obtained using a CBCT unit with a flat panel image detector of amorphous silicon (i-CAT® Model 17-19; Imaging Sciences International Inc., Hatfield, Pennsylvania, USA). All images were performed using standard exposure acquisition parameters and standard patient positioning protocol. Patients were exposed in the sitting position, head adjusted using the headrest, and the occlusal plane parallel to the floor of the room, the mid-

sagittal plan aligned perpendicular to the horizontal plan, using vertical and horizontal alignment beams recommended by the manufacturer. Exposure acquisition parameters were as follows: a tube voltage of 120 kVp, a tube current of 23.87 mA, 6 cm FOV, 0.25 mm voxel size, and 40s scan time with high-resolution bone filter. All images were performed using the radiation protection standards, maintaining the: As Low As Reasonably Achievable (ALARA) principle.

CBCT images were processed and evaluated using a workstation computer unit (Hp LP2475W LCD TFT Monitor, China). The PC workstation used Windows® 7 Professional 32-bit with XP Mode operating system (Microsoft Corporation, Redmond, WA, USA) with pre-installed software: InVivoDental5 Version 5.2 Anatomage, 2010; USA. All CBCT image measurements were obtained using the same software tools under standard conditions; dimly lit room, the same workstation computer unit and the same display monitor. Measurments in each subject were obtained on both sides: Right (R) and Left (L).

3.3. Image Parameters:

The specific objective of this study is to identify a method of CBCT image analysis method to assess the visibility and the course of the IANC, as a continuous unit, with its associate canals starting from the mandibular foramen, branching at the level of mental foramen, continuing as the mandibular incisive canal into the interforaminal region, ending at the midline, and then applying this method to the selected CBCT image sample. The IANC with its associate canals most likely encountered, and observed in CBCT images are as follows:

1. Mandibular Foramen (MaF)
2. Mandibular Canal (MaC)
3. Mental Foramen (MeF)
4. Mental Canal (MeC), or Anterior Loop (AL).
5. Mandibular Incisive Canal (MIC)
6. Lateral Lingual Vascular Canals (LLVCs), or Paramental Canals.
7. Nutrient Canals (NCs)
8. Lingual Canal (LC)
9. Lingual Foramen (LF)

By means of CBCT, these structures will be subjected to a new 3-D measurement scheme, as parameters, and then a CBCT image anatomy categorization of the IANC existing conditions will be assembled in accordance. The general anatomical parameters suggested in detecting, measuring, and evaluating the visibility and the course of the IANC with its associations and\or accessory canals for both R and L sides in this study are as follows:

1. Mandibular Foramen Number (MaFN)
2. Mandibular Canal Number (MaCN)
3. Mental Foramen Number (MeFN)
4. Mental Canal Length (MeCLe) or Anterior Loop length (ALL)
5. Mental Canal location (MeCl)
6. Mental Canal Orientation (MeCO)
7. Mental Canal Angulation (MeCA)
8. Mandibular Incisive Canal visibilty (MIC)
9. Lateral Lingual Vascular Canals' Number (LLVCsN)
10. Lateral Lingual Vascular Canals' Length (LLVCsLe)
11. Lateral Lingual Vascular Canals' Orientation (LLVCsO)
12. Lateral Lingual Vascular Canals' range between teeth (LLVCsr)
13. Lateral Lingual Vascular Canals' Height (LLVCsH)
14. Lateral Lingual Vascular Canals' Aspect (LLVCsA)
15. Nutrient Canals Number (NCsN)
16. Nutrient Canals Range (NCsR)
17. Lingual Canal Number (LCN)
18. Lingual Canal Aspect (LCA)
19. Lingual Canal location (LCl)
20. Lingual Canal in relation to Genial Tubercles (LCGT)
21. Lingual Canal resembling allocated figures (LCfig)
22. Lingual Foramen Number (LFN)
23. Lingual Foramen Aspect (LFA)
24. Lingual Foramen location (LFl)
25. Lingual Canal Class (LC Class)

All of these parameters are interpreted in statistical terms and described in (Appendix 2).

3.4. Method:

All CBCT images were evaluated and processed using reconstructed multi-plane views: axial, coronal, sagittal, reformatted panoramic, and cross-sectional. These reconstructions were analyzed to identify and measure the previously mentioned parameters in the same order, and for every patient as described in the following procedure:

1. **iCATVision** software was opened and the patient of interest was selected according to the ID number on the list. Then, **CT** option was clicked, and **Start InvivoDental** was chosen, leading to an external application in the form of **DICOM** file.
2. In the **Invivo5 DICOM** file, the **Superimposition** option was clicked, and in regards to the 3-D reconstructed format, Right **3\4 view**, and then **Left 3\4 view** were chosen to observe the Mental Foramen Number (MeFN) on both right and left sides (Figure 3.2). The cursor in the mouse was used to perform free hand movement to observe Mandibular Foramen Number (MaFN).
3. The **Section** option was clicked; axial, sagittal, and coronal plans on 3-D section were adjusted with the 3-D reconstructed image of the head in an upright position (Figure 3.3). In general, the aim was to simultaneously slide the plan through one section, such as the axial section, and observe the structures on another section, such as the sagittal section, by moving the cursor very slowly at the level of the mandible for both right and left sides.
4. The horizontal plan was moved slowly from the back forewords on both the axial and coronal sections, simultaneously, to observe the Mandibular Foramen Number (MaFN), Mandibular Canal Number (MaCN), Mental Foramen Number (MeFN), Mental Canal location (MeCl), Mental Canal Orientation (MeCO), and Mental Canal Length (MeCLe).
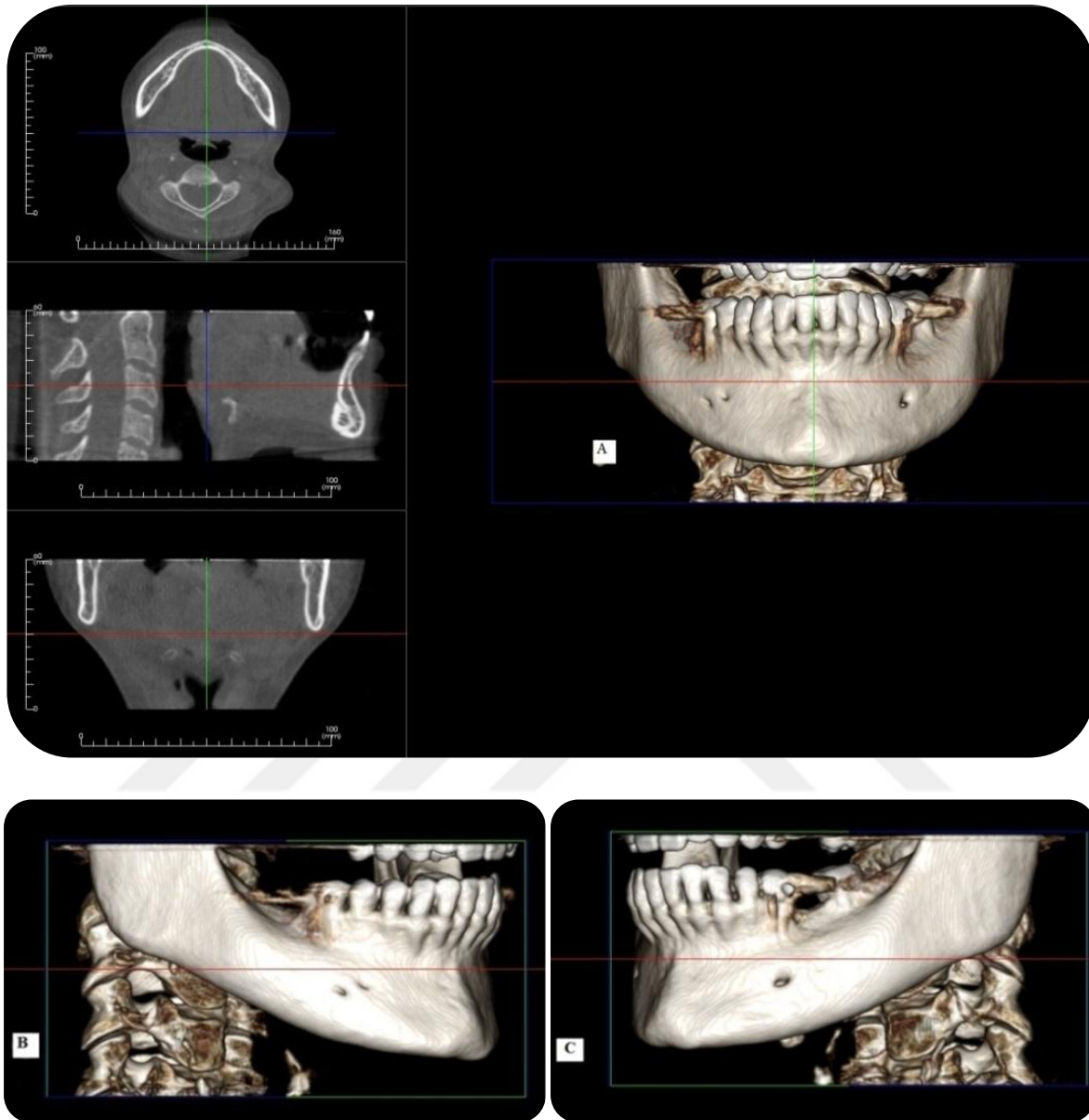
Figure 3.2. The reconstructed 3-D format in Superimposition option to detect Mental Canal Number (MeCN), showing 2 Mental Foramina on the right side: A: Front view, B: cropped Right 3\4 view and C: cropped Left 3\4 view (Images obtained with i-CAT® Model 17-19; CBCT Imaging Unit: InVivoDental5 Version 5.2 Anatomage, software): Dentomaxillofacial Radiology Department; Faculty of Dentistry- University of Yeditepe.
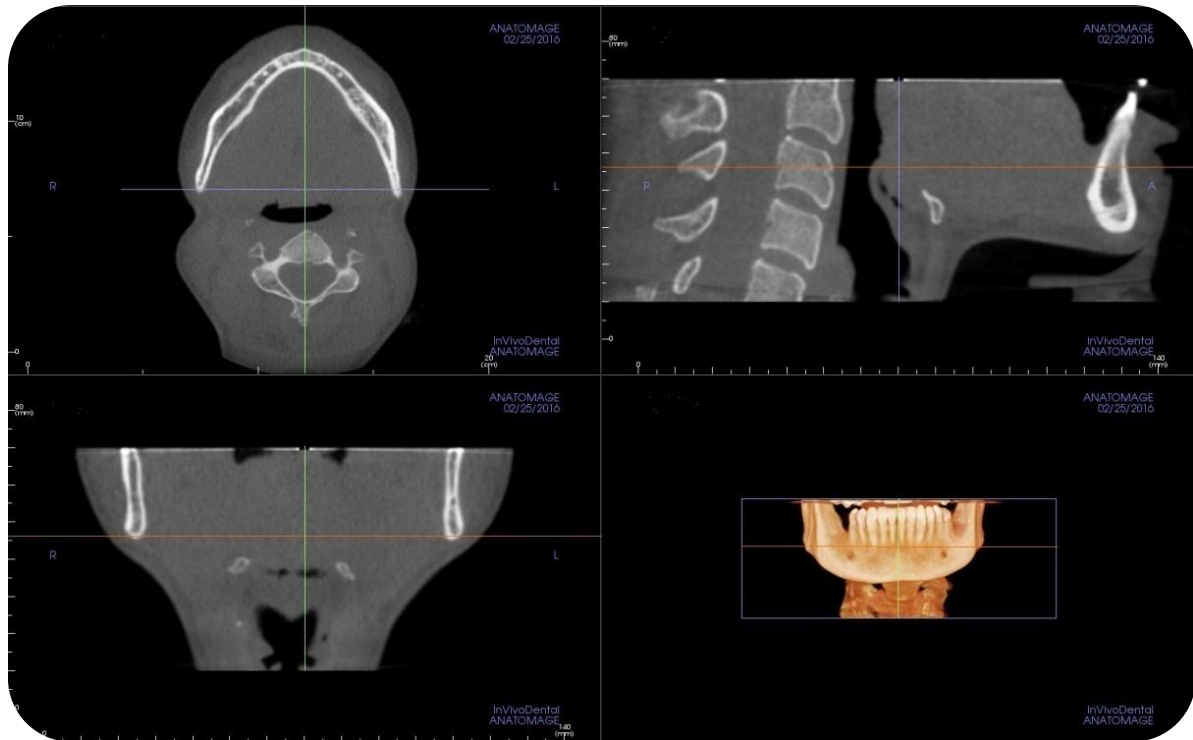
Figure 3.3. The **Section** Window illustrating the three plans; axial, sagittal, coronal on section, and the 3-D reconstructed image of the head in an upright position (Image obtained with i-CAT® Model 17-19; CBCT Imaging Unit: InVivoDental5 Version 5.2 Anatomage, software): Dentomaxillofacial Radiology Department; Faculty of Dentistry- University of Yeditepe.

5. Mental Canal Length (MeCLe) was then measured by placing the "**Distance Measurement**" tool along the two ends of the canal (Figure 3.4). The Mental Canal Angulation (MeCA) was calculated using "**Angle Measurement**" tool by adjusting the horizontal plan at the lower border of the mental canal and then placing the upper end of the tool at the canal opening, making the lower end coinciding with the horizontal plan at the end of the canal (Figure 3.5).

6. With the horizontal plan at the level of the Mental Canals, and by using the free hand movement of the cursor, the vertical plan was slowly dragged on the axial section towards the midline, and simultaneously on the sagittal section, the continuity of the Mental Canal (MeC) with the following structures was observed side by side carefully: Mandibular Incisive Canal (MIC), Lateral Lingual Vascular Canals' Number (LLVCsN), Lateral Lingual Vascular Canals' Orientation (LLVCsO), Lateral Lingual Vascular Canals' range between

teeth (LLVCsr), and Lateral Lingual Vascular Canals' Aspect (LLVCsA). In order to grade the visibility of the MIC, a three-point rating scale was used (refer to Appendix 2, No.8):

1) Good visibility
2) Moderate visibility
3) No visibility
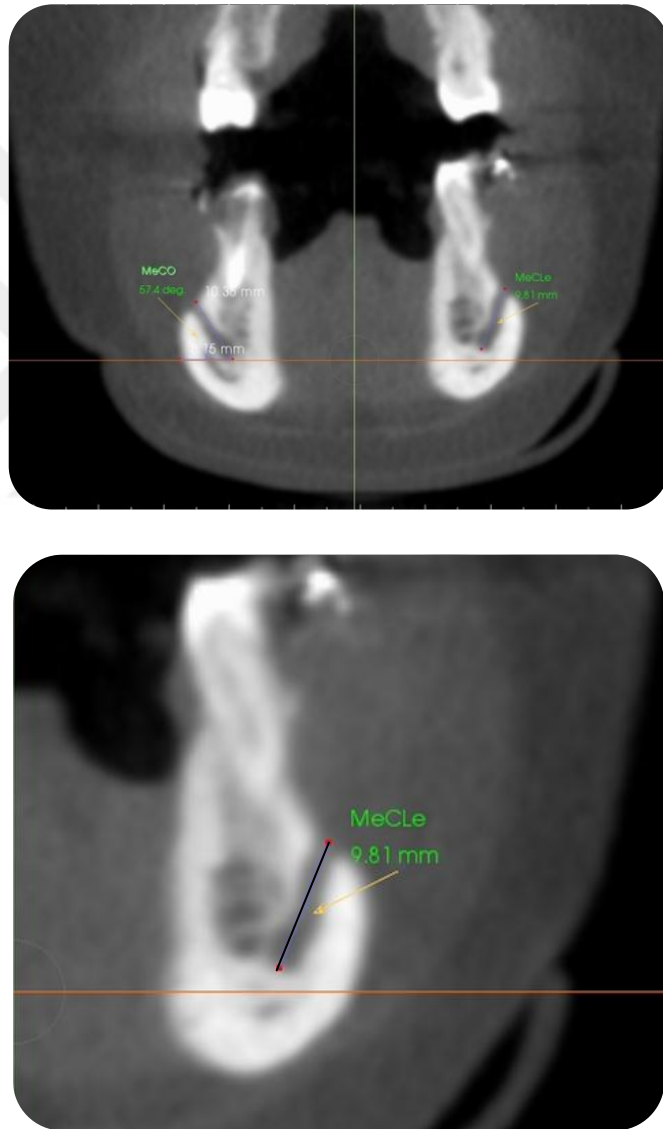
Figure 3.4. Above: coronal section showing the right and left Mental Canals. Below: cropped coronal section illustrating the Mental Canal Length between the two red dots (MeCLe= 9.81 mm) measurement, using "Distance Measurement" Tool (Images obtained with i-CAT® Model 17-19; CBCT Imaging Unit: InVivoDental5 Version 5.2 Anatomage, software): Dentomaxillofacial Radiology Department; Faculty of Dentistry- University of Yeditepe.
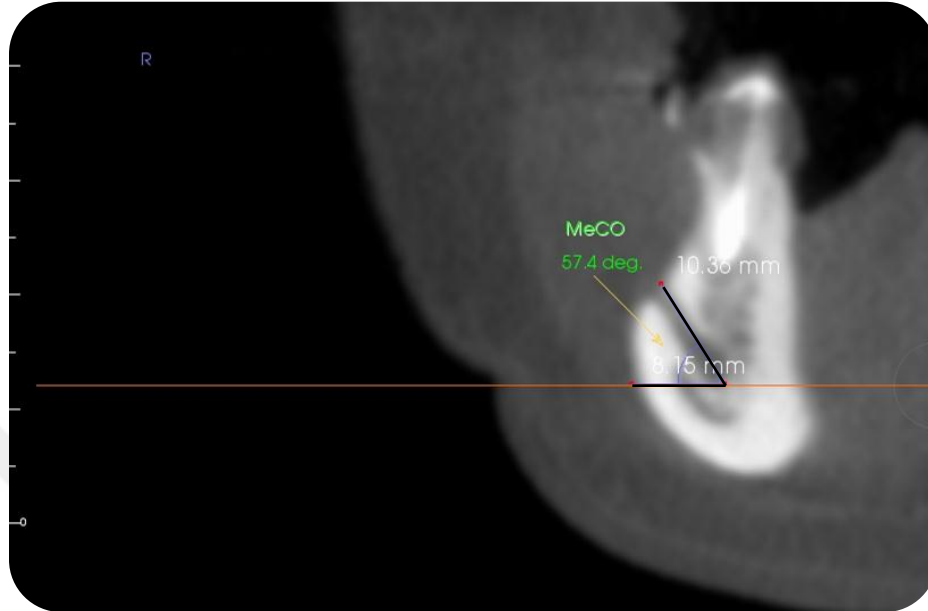
Figure 3.5. Cropped coronal section illustrating the superior Mental Canal Orientation (MeCO) and Mental Canal Angulation (MeCA= 57^0) measurement, using "Angle Measurement" tool; notice the lower end of the tool coinciding with the horizontal plan (Images obtained with i-CAT® Model 17-19; CBCT Imaging Unit: InVivoDental5 Version 5.2 Anatomage, software): Dentomaxillofacial Radiology Department; Faculty of Dentistry-University of Yeditepe.

7. The Lateral Lingual Vascular Canals' Length can be then measured by placing the "**Distance Measurement**" tool along the two ends of the canal, whereas the Lateral Lingual Vascular Canals' Height was measured in mm by means of "**Distance Measurement**" tool; The canal's height was measured from the highest point of the canal's upper border to the lower border of the mandible in proportion to the total height of the mandibular bone divided by 3 (Appendix 2, No.13) (Figure 3.6).

8. On the axial section, with the horizontal plan at the level of the Mental canals, and the vertical plan in the region of the midline, simultaneously, the cursor was dragged slowly, and the following structures were observed on the sagittal section to detect: the Lingual Canal Number (LCN), Lingual Canal Aspect (LCA), Lingual Canal location (LCl), Lingual Canal

in relation to Genial Tubercles (LCGT), Lingual Foramen Number (LFN), and Lingual Foramen Aspect (LFA).

Figure 3.6. Cropped Sagittal cross section illustrating the Lateral Lingual Vascular Canals' Length (LLVCsLe=5.42mm), Lateral Lingual Vascular Canals' Height (LLVCsH=8.23mm) measurements, using "Distance Measurement" tool perpendicular to the horizontal line adjusted as a tangent at the lower border of the mandible, and the total height of mandibular bone =29.05 mm; the total height of bone is divided into one thirds (29.05 ÷ 3= 9.68 mm) so each third= 9.68 mm, and the LLVCsH, which is 8.23 mm is less than one third, indicating that this LLVC is located in the lower one third (Images obtained with i-CAT® Model 17-19; CBCT Imaging Unit: InVivoDental5 Version 5.2 Anatomage, software): Dentomaxillofacial Radiology Department; Faculty of Dentistry-University of Yeditepe.

9. The Lingual Canal type or figure (LCfig) was matched with one of the 20 Lingual Canal figures detected in advance (refer to Results section: Figure 4.7). Whenever there was no match with the figures existing already, the observer was free to establish a new type and a new figure number. Lingual Canal Class (LC Class) was then determined according to the established 20 figures and to the LC Classification table (Appendix 2, No.25).

10. Next, the **Super Pano** option was selected and the panoramic section was constructed by means of both **Upper- lower Limit** and **Focal trough**.

11. Following that, the **Arch Section** option was selected, and the central focal trough plan was, slowly, moved forewords and backwards by the scrolling button on the mouse through the coronal sections on the panoramic window (Figure 3.7) (Figure 3.8) to observe the Nutrient Canals Number (NCsN) and Range (NCsR) between teeth (Figure 3.9), and to re-observe the complete continuous course of the IANC, enabling the clear detection of any canal variations and\or associations.

12. At the **Arch Section,** double checking the parameters was achieved by moving the cursor very slowly and gradually sliding the vertical plan from the right side to the left side on the panoramic window; starting from the right MaF, and ending at the left MaF, while observing the cross-sections of the anatomical structures on the 3 cross section windows available on the **Arch Section** option (Figure 3.8).

3.5. Repeatability and Reliability:

For test- retest reliability, and internal consistency, two caliberated experienced dentomaxillofacial radiologists (observers); first observer: El-Zuki Mervet (E-ZM), and second observer: Fişekçioğlu Erdoğan (FE), assessed the IANC CBCT images independently, implementing the above procedure. As for the intra-observer agreement analysis, all of the 200 images were examined and then re-examined by E-ZM to utilize the "Intra-class Correlation Coefficient (ρ)" after a one month period to minimize measurement bias. As for the inter-observer agreement analysis, 30 images were randomly selected and examined by FE to utilize "Fleiss's Kappa test (k)", and then the same 30 images were re-examined after a one month period to utilize the "Intra-class Correlation Coefficient (ρ)".
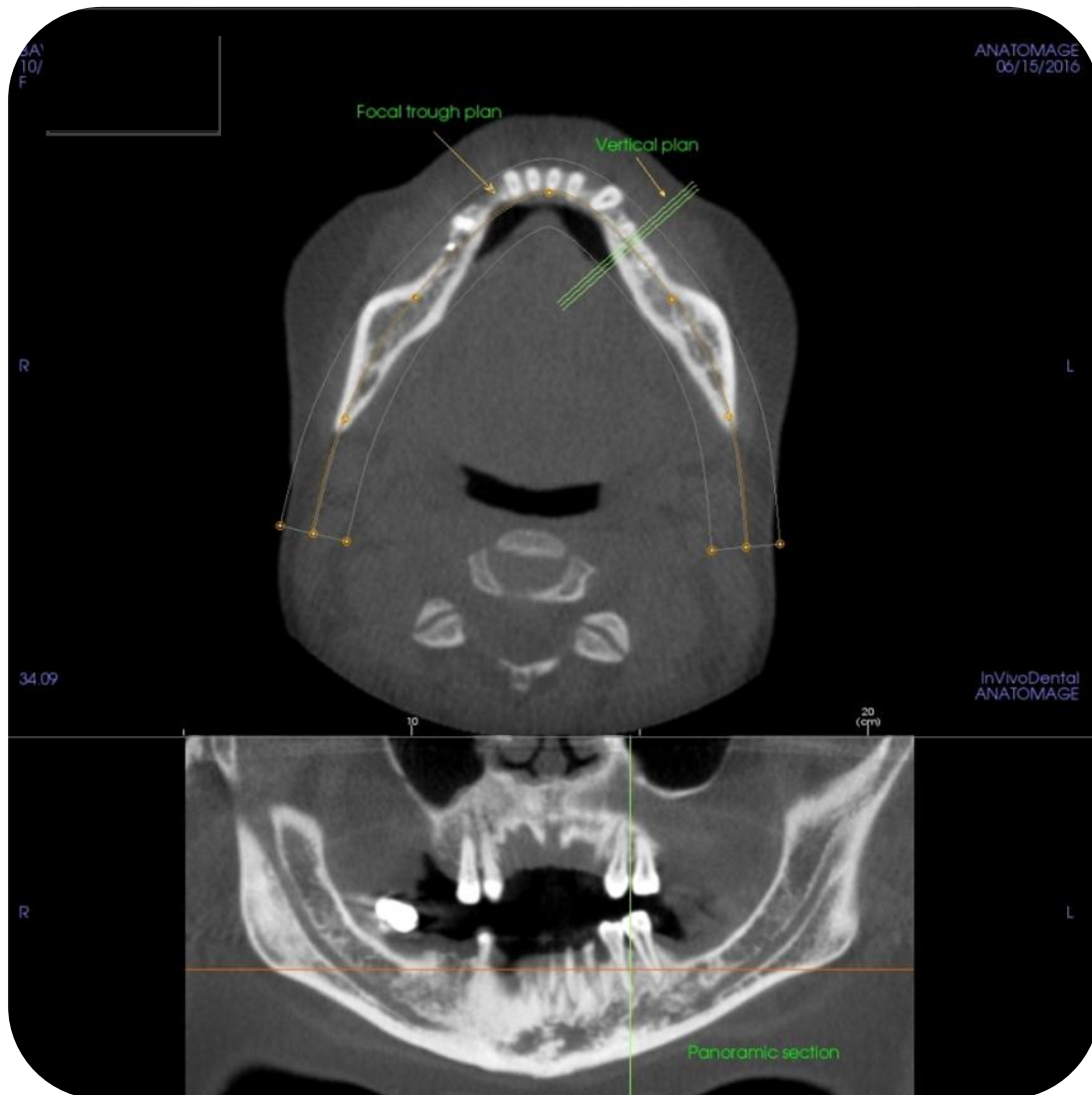
Figure 3.7. The Arch Section option (cropped); Above: The axial section showing the focal trough plan and vertical plan. Below: The panoramic section with the same plans in different orientation (Images obtained with i-CAT® Model 17-19; CBCT Imaging Unit: InVivoDental5 Version 5.2 Anatomage, software): Dentomaxillofacial Radiology Department; Faculty of Dentistry- University of Yeditepe.
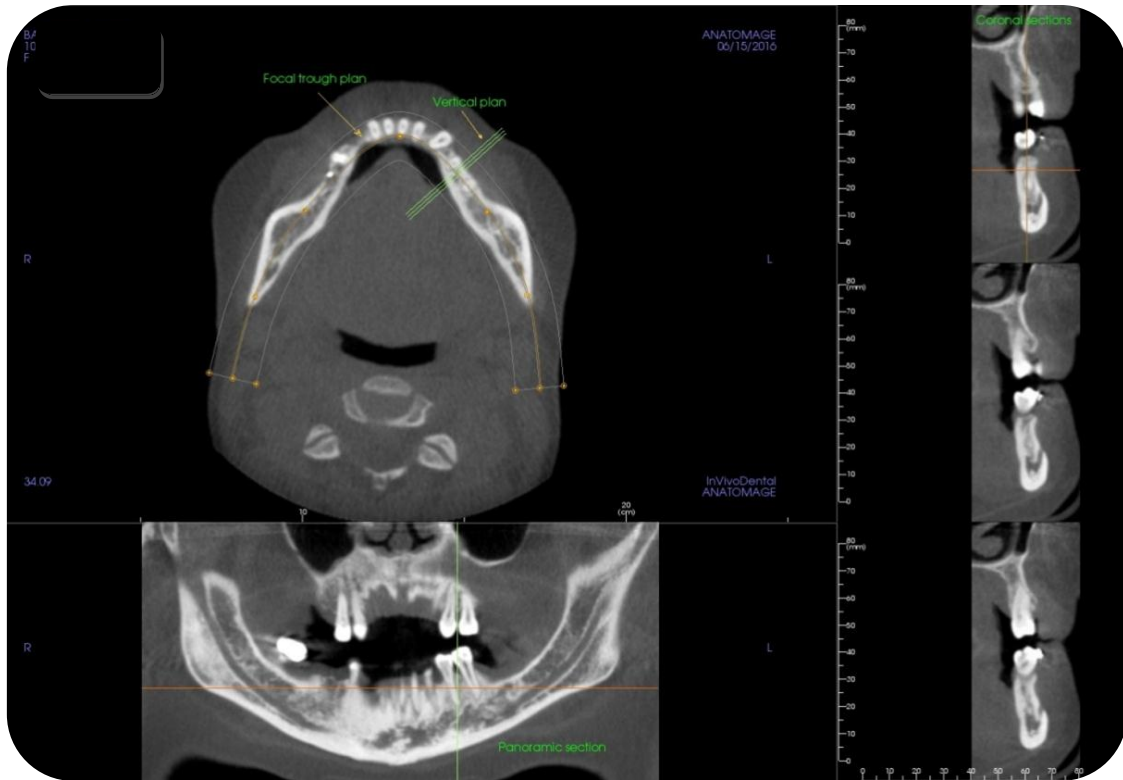
Figure 3.8. Arch Section option; Above: The axial section. Below: The panoramic section. Left side: 3 cross sectional windows (Images obtained with i-CAT® Model 17-19; CBCT Imaging Unit: InVivoDental5 Version 5.2 Anatomage, software): Deneomaxillofacial Radiology Department; Faculty of Dentistry- University of Yeditepe.
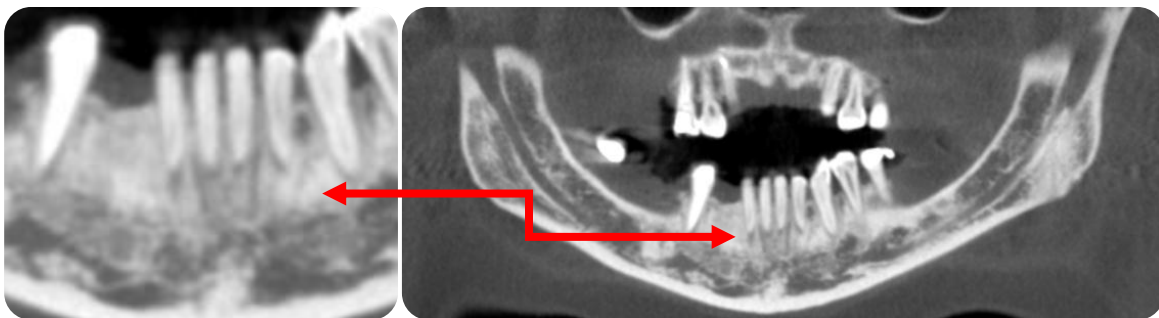
Figure 3.9. The Arch Section option (cropped); the panoramic section and the magnification of the lower anterior segment to reveal the Nutrient Canals (Red arrow), running vertically between the lower incisor teeth (Images obtained with i-CAT® Model 17-19; CBCT Imaging Unit: InVivoDental5 Version 5.2 Anatomage, software): Dentomaxillofacial Radiology Department; Faculty of Dentistry- University of Yeditepe.

4. RESULTS

4.1. Repeatability and Reliability of Results:

The sample consisted of 200 Turkish patients; referred to the Dentomaxillofacial Radiology Department in the Faculty of Dentistry -University of Yeditepe, for CBCT imaging intended for several clinical reasons. For 200 images, the intra-observer and inter-observer agreement repeatability was tested and the results revealed no statistically significant differences ($p>0.05$), indicating reliability. As regarding the "intra-observer" reliability "Infraclass Correlation Coefficient (ρ)" for the first observer E-ZM, observation reliability ranged between 0.831-1.000 for the 200 images. For the second observer FE, observation reliability ranged between 0.965-1.000 for the randomly selected 30 images. As regarding the "inter-observers' agreement analysis, Fleiss's Kappa test (k) was utilized; E-ZM and FE observation agreement for the same 30 images ranged between 0.864- 1.000. Values > 0.7 were accepted as reliable and the first measurements were calculated and utilized for statistical data analysis.

4.2. Statistical Analysis:

All statistical analyses were performed using Statistical Package for Social Science (IBM SPSS® Inc., version 24.0, Chicago, IIIinois, USA). No distinctions were made in regards to either age or gender. All measurements are presented as Mean (M) ± Standard Deviation (SD) values, and the threshold for statistical significance was set at ($p< 0.05$). For continuous variables, descriptive statistics were presented as M ± SD values. As for categorical variables, descriptive statistics were presented as frequencies and percentages.The Chi-square test (x^2 test) were used to investigate the differences in frequency, and the morphological characteristics of anatomic parameters between genders and between right and left sides. Mean differences between genders were investigated by two independent samples T-test.

4.2.1. Descriptive Statistics:

The sample in this study (n=200) consisted of 133 female (66.5%) and 67 male (33.5%) aged between 15 to 76 years; mean age 42.68 years. The frequency of one mandibular foramen

in both genders at right and left sides was 200 (100%). The frequency of a solitary Mental Foramen on the right side was 194 (97%), and 196 (98%) on the left side, as the frequency of two mental foramina on the right side was 6 (3%), and 4 (2%) on the left side. As regarding the Mandibular Canal: the frequencies of a single canal were 181 (90.5%) and 186 (93%) on the right and left sides respectively; the frequency of BMC in general was 18 (9%) on the right and 14 (7%) on the left, and the frequency of only one (0.5%) TMC on the right side (Table 4.1). In this study, out of the five types of BMC (Table 2.1), only two types were detected; 13 (6.5%) Dental BMC, and 19 (9.5%) (Table 4.2) RMC types are displayed according to Von Arx et al. (89) classification (Figure 2.10) as frequency and percentage (Table 4.3).

Table 4.1. Frequency and percentage of Mandibular Canal Number (MaCN) on right, and left sides of the mandible.

MaCN	Right		Left	
	Frequency	**(%)**	**Frequency**	**(%)**
1 Canal	181	90.5	186	93
2 Canals	18	9	14	7
3 Canals	1	0.5	0	0
Total	200	100	200	100

Table 4.2. Frequency and percentage of Bifid Mandibular Canals (BMC) types on right and left sides.

BMC	Right		Left	
	Frequency	**(%)**	**Frequency**	**(%)**
Dental BMC	8	44	5	36
Retromolar BMC:	10	56	9	64
Forward BMC	-	-	-	-
Bucco-lingual BMC	-	-	-	-
Superior BMC	-	-	-	-
Total	18	100	14	100

48

Table 4.3. Distribution of the RMC (n=19) according to type: Type A1; Verticle course, Type A2; Vertical course with horizontal branch, Type B1; Curved course, Type B2; Curved with horizontal branch, and Type C; Horizontal course.

Type	Frequency	(%)
A1	7	36.8
A2	-	-
B1	10	52.6
B2	1	5.3
C	1	5.3
Total	19	100

As regarding the Mental Canal or Anterior Loop location on coronal sections: 139 (69.5%) were simultaneously symmetrical, 47 (23.5%) of the right side loops were located in close proximity to the midline; mesial to the left side loops, and 14 (7%) of the right side loops were located far from the midline; distal to the left side loops. On the right side, 195 (97.5%) of the anterior loops had a superior orientation, and 5 (2.5%) had a horizontal orientation. The superior and horizontal orientations of the AL on the left side were 189 (94.5%) and 11 (5.5%) respectively. There was no AL with an inferior direction.

As regarding the Mental Canal Angulations in general, the minimum and maximum angles ranged from (0^0 to 83^0) with mean of 41.5^0. On the right side: 5 (2.5%) of the angles were equal to zero degree, 96 (48%) were more than zero and less than 45 degrees, and 99 (49.5%) were more than 45 degrees and less than 90 degrees. As regarding the Mental Canal Angulation on the left side: 11 (5.5%) were equal to zero degree, 65 (32.5%) were more than zero and less than 45 degrees, and 124 (62%) were more than 45 degrees and less than 90 degrees (Table 4.4).

Table 4.4 The frequency and percentage of Mental Canal Angulation (MeCA) on both right and left sides.

MeCA	Right		Left	
	Frequency	**(%)**	**Frequency**	**(%)**
Horizontal:				
Zero^0	5	2.5	11	5.5
Superior:				
0^0>45^0	96	48	65	32.5
Superior:				
45^0>90^0	99	49.5	124	62
Total	200	100	200	100

The frequency of the visibility of the Mandibular Incisive Canal was the same on both right and left sides; 200 (100%), with 134 (67%) images of good visibility on the right and 133 (66.5%) images of good visibility on the left. Frequency of moderate visibility of MIC on the right and left sides were 66 (33%) and 67 (33.5%) correspondingly.

As regarding Lateral Lingual Vascular Canals, there were no lateral canals on the right side in 109 (54.5%) of the images, and no lateral canals in 111 (55.5%) of the images on the left. One lateral canal was detected on the right side of 85 (42.5%) of the images and 81 (40.5%) on the left side. Two lateral canals were seen on the right side of 6 (3%) of the images, and 8 (4%) on the left side (Table 4.5).

Table 4.5. The frequency and percentage of the Lateral Lingual Vascular Canals Number (LLVCsN) on both right and left sides.

LLVCsN	Right		Left	
	Frequency	**(%)**	**Frequency**	**(%)**
No canals	109	54.5	111	55.5
1 Canal	85	42.5	81	40.5
2 Canals	6	3	8	4
Total	200	100	200	100

As regarding the LLVCs frequency unilaterally, there was one unilateral canal in 54 (48.2%) of the cases, and two unilateral canals in 5 (4.5%) of the cases. For bilateral canals, there was one bilateral canal in 46 (41%) of the cases, two bilateral canals in only one case (1%), one canal on one side and two canals on the other side in 6 (5.3%) of the cases (Table 4.6). The general frequency of bilateral LLVCs in the current study was 53 (47.35%), and 59 (52.7%) of unilateral LLVCs.

Table 4.6 The frequency and percentage of Lateral Lingual Vascular Canals Number (LLVCsN) Types: unilaterally and bilaterally.

LLVCs Types	Number of canals	Frequency	%
Unilateral	1 canal	54	48.2
	2 canals	5	4.5
	1 canal	46	41
Bilateral	2 canals	1	1
	1 canal & 2 canals	6	5.3
Total		112 (56%)	100

The orientation of the first lateral canal (when there was one in number) varied from 12 (6%) superior, 23 (11.5%) horizontal and 56 (28%) inferior on the right side. The orientation of the first lateral canal (when there was one in number) varied from 10 (5%) superior, 21 (10.5%) horizontal and 58 (29%) inferior on the left side. The orientation of the second lateral canal (when there were two in numbers) varied from 2 (1%) superior, 1 (0.5%) horizontal and 3 (1.5%) inferior on the right side. The orientation of the second lateral canal (when there were two in numbers) varied from 1 (0.5%) superior, 4 (2%) horizontal and 3 (1.5%) inferior on the left side.

As regarding the location of lateral canals; on the right side, the location of 8 (4%) of the first lateral canal (when there was one in number) ranged between teeth number 41 and 42, 12 (6%) ranged between teeth number 42 and 43, 60 (30%) ranged between teeth number 43 and 44, and 10 (5%) ranged between teeth number 44 and 45 (Figure 4.1). Whereas, the location of 2 (1%) of the second lateral canal (when there were two in number) ranged between teeth number 41 and 42, 1 (0.5%) ranged between teeth number 42 and 43, and 2 (1%) ranged between teeth number 43 and 44 (Figure 4.2). As regarding the left side, the location of 12 (6%) of the first lateral canal (when there was one in number) ranged between teeth number 31 and 32, 25 (12.5%) ranged between teeth number 32 and 33, 45 (22.5%) ranged between teeth number 33 and 34, and 5 (2.5%) ranged between teeth number 34 and 35 (Figure 4.1). Whereas, the location of 2 (1%) of the second lateral canal (when there were two in number) ranged between teeth number 31 and 32, 3 (1.5%) ranged between teeth number 32 and 33, and 3 (1.5%) ranged between teeth number 33 and 34. There was one lateral canal (0.5%) slightly to the right of the midline, and 2 (1%) slightly to the left of the midline between teeth number 31 and 41 when there was one in number (Figure 4.1). Whereas, there was one lateral canal (0.5%) at the midline between teeth number 31 and 41 when there were two canals on one or both sides (Figure 4.2).
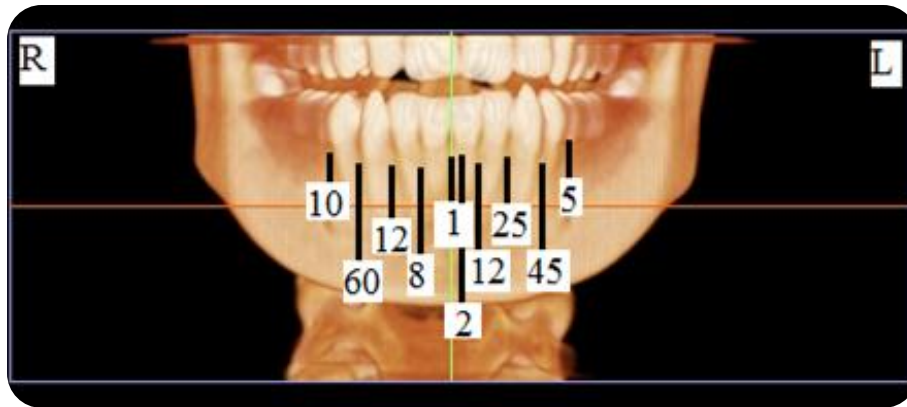
Figure 4.1. The frequency of the location of Lateral Lingual Vascular Canals ranging between mandibular teeth (LLVCsr) when there was one canal on one or both sides (Images obtained with i-CAT® Model 17-19; CBCT Imaging Unit: InVivoDental5 Version 5.2 Anatomage, software): Dentomaxillofacial Radiology Department; Faculty of Dentistry, University of Yeditepe.


Figure 4.2. The frequency of the location of Lateral Lingual Vascular Canals ranging between mandibular teeth (LLVCsr) when there were two canals on one or both sides (Images obtained with i-CAT® Model 17-19; CBCT Imaging Unit: InVivoDental5 Version 5.2 Anatomage, software): Dentomaxillofacial Radiology Department; Faculty of Dentistry, University of Yeditepe.

As regarding the LLVCsH on the right side, 20 (10%) of the first canals (when there was one canal on one or both sides) were present in the upper one third of the mandibular height at that level (the level where the lateral lingual vascular canal was detected), 70 (35%) were present in the middle one third of the mandibular height at that level, and 1 (0.5%) was present in the

lower one third of the mandibular height at that level (Figure 4.3). When there were two canals on the right side, 4 (2%) were present in the upper one third, 2 (1%) were present in the middle one third of the mandibular height at that level, and no canals were present in the lower one third of the mandibular height at that level (Figure 4.4). As regarding the LLVCsH on the left side, 20 (10%) were present in the upper one third, 68 (34%) were present in the middle one third of the mandibular height at that level, and none in the lower one third of the mandibular height at that level (Figure 4.3). When there were two canals on the left side, 3 (1.5%) were present in the upper one third, 5 (2.5%) were present in the middle one third of the mandibular height at that level, and none in the lower one third of the mandibular height at that level (Figure 4.4).

Figure 4.3. The frequency of the Lateral Lingual Vascular Canals Heights, ranging between upper 1\3, middle 1\3, and lower 1\3 of the mandibular height, when there was one canal on one or both sides (Images obtained with i-CAT® Model 17-19; CBCT Imaging Unit: InVivoDental5 Version 5.2 Anatomage, software): Dentomaxillofacial Radiology Department; Faculty of Dentistry, University of Yeditepe.

Figure 4.4. The frequency of the Lateral Lingual Vascular Canals' Heights, ranging between upper 1\3, middle 1\3, and lower 1\3 of the mandibular height, when there were two canals on one or both sides (Images obtained with i-CAT® Model 17-19; CBCT Imaging Unit: InVivoDental5 Version 5.2 Anatomage, software): Dentomaxillofacial Radiology Department; Faculty of Dentistry, University of Yeditepe.

The frequency of the first Lateral Lingual Vascular Canals Aspect (when there was one canal in number, either on one or both sides) were 87 (43.5%) canals opening on the lingual aspect, and 4 (2%) opening on the labial aspect for the right side. For the same right side (when there were two canals in number, either on one or both sides), there were 5 (2.5%) canals opening on the lingual aspect, and 1 (0.5%) opening on the labial aspect. On the left side, the frequency of the first LLVCsA (when there was one canal in number, either on one or both sides) were 85 (42.5%) canals opening on the lingual aspect, and 3 (1.5%) opening on the labial aspect. For the same left side (when there were two canals in number, either on one or both sides), there were 5 (2.5%) canals opening on the lingual aspect, and 1 (0.5%) opening on the labial aspect.

As regarding the frequency of Nutrient Canals (NCs), the canals were detected in 192 (96%) of the cases. When detected, the number of bilateral canals was variable; the minimum was at least one NC, and the maximum number was 4 canals on each side. However, there were 8 (4%) cases of unilateral NCs. As regarding their bilateral symmetrical range between teeth: total=140 (73%): 2 (1%) of the NCs were detected between the lower first incisors, 22 (11.5%) between the lower second incisors, 62 (32.2%) between the lower canines, 40 (21%) between the lower first premolars, and 14 (7.3%) between the lower second premolars. The other 52 (27%) cases of the detected NCs were asymmetric.

As regarding the Lingual Canals Number, 3 (1.5%) of the images showed no lingual canals, 92 (46%) had only one, 100 (50%) had two canals, and 5 (2.5%) had three canals (Figure 4.5).

According to their location in relation to Genial Tubercles (GT); 63 (31.5%) were above GT, 27(13.5%) were below GT, 5 (2.5%) through or at GT, 77(38%) were above and below GT, 5 (2.5%) were above, below and through GT, 15 (7.5%) were above and through GT, 5 (2.5%) were below and through GT, and 3 (1.5%) showed no lingual canals (Figure 4.6).

As regarding the Lingual Canals types, the frequency and percentage were assigned according to each of the 20 figures (Figure 4.7). When the lingual canal aspect was concerned, 193 (96.5%) of the images had a lingual canal opening on the lingual aspect of the mandible, 1 (0.5%) had a lingual canal opening on the labial aspect, and 3 (1.5%) had canals opening on both lingual and labial aspects at the same time. As regarding the location of the lingual canals in relation to the midline when they were present, 120 (60%) of the canals were at the midline, 42 (21%) were on the right to the midline, and 35 (17.5%) were left to the midline (Figure 4.8).
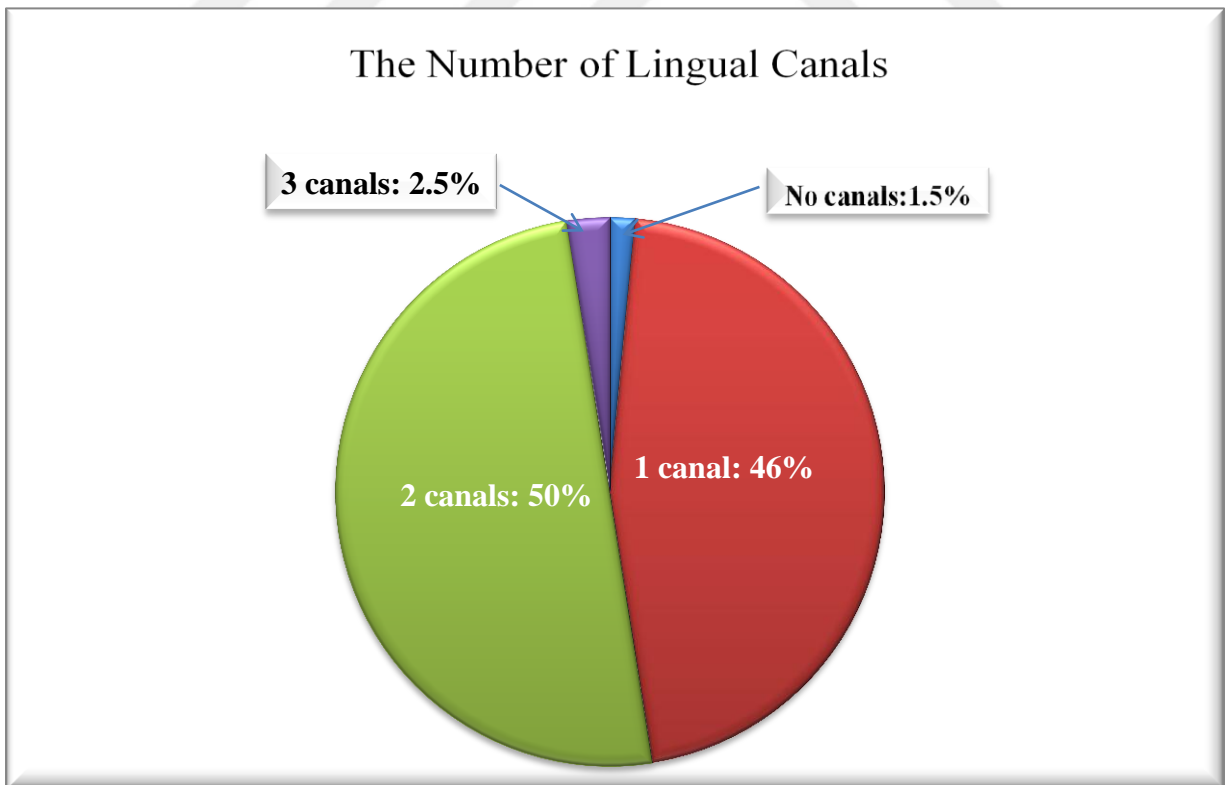
Figure 4.5. A pie chart showing the percentage of Lingual Canals Number in 200 images.

The Location of Lingual Canals

- Above 31.5%
- Below 13.5%
- Through 2.5%
- Above & below 38%
- Above, below & through 2.5%
- Above & through 7.5%
- Below & through 2.5%
- No LC 1.5%
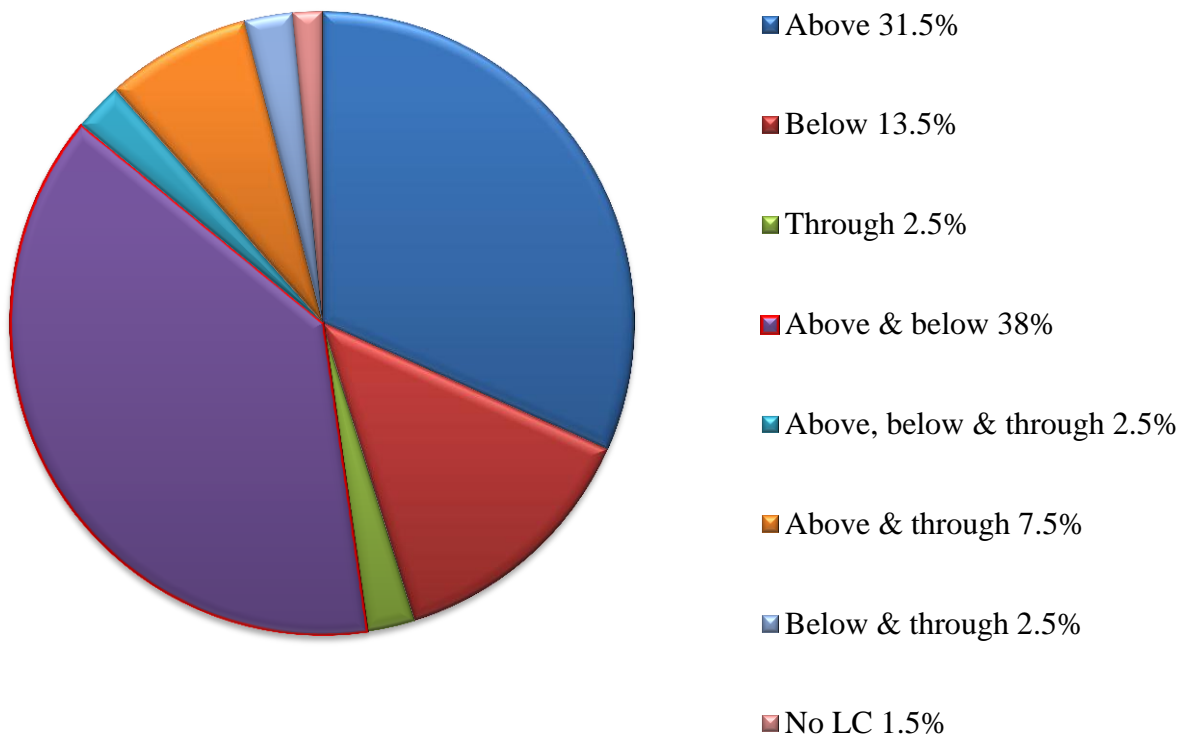
Figure 4.6. A pie chart, showing the percentage of the Lingual Canals Location in relation to Genail tubercles in 200 images.
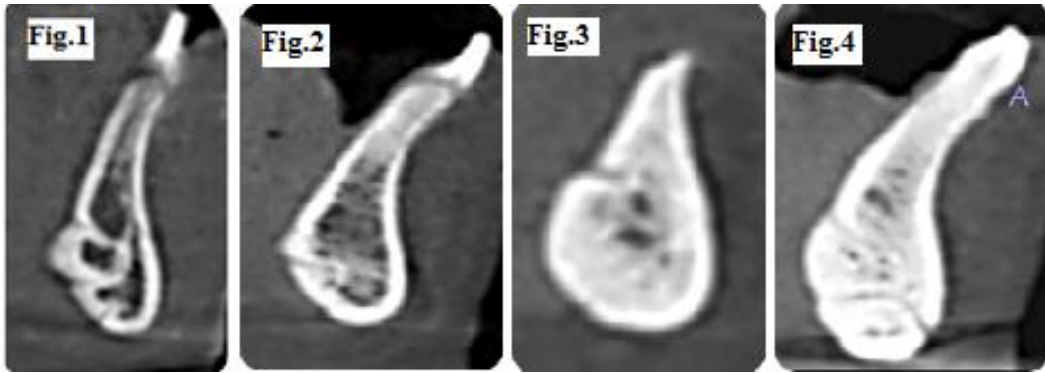
Fig. 1: LC No.: 3 Above (Superior) At (Horizontal) Below (Inferior)	Fig. 2: LC No.: 1 At (Superior)	Fig. 3: LC No.: 1 Above (Horizontal)	Fig.:4: LC No.: 2 Above (Superior) Below (Inferior)*
Freq.: 5 (2.5%)	Freq.: 2 (1%)	Freq.: 3 (1.5%)	Freq.: 1 (0.5%)
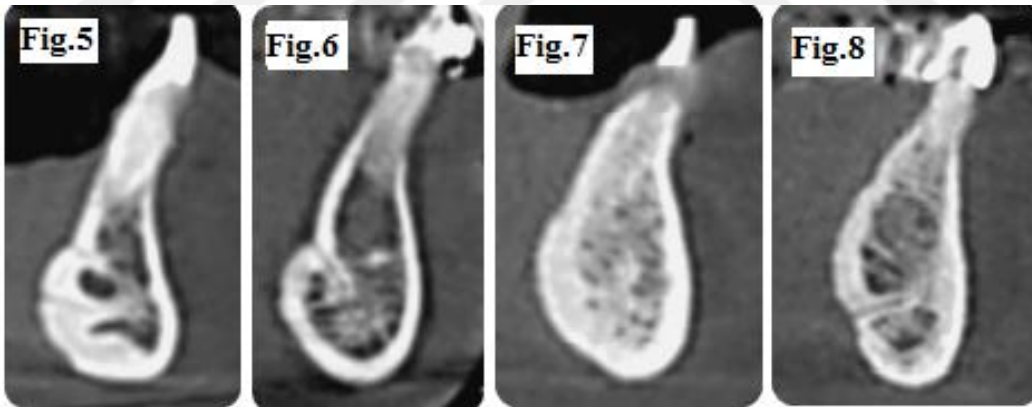
Fig. 5: LC No.: 2 Above (Superior) At (Superior)	Fig. 6: LC No.: 1 Above (Superior)	Fig. 7: LC No.: 0	Fig.8: LC No.: 1 Below (Inferior)
Freq.: 9 (4.5%)	Freq.: 58 (29%)	Freq.: 3 (1.5%)	Freq.: 23 (11.5%)

Fig. 9: LC No.: 2	Fig. 10: LC No.: 2	Fig. 11: LC No.: 1	Fig.12: LC No.: 2
Above (Superior) Below (Inferior)	Above (Superior) Below(Horizontal)	At (Horizontal)	Above (Superior) Below (Superior)
Freq.: **60 (30%)**	Freq.: **12 (6%)**	Freq.: **2 (1%)**	Freq.: **2 (1%)**
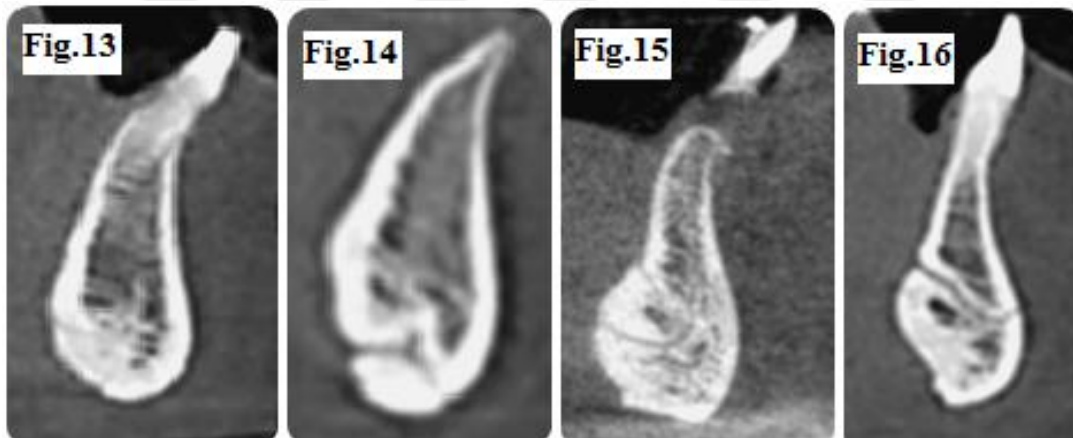
Fig. 13: LC No.: 2	Fig.14: LC No.: 2	Fig.15: LC No.: 2	Fig.16: LC No.: 1
At (Superior) Below (Inferior)	Below(Horizontal) Below(Inferior)*	Above (Superior) At (Superior)	Above (Superior)*
Freq.: **4 (2%)**	Freq.: **1 (0.5%)**	Freq.: **6 (3%)**	Freq.: **2 (1%)**
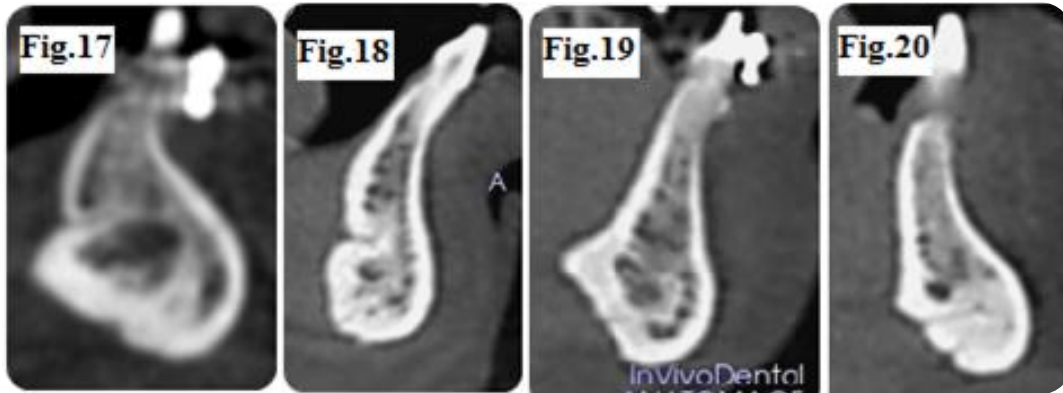
Fig. 17: LC No.: 2 Above(Inferior) Below (Inferior)	Fig.18: LC No.: 2 Above (Horizontal) Below(Inferior)	Fig.19: LC No.: 1 Below(Horizontal)	Fig.20: LC No.: 2 Below (Inferior) Below (Inferior)
Freq.: 1 (0.5%)	Freq.: 1 (0.5%)	Freq.: 3 (1.5%)	Freq.: 2 (1%)

Figure4.7. The frequency and percentage of the Lingual Canal types assigned as 20 figures. Each figure is described according to the LC number, LC location in relation to GT (above\At\below), and the direction or orientation of the canal (superior\horizontal\inferior). * The canal continues to the labial aspect (Images obtained with i-CAT® Model 17-19; CBCT Imaging Unit: InVivoDental5 Version 5.2 Anatomage, software): Dentomaxillofacial Radiology Department; Faculty of Dentistry, University of Yeditepe.
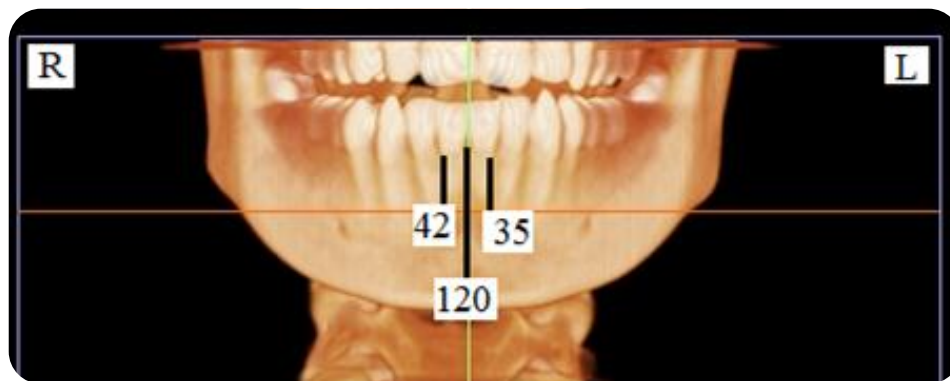
Figure 4.8. The frequency and percentage of Lingual Canal location in relation to the midline in 200 images (Note that there were no lingual canals detected in 3 images). (Images obtained with i-CAT® Model 17-19; CBCT Imaging Unit: InVivoDental5 Version 5.2 Anatomage, software): Dentomaxillofacial Radiology Department; Faculty of Dentistry, University of Yeditepe.

As regarding the Lingual Foramen, the result analysis showed a frequency of 3 (1.5%) images with no LF, 93 (46.5%) with one foramen, 99 (49.5%) with two foramina, and 5 (2.5%) with three foramina. The frequency of the aspects on which the LF opened, when they were present, was as follows: 194 (97%) opened on the lingual aspect and 3 (1.5%) opened on both lingual and labial sides.

4.2.2. Arithmetic Means and Standard Deviations of the Measurements:

As regarding the age, for 200 images M = 42.68, SD =16.05542, and the p-value =0.094. As for the gender (female, male, and both female and male or total), the M, SD, and p-value for the MaF and MaCs number for right and left sides were deliberated (Table 4.7).

Table 4.7. Mean (M), Standard Deviation (SD), and p-value (p) for Mandibular Foramen (MaFN) and canal (MaCN) numbers for right (R) and left (L) sides in females and males separately, and together.

Parameter	Female		Male		Total		
	n=133		n=67		n=200		
	M	*SD*	*M*	*SD*	*M*	*SD*	*p*
MaFNR	1.000	0.000	1.000	0.000	1.000	0.000	-*
MaFNL	1.000	0.000	1.000	0.000	1.000	0.000	-*
MaCNR	1.248	0.772	1.104	0.464	1.200	0.687	0.182
MaCNL	1.188	0.687	1.104	0.526	1.160	0.637	0.609
* No statistics are computed, because MaFN is a constant.							

As regarding the gender: M, SD, and p-value for the Mental Foramen Number and Mental Canal: length, location, orientation, and aspect for both sides were deliberated (Table 4.8).

Table 4.8. Mean (M), Standard Deviation (SD), and p-value (*p*) for mental foramen number (MeFN) and Mental Canal; length (MeCLe), location (MeCl), orientation (MeCO), and angulation (MeCA) on right (R) and left (L) sides in females and males separately, and together. Note: MaCA ranged from 0^0 to 83^0.

Parameter	Female		Male		Total		
	n=133		n=67		n=200		
	M	*SD*	*M*	*SD*	*M*	*SD*	*p*
MeFNR	1.037	0.190	1.014	0.122	1.030	0.171	0.666
MeFNL	1.022	0.149	1.014	0.122	1.020	0.140	1.000
MeCLeR	6.119	1.573	7.466	1.742	6.570	1.747	0.000*
MeCLeL	6.041	1.655	6.705	1.417	6.264	1.607	0.006*
MeClR	1.368	0.621	1.388	0.601	1.375	0.613	0.699
MeClL	1.511	0.831	1.597	0.888	1.540	0.849	0.699
MeCOR	1.015	0.122	1.044	0.208	1.025	0.156	0.337
MeCOL	1.060	0.238	1.044	0.208	1.055	0.228	0.754
MeCAR	46.278	11.372	48.417	15.597	46.995	12.942	0.321
MeCAL	47.639	16.341	51.880	16.768	49.060	16.565	0.087

*P < 0.05 is accepted as statistically significant.

As regarding the gender: M, SD, and *p*-value for the Mandibular Incisive Canal visibility, on right and left sides, were deliberated (Table 4.9).

Table 4.9. Mean (M), Standard Deviation (SD), and p-value (*p*) for Mandibular Incisive Canal (MIC) visibility on right (R) and left (L) sides in females and males separately, and together.

Parameter	Female		Male		Total		
	n=133		n=67		n=200		
	M	*SD*	*M*	*SD*	*M*	*SD*	*p*
MIC(R)	1.315	0.466	1.358	0.483	1.330	0.471	0.633
MIC(L)	1.323	0.469	1.358	0.483	1.335	0.473	0.622

*P < 0.05 is accepted as statistically significant

As regarding the gender: M, SD, and p-value for the lateral lingual vascular canals'; number (LLVCN), length (LLVCLe), orientation (LLVCO), range (LLVCr), height (LLVCH), and aspect (LLVCA) (when there was one canal 'a', or two canals 'b' on one or both sides) on right (R) and left (L) sides in females and males separately, and together for both right and left sides were deliberated (Table 4.10).

Table 4.10. Mean (M), Standard Deviation (SD), and p-value (*p*) for Lateral Lingual Vascular Canals (LLVCs).

Parameter	Female		Male		Total		
	n=133		n=67		n=200		
	M	*SD*	*M*	*SD*	*M*	*SD*	*p*
LLVCNR	0.428	0.540	0.597	0.578	0.485	0.557	0.129
LLVCNL	0.458	0.557	0.537	0.611	0.485	0.575	0.545
LLVCLeRa	2.108	2.671	2.893	2.742	2.371	2.713	0.053
LLVCLeRb	0.105	0.785	0.181	0.857	0.131	0.808	0.535
LLVCLeLa	2.297	2.807	2.625	2.890	2.407	2.832	0.440
LLVCLeLb	0.151	0.884	0.247	1.014	0.183	0.928	0.448
LLVCORa	0.985	1.279	1.417	1.394	1.130	1.331	0.076
LLVCORb	0.030	0.211	0.134	0.625	0.065	0.401	0.058
LLVCOLa	1.075	1.329	1.238	1.382	1.130	1.346	0.859
LLVCOLb	0.060	0.364	0.149	0.609	0.090	0.461	0.473
LLVCrRa	1.142	1.436	1.656	1.934	1.315	1.633	0.002*
LLVCrRb	0.097	0.960	0.119	0.564	0.105	0.847	0.112
LLVCrLa	1.157	1.770	1.268	1.452	1.195	1.667	0.252
LLVCrLb	0.060	0.364	0.134	0.574	0.085	0.445	0.622
LLVCHRa	1.142	1.409	1.522	1.428	1.270	1.423	0.086
LLVCHRb	0.045	0.298	0.119	0.564	0.070	0.407	0.127
LLVCHLa	1.180	1.397	1.298	1.435	1.220	1.407	0.768
LLVCHLb	0.082	0.477	0.149	0.609	0.105	0.524	0.446
LLVCARa	0.421	0.525	0.582	0.554	0.475	0.539	0.135
LLVCARb	0.030	0.211	0.044	0.208	0.035	0.209	0.349
LLVCALa	0.436	0.527	0.492	0.532	0.455	0.528	0.744
LLVCALb	0.030	0.211	0.044	0.208	0.035	0.209	0.349

*P < 0.05 is accepted as statistically significant

As regarding the gender: M, SD, and p-value for the Lingual Canals'; number, aspect , location in relation to the midline, location in relation to the genial tubercles, and in relation to the 20 figures allocated by the first observer were deliberated (Table 4.11).

Table 4.11. Mean (M), Standard Deviation (SD), and p-value (*p*) for Lingual Canals'; number (LCN), aspect (LCA), location (LCl), location in relation to Genail Tubercle (LCGT), and in relation to the 20 allocated figures (LCfig) on right (R) and left (L) sides in females and males separately, and together.

Parameter	Female		Male		Total		
	n=133		n=67		n=200		
	M	*SD*	*M*	*SD*	*M*	*SD*	*p*
LCN	1.488	0.572	1.626	0.573	1.535	0.574	0.376
LCA	1.000	0.213	1.059	0.384	1.020	0.282	0.317
LCI	1.533	0.783	1.567	0.820	1.545	0.794	0.954
LCGT	2.744	1.760	3.358	1.702	2.950	1.761	0.020*
LCfig	8.037	3.432	8.611	3.237	8.230	3.371	0.256

*P < 0.05 is accepted as statistically significant.

As regarding the gender: M, SD, and p-value for the Lingual Foramina; number, aspect, and location were deliberated (Table 4.12).

Table 4.12. Mean (M), Standard Deviation (SD), and p-value (*p*) for Lingual Foramina; Number (LFN), Aspect (LFA), and location (LFl) on both right (R) and left (L) sides in females and males separately, and together.

Parameter	Female		Male		Total		
	n=133		n=67		n=200		
	M	*SD*	*M*	*SD*	*M*	*SD*	*p*
LFN	1.473	0.571	1.641	0.569	1.530	0.575	0.196
LFA	1.000	0.213	1.044	0.366	1.015	0.274	0.471
LFl	1.548	0.792	1.641	0.847	1.580	0.810	0.859

*P < 0.05 is accepted as statistically significant

4.2.3. Comparison of Measurements in Terms of Gender:

4.2.3.1 Group Statistics:

For continuous type of data, the arithmetic means of the measurements were compared in terms of gender. For group statistics, data is summerized as tables in regards to age (Table 4.13), Mental Canal Length (Table 4.14), Lateral Lingual Vascular Canals' Length (Table 4.15), Lingual Canal in relation to genial tubercles, and in accordance to types assigned in the 20 figures (Table 4.16).

Table 4.13. Group statistics for Age.

Parameter	Gender	*N*	*M*	*SD*	*Std. Error Mean*
Age	Female	133	44.0301	15.84199	1.37368
	Male	67	40.0000	16.25833	1.98627

Table 4.14. Group statistics for Mental Canal Length (MeCLe) and Angulation (MeCA) for bothe right (R) and left (L) sides.

Parameter	Gender	*N*	*M*	*SD*	*Std. Error Mean*
MeCLe(R)	Female	133	6.1194	1.57309	0.13640
	Male	67	7.4666	1.74229	0.21285
MeCLe(L)	Female	133	6.0415	1.65559	0.14356
	Male	67	6.7055	1.41754	0.17318
MeCA(R)	Female	133	46.2782	11.37272	0.98614
	Male	67	48.4179	15.59735	1.90552
MeCA(L)	Female	133	47.6391	16.34168	1.41700
	Male	67	51.8806	16.76895	2.04865

Table 4.15. Group statistics for Lateral Lingual Vascular Canals' Length for both right and left sides (when there was one canal 'LLVCLeRa\ LLVCLeLa' or two canals 'LLVCLeRb\ LLVCLeLb' on one or both sides).

Parameter	Gender	*N*	*M*	*SD*	*Std. Error Mean*
LLVCLe(Ra)	**Female**	133	2.1087	2.67106	0.23161
	Male	67	2.8931	2.74293	0.33510
LLVCLe(Rb)	**Female**	133	0.1057	0.78527	0.06809
	Male	67	0.1812	0.85704	0.10470
LLVCLe(La)	**Female**	133	2.2973	2.80749	0.24344
	Male	67	2.6258	2.89031	0.35311
LLVCLe(Lb)	**Female**	133	0.1512	0.88453	0.07670
	Male	67	0.2479	1.01456	0.12395

Table 4.16. Group statistics for Lingual Canal in relation to genial tubercles (LCGT) and in relation to the 20 figures (LCfig).

	Gender	*N*	*M*	*SD*	*Std. Error Mean*
LCGT	**Female**	133	2.7444	1.76091	0.15269
	Male	67	3.3582	1.70295	0.20805
LCfig	**Female**	133	8.0376	3.43204	0.29760
	Male	67	8.6119	3.23782	0.39556

4.2.3.2. Independent Samples T-Test:

For continuous type of data, the arithmetic means of the measurements were compared in terms of gender, using independent sample t-test. This section followed the design of "Statistics Help for Students" (146) in describing the data.

An independent samples t-test was conducted to compare Mental Canal (Anterior Loop) length in both females and males (range 2.40 mm- 10.78mm). As for the mental canal length on the right side, there was a significant difference in this measurement for females (M=6.12, SD=1.57) and for males (M=7.47, SD=1.74); t (198) = -5.512, *p*= 0.00. As for the Mental Canal length on the left side, there was a significant difference in this measurement for females (M=6.04, SD=1.65) and for males (M=6.71, SD=1.42); t (198) = 2.81, *p*= 0.006. These results suggest that the Mental Canal Length for both right and left sides is affected by gender.

An independent samples t-test was conducted to compare Lateral Lingual Vascular Canal Length in both females and males. As for the lateral lingual vascular canal length on the right side, there was not a significant difference in this measurement neither for females (M=2.11, SD=2.76) nor for males (M=2.89, SD=2.74); t (198) = -1.943, *p*= 0.053. As for the Lateral Lingual Vascular Canal Length on the left side, there was not a significant difference in this measurement neither for females (M=2.329, SD=2.81) nor for males (M=2.63, SD=2.89); t (198) = 0.77, *p*= 0.440. These results suggest that the Lateral Lingual Vascular Canal Length on both right and left sides is not affected by gender.

An independent samples t-test was conducted to compare Lingual Canal location in relation to genial tubercles for both females and males. There was a significant difference for females (M=2.74, SD=1.76) and for males (M=3.35, SD=1.72); t (198) = 2.35, *p*= 0.02. This suggests that the Lingual Canal location in relation to genial tubercles is affected by gender.

An independent samples t-test was conducted to compare Lingual Canal types in relation to the assigned 20 figures for both females and males. There was not a significant difference for females (M=8.04, SD=3.43) and for males (M=8.61, SD=3.24); t (198) = 1.138, *p*= 0.256. This suggests that the Lingual Canal configurations are not affected by gender.

An independent samples t-test was conducted to compare Lingual Canal Number for both females and males. There was a significant difference for females (M=3.71, SD=1.72) and for males (M=4.33, SD=1.73); t (198) = -2.378, *p*= 0.018. This suggests that the Lingual Canal Number is affected by gender.

4.2.4. Categorical Data Comparison with Chi-square Test or Fisher's Exact Test:

The data was subjected to cross-tabulation between distribution of the measurements among gender, and then to Chi-square tests. The results of the comparison are for Mandibular Canal Number in relation to gender (Table 4.17), for Mental Foramen Number in relation to gender (Table 4.18), for Mental Canal location in relation to gender (Table 4.19), for Mental Canal Orientation in relation to gender (Table 4.20), for the visibility of Mandibular Incisive Canal in relation to gender (Table 4.21), for Lateral Lingual Vascular Canals Number in relation to gender (Table 4.22), for Lateral Lingual Vascular Canals Orientation in relation to gender (when there is one canal on one or both sides) (Table 4.23), for Lateral Lingual Vascular Canals Orientation in relation to gender (when there are two canals on one or both sides) (Table 4.24), for Lateral Lingual Vascular Canals range between mandibular teeth in relation to gender (when there is one canal on one or both sides) (Table 4.25), of Lateral Lingual Vascular Canals range between mandibular teeth in relation to gender (when there are two canals on one or both sides) (Table 4.26), of Lateral Lingual Vascular Canals Height in relation to gender (when there is one canal on one or both sides) (Table 4.27), for Lateral Lingual Vascular Canals Height in relation to gender (when there are two canals on one or both sides) (Table 4.28), of Lateral Lingual Vascular Canals Aspect in relation to gender (when there is one canal on one or both sides)

(Table 4.29), of Lateral Lingual Vascular Canals Aspect in relation to gender (when there are two canals on one or both sides) (Table 4.30), of the number of Lingual Canals in relation to gender (Table 4.31), for the aspect of Lingual Canals in relation to gender (Table 4.32), for the location of Lingual Canals in relation to gender (Table 4.33), of the number of Lingual Foramina in relation to gender (Table 4.34), for the aspect of Lingual Foramina in relation to gender (Table 4.35), and for the location of Lingual Foramina in relation to gender (Table 4.36).

Table 4.17. Categorical comparison for Mandibular Canal Number (MaCN) in relation to gender for both right (R) and left (L) sides.

Parameter	Measurement	Female		Male		p-value
		n	(%)	n	(%)	
MaCN(R)	1 canal	118	(65.2)	63	(34.8)	0.182[a]
	2 canals:					
	DentoBMC	6	(75)	2	(25)	
	RetroBMC	9	(90)	1	(10)	
	3 canals	0	(0)	1	(100)	
MaCN(L)	1 canal	122	(65.6)	64	(34.4)	0.609[a]
	2 canals:					
	DentoBMC	4	(80)	1	(20)	
	RetroBMC	7	(77.8)	2	(22.2)	
	3 canals	0	(0)	0	(0)	

*P< 0.05 is accepted as statistically significant.
a: Pearson Chi-square test; *P* value < 0.05 is accepted as statistically significant.
b: Fisher's Exact test; *P* value < 0.05 is accepted as statistically significant.

Table 4.18. Categorical comparison for Mental Foramen Number (MeFN) in relation to gender for both right (R) and left (L) sides.

Parameter	Measurement	Female n	(%)	Male n	(%)	*p-value*
MeFN(R)	1 foramen	128	(66)	66	(34)	0.666[b]
	2 foramina	5	(83.3)	1	(16.7)	
MeFN(L)	1 foramen	122	(65.6)	64	(34.4)	1.000[b]
	2 foramina	130	(66.3)	66	(33.7)	

*P< 0.05 is accepted as statistically significant

a: Pearson Chi-square test; *P* value < 0.05 is accepted as statistically significant.

b: Fisher's Exact test; *P* value < 0.05 is accepted as statistically significant.

Table 4.19. Categorical data comparison for Mental Canal location (MeCl) in relation to gender for both (R) and left (L) sides.

Parameter	Measurement	Female n	(%)	Male n	(%)	*p-value*
MeCl(R)	Symmetrical	94	(67.6)	45	(32.4)	0.699[a]
	Mesial	29	(61.7)	18	(38.3)	
	Distal	10	(71.4)	4	(28.6)	
MeCl(L)	Symmetrical	94	(67.6)	45	(32.4)	0.699[a]
	Mesial	10	(71.4)	4	(28.6)	
	Distal	29	(61.7)	18	(38.3)	

*P< 0.05 is accepted as statistically significant.

a: Pearson Chi-square test; *P* value<0.05accepted as statistically significant

b: Fisher's Exact test; *P* value < 0.05 accepted as statistically significant.

Table 4.20. Categorical comparison for Mental Canal Orientation (MeCO) in relation to gender for both right (R) and left (L) sides.

Parameter	Measurement	Female		Male		p-value
		n	(%)	n	(%)	
MeCO(R)	Superior	131	(67.2)	64	(32.8)	0.337[b]
	Horizontal	2	(40)	3	(60)	
MeCO(L)	Superior	125	(66.1)	64	(33.9)	0.754[b]
	Horizontal	8	(72.7)	3	(27.3)	

*P< 0.05 is accepted as statistically significant

a:Pearson Chi-square test; *P* value<0.05 accepted as statistically significant.

b: Fisher's Exact test; *P* value < 0.05 accepted as statistically significant.

Table 4.21. Categorical comparison for the visibility of Mandibular Incisive Canal (MIC) in relation to gender for both right (R) and left (L) sides.

Parameter	Measurement	Female		Male		p-value
		n	(%)	n	(%)	
MIC(R)	Good	91	(67.9)	43	(32.1)	0.547[a]
	Moderate	42	(63.6)	24	(36.4)	
MIC(L)	Good	90	(67.7)	43	(32.3)	0.622[a]
	Moderate	43	(64.2)	24	(35.8)	

*P< 0.05 is accepted as statistically significant

a: Pearson Chi-square test; *P* value < 0.05 is accepted as statistically significant.

b: Fisher's Exact test; *P* value < 0.05 is accepted as statistically significant.

Table 4.22. Categorical comparison for Lateral Lingual Vascular Canals Number (LLVCN) in relation to gender for both right (R) and left (L) sides.

Parameter	Measurement	Female		Male		p-value
		n	(%)	n	(%)	
LLVCN(R)	No canals	79	(72.5)	30	(27.5)	0.129[a]
	1 canals	51	(60)	34	(40)	
	2 canals	3	(50)	3	(50)	
LLVCN (L)	No canals	76	(68.5)	35	(31.5)	0.545[a]
	1 canals	53	(65.4)	28	(34.6)	
	2 canals	4	(50)	4	(50)	

*P< 0.05 is accepted as statistically significant

a: Pearson Chi-square test; *P* value < 0.05 is accepted as statistically significant.

b: Fisher's Exact test; *P* value < 0.05 is accepted as statistically significant.

Table 4.23. Categorical comparison for Lateral Lingual Vascular Canals Orientation (LLVCO1) in relation to gender (when there is one canal on one or both sides) for right (R) and left (L) sides.

Parameter	Measurement	Female		Male		p-value
		n	(%)	n	(%)	
LLVCO1(R)	No canals	79	(72.5)	30	(27.5)	0.076[a]
	Superior	7	(58.3)	5	(41.7)	
	Horizontal	17	(73.9)	6	(26.1)	
	Inferior	30	(53.6)	26	(46.4)	
LLVCO1(L)	No canals	76	(68.5)	35	(31.5)	0.859[a]
	Superior	7	(70)	3	(30.6)	
	Horizontal	14	(66.7)	7	(33.3)	
	Inferior	36	(62.1)	22	(37.9)	

*P< 0.05 is accepted as statistically significant

a: Pearson Chi-square test; *P* value < 0.05 is accepted as statistically significant.

b: Fisher's Exact test; *P* value < 0.05 is accepted as statistically significant.

Table 4.24. Categorical comparison for Lateral Lingual Vascular Canals Orientation (when there are two canals on one or both sides) (LLVCO2) in relation to gender for right (R) and left (L) sides.

Parameter	Measurement	Female		Male		*p*-value
		n	(%)	n	(%)	
LLVCO2(R)	No canals	130	(67)	64	(33)	0.058[a]
	Superior	2	(100)	0	(0)	
	Horizontal	1	(100)	0	(0)	
	Inferior	0	(0)	3	(100)	
LLVCO2(L)	No canals	129	(67.2)	63	(32.8)	0.473[a]
	Superior	1	(100)	0	(0)	
	Horizontal	2	(50)	2	(50)	
	Inferior	1	(33.3)	2	(66.7)	

*P< 0.05 is accepted as statistically significant

a: Pearson Chi-square test; *P* value < 0.05 is accepted as statistically significant.

b: Fisher's Exact test; *P* value < 0.05 is accepted as statistically significant.

Table 4.25. Categorical comparison for Lateral Lingual Vascular Canals range between mandibular teeth (when there is one canal on one or both sides) (LLVCr1) in relation to gender for right (R) and left (L) sides.

Parameter	Measurement	Female		Male		*p-value*
		n	(%)	n	(%)	
LLVCr1(R)	No canals	79	(72.5)	30	(27.5)	0.002*[a]
	31 and 41	0	(0)	1	(100)	
	41 and 42	3	(37.5)	5	(62.5)	
	42 and 43	6	(50)	6	(50)	
	43 and 44	43	(71.7)	17	(28.3)	
	44 and 45	2	(20)	8	(80)	
LLVCr1(L)	No canals	76	(68.5)	35	(31.5)	0.252[a]
	31 and 41	2	(100)	0	(0)	
	31 and 32	9	(75)	3	(25)	
	32 and 33	16	(64)	9	(36)	
	33 and 34	29	(64.4)	16	(35.6)	
	34 and 35	1	(20)	4	(80)	

*P< 0.05 is accepted as statistically significant

a:Pearson Chi-square test; *P* value<0.05 accepted as statistically significant.

b:Fisher's Exact test; *P* value < 0.05 accepted as statistically significant.

Table 4.26. Categorical comparison for Lateral Lingual Vascular Canals range between mandibular teeth (when there are two canals on one or both sides) (LLVCr2) in relation to gender for right (R) and left (L) sides.

Parameter	Measurement	Female		Male		*p-value*
		n	(%)	n	(%)	
LLVCr2(R)	No canals	130	(67)	64	(33)	0.112[a]
	31 and 41	1	(100)	0	(0)	
	41 and 42	2	(100)	0	(0)	
	42 and 43	0	(0)	1	(100)	
	43 and 44	0	(0)	2	(100)	
	44 and 45	0	(0)	0	(0)	
LLVCr2(L)	No canals	129	(67.2)	63	(32.8)	0.622[a]
	31 and 41	0	(0)	0	(0)	
	31 and 32	1	(50)	1	(50)	
	32 and 33	2	(66.7)	1	(33.3)	
	33 and 34	1	(33.3)	2	(66.7)	
	34 and 35	0	(0)	0	(0)	

*P< 0.05 is accepted as statistically significant

a:Pearson Chi-square test;*P* value<0.05 accepted as statistically significant.

b: Fisher's Exact test; *P* value < 0.05 is accepted as statistically significant.

Table 4.27. Categorical comparison for Lateral Lingual Vascular Canals Height (when there is one canal on one or both sides) (LLVCH1) in relation to gender for right (R) and left (L) sides.

Parameter	Measurement	Female n	(%)	Male n	(%)	*p-value*
LLVCH1(R)	No canals	79	(72.5)	30	(27.5)	0.086[a]
	Upper 1\3	10	(50)	10	(50)	
	Middle 1\3	44	(62.9)	26	(37.1)	
	Lower 1\3	0	(0)	1	(100)	
LLVCH1(L)	No canals	76	(67.9)	36	(32.1)	0.768[a]
	Upper 1\3	0	(0)	0	(0)	
	Middle 1\3	14	(70)	6	(30)	
	Lower 1\3	43	(63.2)	25	(36.8)	

*P< 0.05 is accepted as statistically significant

a: Pearson Chi-square test; *P* value < 0.05 is accepted as statistically significant.

b: Fisher's Exact test; *P* value < 0.05 is accepted as statistically significant.

Table 4.28. Categorical comparison for Lateral Lingual Vascular Canals Height (when there are two canals on one or both sides) (LLVCH2) in relation to gender for right (R) and left (L) sides.

Parameter	Measurement	Female		Male		*p-value*
		n	(%)	n	(%)	
LLVCH2(R)	No canals	130	(67)	64	(33)	0.127[a]
	Upper 1\3	0	(0)	0	(0)	
	Middle 1\3	3	(75)	1	(25)	
	Lower 1\3	0	(0)	2	(100)	
LLVCH2(L)	No canals	129	(67.2)	63	(32.8)	0.446[a]
	Upper 1\3	0	(0)	0	(0)	
	Middle 1\3	1	(33.3)	2	(66.7)	
	Lower 1\3	3	(60)	2	(40)	

*P< 0.05 is accepted as statistically significant

a: Pearson Chi-square test; *P* value < 0.05 is accepted as statistically significant.

b: Fisher's Exact test; *P* value < 0.05 is accepted as statistically significant.

Table 4.29. Categorical comparison for Lateral Lingual Vascular Canals Aspect (LLVCA1) in relation to gender (when there is one canal on one or both sides) for right (R) and left (L) sides.

Parameter	Measurement	Female		Male		p-value
		n	(%)	n	(%)	
LLVCA1(R)	No canals	79	(72.5)	30	(27.5)	0.135[a]
	Lingual	52	(59.8)	35	(40.2)	
	Labial	2	(50)	2	(50)	
	Both	0	(0)	0	(0)	
LLVCA1(L)	No canals	77	(68.8)	35	(31.3)	0.744[a]
	Lingual	54	(63.5)	31	(36.5)	
	Labial	2	(66.7)	1	(33.3)	
	Both	0	(0)	0	(0)	

*P< 0.05 is accepted as statistically significant

a: Pearson Chi-square test; *P* value < 0.05 is accepted as statistically significant.

b: Fisher's Exact test; *P* value < 0.05 is accepted as statistically significant.

Table 4.30. Categorical comparison for Lateral Lingual Vascular Canals Aspect (when there are two canals on one or both sides) (LLVCA2) in relation to gender for right (R) and left (L) sides.

Parameter	Measurement	Female		Male		*p-value*
		n	(%)	n	(%)	
LLVCA2(R)	No canals	130	(67)	64	(33)	0.349[a]
	Lingual	2	(40)	3	(60)	
	Labial	1	(100)	0	(0)	
	Both	0	(0)	0	(0)	
LLVCA2(L)	No canals	130	(67)	64	(33)	0.349[a]
	Lingual	2	(40)	3	(60)	
	Labial	1	(100)	0	(0)	
	Both	0	(0)	0	(0)	

*P< 0.05 is accepted as statistically significant

a: Pearson Chi-square test; *P* value < 0.05 is accepted as statistically significant.

b: Fisher's Exact test; *P* value < 0.05 is accepted as statistically significant.

Table 4.31. Categorical comparison for the Lingual Canal Number (LCN) in relation to gender for right (R) and left (L) sides.

Parameter	Measurement	Female	Male	*p-value*
		n (%)	n (%)	
LCN	No canals	2 (66.7)	1 (33.3)	0.376[a]
	1 canal	67 (72.8)	25 (27.2)	
	2 canals	61 (61)	39 (39)	
	3 canals	3 (60)	2 (40)	

*P< 0.05 is accepted as statistically significant

a: Pearson Chi-square test; *P* value < 0.05 is accepted as statistically significant.

b: Fisher's Exact test; *P* value < 0.05 is accepted as statistically significant.

Table 4.32. Categorical comparison for the Lingual Canal Aspect (LCA) relation to gender.

Parameter	Measurement	Female		Male		p-value
		n	(%)	n	(%)	
LCA	No canals	2	(66.7)	1	(33.3)	0.317[a]
	Lingual	130	(67.4)	63	(32.6)	
	Labial	0	(0)	1	(100)	
	Both aspects	1	(33.3)	2	(66.7)	

*P< 0.05 is accepted as statistically significant

a: Pearson Chi-square test; *P* value < 0.05 is accepted as statistically significant.

b: Fisher's Exact test; *P* value < 0.05 is accepted as statistically significant.

Table 4.33. Categorical comparison for the Lingual Canal location (LCl) in relation to gender.

Parameter	Measurement	Female		Male		p-value
		n	(%)	n	(%)	
LCl	No canals	2	(66.7)	1	(33.3)	0.954[a]
	Midline	80	(66.7)	40	(33.3)	
	Mesial	29	(69)	13	(31)	
	Distal	22	(62.9)	13	(37.1)	

*P< 0.05 is accepted as statistically significant

a: Pearson Chi-square test; *P* value < 0.05 is accepted as statistically significant.

b: Fisher's Exact test; *P* value < 0.05 is accepted as statistically significant.

Table 4.34. Categorical comparison for the Lingual Foramen Number (LFN) in relation to gender.

Parameter	Measurement	Female n	(%)	Male n	(%)	*p-value*
LFN	No foramen	2	(66.7)	1	(33.3)	0.196[a]
	One foramen	69	(74.2)	24	(25.8)	
	2 foramina	59	(59.6)	40	(40.4)	
	3 foramina	3	(60)	2	(40)	

*P< 0.05 is accepted as statistically significant

a: Pearson Chi-square test; *P* value < 0.05 is accepted as statistically significant.

b: Fisher's Exact test; *P* value < 0.05 is accepted as statistically significant.

Table 4.35. Categorical comparison for the Lingual Foramen Number (LFA) in relation to gender.

Parameter	Measurement	Female n	(%)	Male n	(%)	*p-value*
LFA	No foramen	2	(66.7)	1	(33.3)	0.471[a]
	Lingual	130	(67)	64	(33)	
	Labial	0	(0)	0	(0)	
	Both aspects	1	(33.3)	2	(66.7)	

*P< 0.05 is accepted as statistically significant

a: Pearson Chi-square test; *P* value < 0.05 is accepted as statistically significant.

b: Fisher's Exact test; *P* value < 0.05 is accepted as statistically significant.

Table 4.36 Categorical comparison for the Lingual Foramen location (LFl) in relation to gender.

Parameter	Measurement	Female		Male		*p-value*
		n	(%)	n	(%)	
LFl	None	2	(66.7)	1	(33.3)	0.859[a]
	Midline	79	(68.1)	37	(31.9)	
	Mesial	29	(67.4)	14	(32.6)	
	Distal	23	(60.5)	15	(89.5)	

*P< 0.05 is accepted as statistically significant

a: Pearson Chi-square test; *P* value < 0.05 is accepted as statistically significant.

b: Fisher's Exact test; *P* value < 0.05 is accepted as statistically significant.

4.2.5. Correlation Coefficient:

This section followed the design of "Statistics Help for Students" (147) in describing the data. A Spearman's Correlation Coefficient was computed to assess the relationship between Mental Canal Orientation (MeCO) on the right side of the mandible and Mental Canal Orientation on the left side. There was a statistically significant correlation between the two variables; r=0.523, n=200, *p*= 0.000. A scatter plot summarizes the results (Figure 4.9). Overall, there was a moderate positive correlation between the Mental Canal Orientations on the right side with that of the left side. Increases in the degree of orientation of the mental canal on the right side were correlated with increases in the degree of orientation of the mental canal on the left side.
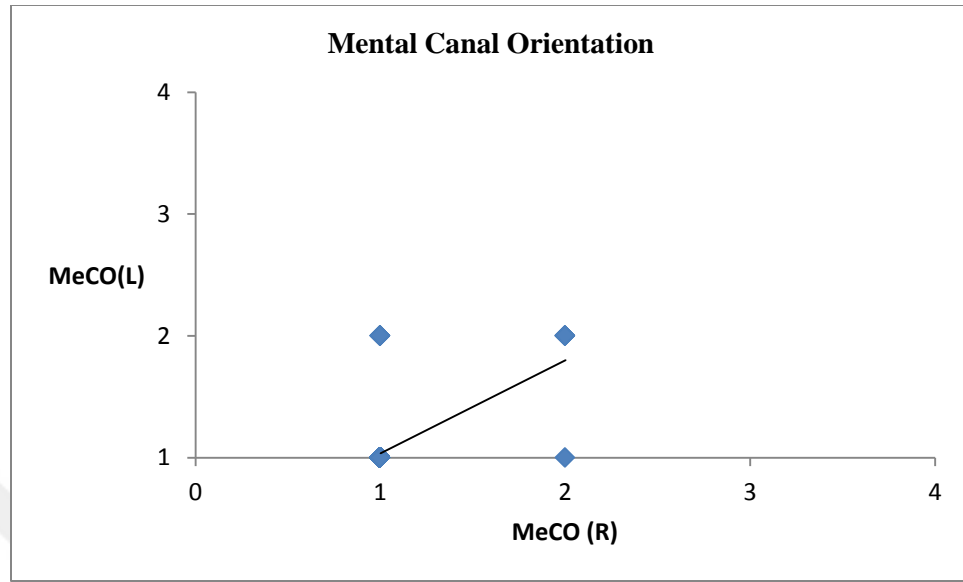
Figure 4.9. Scatter plot showing the correlation coefficient between Mental Canal Orientation on the right side (MeCO(R)) and Mental Canal Orientation on the left side (MeCO(R)).

A Spearman's Correlation Coefficient was computed to assess the relationship between Mental Canal Orientation (MeCO) and Mental Canal location (MeCl) on the same right side. There was no statistically significant correlation between the two variables; r= -0.041, n= 200, p=0.565. The same test was computed to assess the relationship between Mental Canal Orientation (MeCO) and Mental Canal location (MeCl) on the same left side. There was no statistically significant correlation between the two variables; r= -0.029, n= 200, p= 0.682.

A Spearman's Correlation Coefficient was computed to assess the relationship between the Mental Canal Length on the right side (MeCLeR) and the Mental Canal Length on the left side (MeCLeL). There was a statistically significant correlation between the two variables; r=0.360, n=200, p=0.00. Overall, there was a weak positive correlation between the Mental Canal Lengths on right and left sides. The increase of the Mental Canal Length on the right side was correlated with the increase of the Mental Canal Length on the left side.

A Spearman's Correlation Coefficient was computed to assess the relationship between Mental Canal Length (MeCLe) and the Mandibular Incisive Canal (MIC) visibility on the same right side. There was no statistically significant correlation between the two variables; r= 0.013,

n= 200, *p*= 0.850. The same test was computed to assess the relationship between Mental Canal Length and the Mandibular Incisive Canal visibility on the same left side. There was no statistically significant correlation between the two variables; r= -0.029, n= 200, *p*= 0.682.

A Spearman's Correlation Coefficient was computed to assess the relationship between the Mental Canal Length (MeCLe) and Mental Canal Orientation (MeCO) on the same right side. There was no statistically significant correlation between the two variables; r=-0.128, n= 200, *p*=0.071. The same test was computed to assess the relationship between Mental Canal Length and the Mental Canal Orientation on the same left side. There was no statistically significant correlation between the two variables; r= -0.102, n= 200, *p*= 0.150.

A Spearman's Correlation Coefficient was computed to assess the relationship between the Lateral Lingual Vascular Canals Number on the right side (LLVCNR) and the Lateral Lingual Vascular Canals Number on the left side (LLVCNL). There was a statistically significant correlation between the two variables; r= 0.283, n= 200, *p*=0.000. Overall, there was a weak positive correlation between the number of Lateral Lingual Vascular Canal on the right side and that of the left.

A Spearman's Correlation Coefficient was computed to assess the relationship between the Lateral Lingual Vascular Canal Number (LLVCN) and the Mandibular Incisive Canal (MIC) visibility on the same right side. There was no statistically significant correlation between the two variables; r=- 0.134, n= 200, *p*=0.058. The same test was computed to assess the relationship between Lateral Lingual Vascular Canal Number (LLVCsN) and the Mandibular Incisive canal (MIC) visibility on the same left side. There was no statistically significant correlation between the two variables; r= -0.004, n= 200, *p*= 0.954.

A Kendlall's Correlation Coefficient was computed to assess the relationship between the Lingual Canal Number (LCN) at the midline and the Mandibular Incisive Canal (MIC) visibility on the right side. There was no statistically significant correlation between the two variables; r=0.069, n=200, *p*=0.324. The same test was computed to assess the relationship between the Lingual Canal Number and the Mandibular Incisive Canal visibility on the left side. There was no statistically significant correlation between the two variables; r= 0.136, n= 200, *p*= 0.050.

A Spearman's Correlation Coefficient was computed to assess the relationship between the Lateral Lingual Vascular Canal Length on the right side (LLVCLeR) of the mandible and the Lateral Lingual Vascular Canal Length on the left (LLVCLeL). There was a statistically significant correlation between the two variables; r=0.307, n=200, *p*=0.000. Overall, there was a weak positive correlation between the right Lateral Lingual Vascular Canal Length and the left Lateral Lingual Vascular Canal Length. Increases in the right side canals were correlated with increases in that of the left side ones.

A Spearman's Correlation Coefficient was computed to assess the relationship between the Lateral Lingual Vascular Canal Length on the right side (LLVCLeR) of the mandible and Mandibular Incisive Canal (MIC) visibility on the same side. There was a statistically significant correlation between the two variables; r=-0.142, n=200, *p*=0.045. Overall, there was a very weak negative correlation between the two variables. The same test was computed to assess the relationship between the Lingual Canal Length on the left side and the Mandibular Incisive Canal visibility on the same side. There was no statistically significant correlation between the two variables; r= -0.019, n= 200, *p*= 0.792.

A Kendlall's Correlation Coefficient was computed to assess the relationship between the right Lateral Lingual Vascular Canals' Orientation (LLVCOR1) and the left Lateral Lingual Vascular Canals' Orientation (LLVCOL1) when there was one canal. There was a statistically significant correlation between the two variables; r= 0.235, n=200, *p*=0.000. Overall, there was a weak positive correlation between the two variables. The same test was computed to assess the relationship between the right Lateral Lingual Vascular Canals' Orientation (LLVCOR2) and that on the left (LLVCOL2) when there were two canals. There was no statistically significant correlation between the two variables; r= 0.118, n= 200, *p*= 0.092.

A Kendlall's Correlation Coefficient was computed to assess the relationship between the right Lateral Lingual Vascular Canals' Orientation (LLVCOR1) and the right Lateral Lingual Vascular Canals' Height (LLVCHR1) when there was one canal. There was a statistically significant correlation between the two variables; r=0.850, n=200, *p*=0.000. A scatter plot summarizes the results (Figure 4.10). The same test was computed to assess the relationship between the right Lateral Lingual Vascular Canals' Orientation (LLVCOR2) and the right Lateral Lingual Vascular Canals' Height (LLVCHR2) when there were two canals. There is a

statistically significant correlation between the two variables; r=0.997, n=200, *p*=0.000. A scatter plot summarizes the results (Figure 4.11). Overall, there was a very strong positive correlation between the right Lateral Lingual Vascular Canals' Orientation and the right Lateral Lingual Vascular Canals' Height. Increases in the degree of orientation of the Lateral Lingual Canals were correlated with increases in the height of the canals in regards to the overall alveolar bone height at the measurement site.
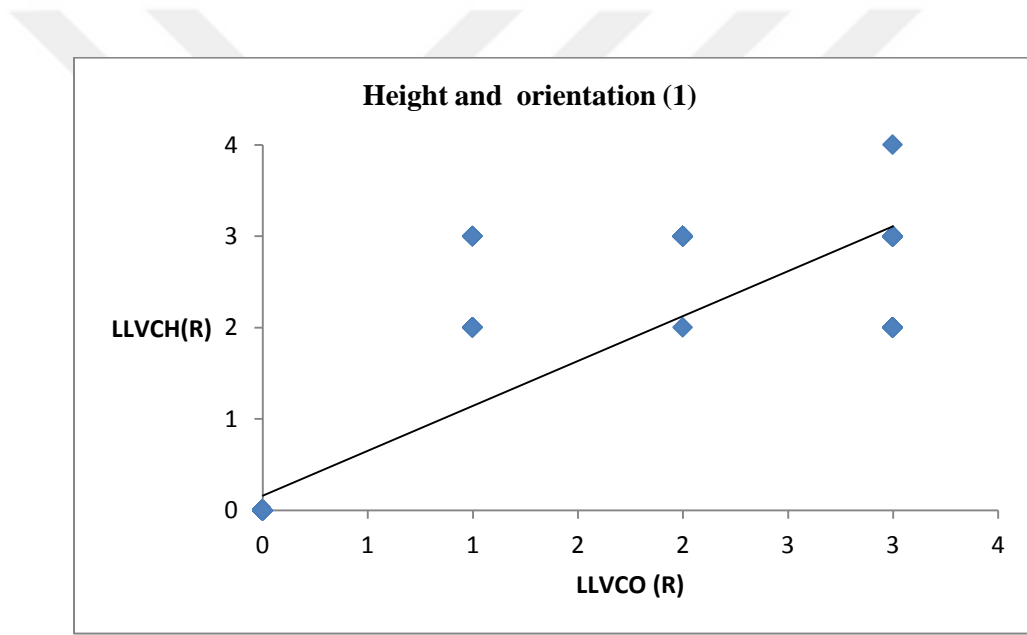
Figure 4.10. Scatter plot showing the correlation coefficient between Lateral Lingual Vascular Canals Orientation on the right side (LLVCO(R)) and the Lateral Lingual Vascular Canals Height on the same side (LLVCH(R)) when there was one canal.
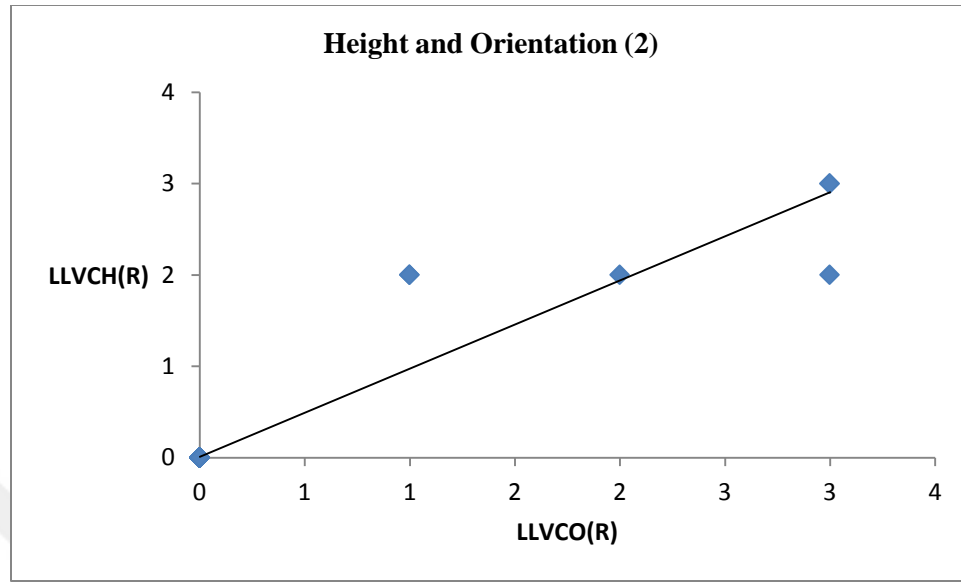
Figure 4.11 Scatter plot showing the correlation coefficient between Lateral Lingual Vascular Canals' Orientation on the right side (LLVCO(R)) and the Lateral Lingual Vascular Canals' Height on the right side (LLVCH(R)) when there were two canals.

A Kendlall's Correlation Coefficient was computed to assess the relationship between the left Lateral Lingual Vascular Canals' Orientation (LLVCOL1) and the left Lateral Lingual Vascular Canals' Height (LLVCHL1) when there was one canal. There was a statistically significant correlation between the two variables; r=0.879, n=200, *p*=0.000. A scatter plot summarizes the results (Figure 4.12). The same test was computed to assess the relationship between the left Lateral Lingual Vascular Canals Orientation (LLVCOL2) and the left Lateral Lingual Vascular Canals Height (LLVCHL2) when there are two canals. There is a statistically significant correlation between the two variables; r=0.992, n=200, *p*=0.000. A scatter plot summarizes the results (Figure 4.13). Overall, there was a very strong positive correlation between the left Lateral Lingual Vascular Canals' Orientation and the left Lateral Lingual Vascular Canals' Height. Increases in the orientation of the Lateral Lingual Canals were correlated with increases in the height of the canals in regards to the overall alveolar bone height at the measurement site.
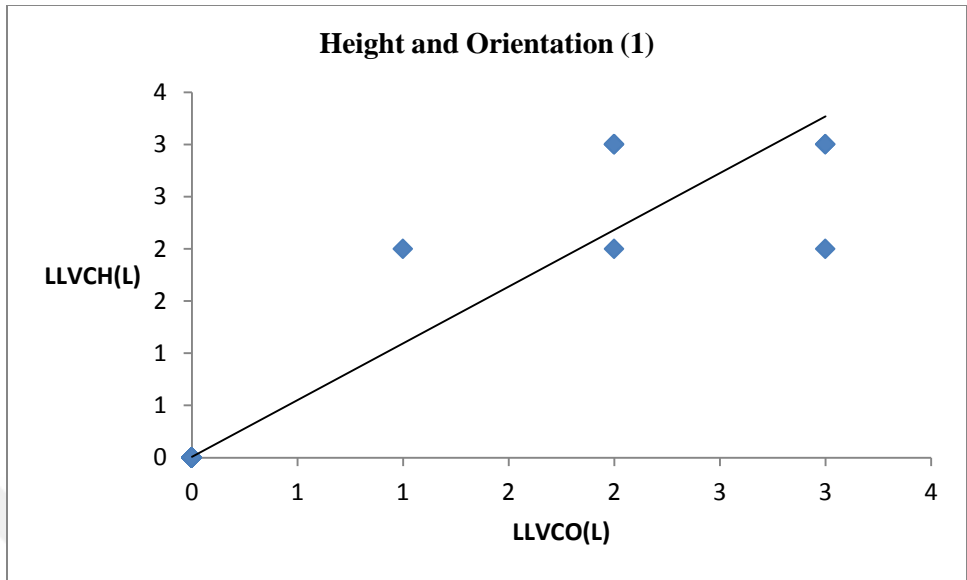
Figure 4.12. Scatter plot showing the correlation coefficient between Lateral Lingual Vascular Canals' Orientation on the left side (LLVCO(L)) and the Lateral Lingual Vascular Canals' Height on the left side (LLVCH(L)) when there was one canal.
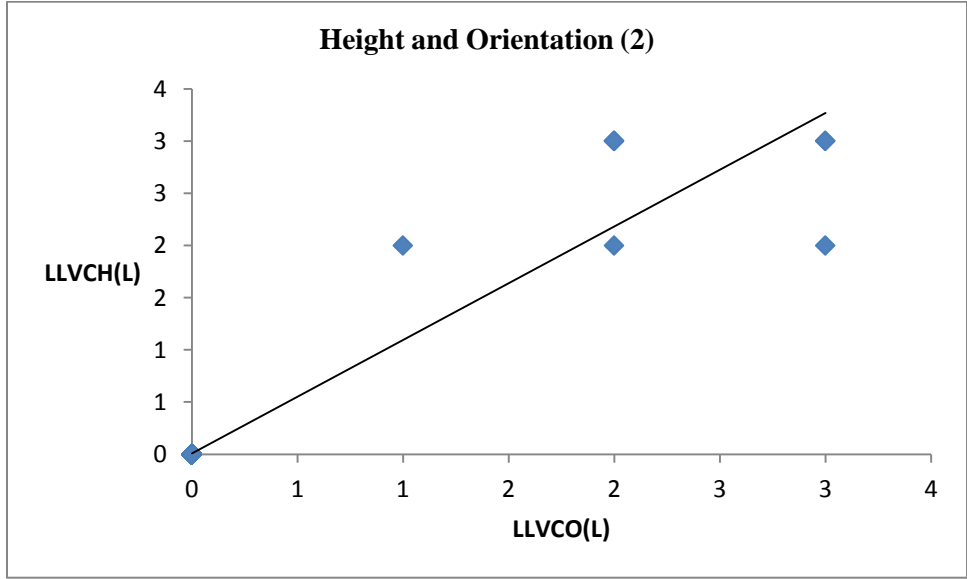
Figure 4.13. Scatter plot showing the correlation coefficient between Lateral Lingual Vascular Canals' Orientation on the left side (LLVCO(L)) and the Lateral Lingual Vascular Canals' Height on the left side (LLVCH(L)) when there were two canals.

A Kendlall's Correlation Coefficient was computed to assess the relationship between the number of the Lingual Canals (LCN) at the midline and the Lateral Lingual Vascular Canals Number on the right side (LLVCNR). There was no statistically significant correlation between the two variables; r=0.056, n=200, *p*=0.412. The same test was computed to assess the relationship between the number of the Lingual Canals (LCN) and the lateral lingual vascular canals' number on the left side (LLVCNL). There was no statistically significant correlation between the two variables; r=-0.022, n=200, *p*=0.745.

A Kendlall's Correlation Coefficient was computed to assess the relationship between the number of Mandibular Canals on the right (MaCNR) side and the number of Mandibular Canals on the left (MaCNL). There was a statistically significant correlation between the two variables; r=0.308, n=200, *p*=0.000. Overall, there was a weak positive correlation between the number of the Mandibular Canals on the right and left sides. Increases in the number of the right Mandibular Canals were correlated with increases in the number of the left Mandibular Canals.

A Kendlall's Correlation Coefficient was computed to assess the relationship between the number of Mandibular Canals on the right side (MaCNR) and the number of Mental Foramina (MeFNR) on the same side. There was no statistically significant correlation between the two variables; r=0.047, n=200, *p*=0.509. The same test was computed to assess the relationship between the number of the Mandibular Canals on the left side (MaCNL) and the number of Mental Foramina on the same side (MeFNL). There is a statistically significant correlation between the two variables; r=0.236, n=200, *p*=0.001. Overall, there was a weak positive correlation between the number of the Mandibular Canals on the left side and the number of Mental Foramina on the same side. Increases in the number of the Mandibular Canals on the left side were correlated with increases in the number of Mental Foramina on the same side.

5. DISCUSSION

In regards to the intra-osseous course of the IANC and its associations and variations in the mandible, the main bulk of literature was assembled from studies and conclusions based on 2-D imaging; mainly panoramic and intraoral periapical radiographs (2, 12, 13, 22, 42, 52, 53, 60, 61, 68, 73, 99, 148, 149). Since the introduction of 3-D imaging; especially CBCT, many of these studies have been recently tagged as false (84). Other studies reported that conventional panoramic radiographs have failed to detect MIC (9, 12, 13, 17, 65, 140, 150-152). Furthermore, bone measurement discrepancies in radiographs were reported; Sonick et al. (153) calculated the average distortion and linear errors in the bone coronal to the mandibular canal and mental foramen as follows: panoramic films: 23.5% (mean 3mm; range 0.5-7.5mm), periapical films: 14% (mean 1.9mm; range 0.0-5.0mm), and CT scans with only linear errors in: 1.8% (0.2mm; range 0.0-0.5mm). This states that the panoramic radiograph is proved to be the most inaccurate image, exhibiting the greatest amount of distortion (153). Accordingly, neither periapical nor panoramic radiography can precisely portray the amount of bone coronal to the mandibular canal and mental foramen (154). Moreover, the information that it provides in regards to the anterior loop of the mental canal is inaccurate and not reliable (140, 155), as false-positive and negative findings occur when diagnosing the anterior loop with panoramic radiographs (154). Accordingly, implant surgery in mandibular anterior region may turn from a simple safe minor surgery into a life-threatening complication, due to inadequate knowledge of the existing anatomy in that particular region (156). On the other hand, CBCT resembles conventional CT in type of images obtained and software capabilities, nevertheless there are no CBCT linear measurement magnifications as those occurring in conventional CT scans (140, 141), hence the CBCT images are sharper and diagnostically clearer as the voxel size of CBCT is 0.1mm, whereas in the CT scan it is 0.5mm at minimum (156). Therefore, CBCT has advantages over panoramic radiography in the detection of anatomical variations and associations in the mandible (53). Nevertheless, panoramic images reformatted from CBCT scan show better diagnostic results than regular digital panoramic images (156, 157), and CBCT scans can be recommended while planning dental implant placement in the mandible, especially in the anterior region (140). In fact, CBCT imaging has been proved to be a gold standard among the various imaging

modalities used in dental implant treatment planning, as it also provides digital preoperative mock-up before proceeding with dental implant placement (156). In this context, all of the findings, parameters and their measurements in the following section in the present study will be only evaluated in accordance to their equivalents in other different CBCT studies, and the benchmark is, indeed, the anatomical studies.

In an effort to elucidate the CBCT imaging anatomy of the IANC, including the MIC with their associations and variations; this study was set out to develop a reliable and consistent method of CBCT imaging analysis to assess the IANC, starting from the mandibular foramen pending to the mandibular midline to involve the entire structure, accommodating all of its encountered associations, variations and anatomical relationships in the same case.

5.1. Mandibular Incisive Canal:

By means of the original iCAT CBCT software program, the assessment of the IANC revealed that the MIC is bilaterally visible in reformatted cross-sections of all the 200 iCAT CBCT images; 400 IANC, with around 67% of the images having good MIC visibility. Furthermore, on both right and left sides, MIC is not affected by gender. These indicate that the MIC is a constant anatomical structure that can be detected on CBCT imaging, and the IANC continues to the midline. This result, accordingly, supports the study's hypothesis, which stated that the visibility of the IANC and its prolongation in CBCT images can be detected as a continuous component.

Based on imaging studies, this result is similar to the results in the following studies: Al-Ani et al. (158) who identified the visibility of MIC in all (100%) of iCAT CBCT scans; also with Patricia et al. (17) who detected MIC, bilaterally, in all of the 100 iCAT CBCT scans; and with Leite et al. (159) who detected MIC, bilaterally, in all of the 250 CBCT scans; for 500 IANC.

Other authors have also found a high prevalence of MIC, using CBCT, with a variable visibility ranging from 71.66% to 97.5%. as follows: Sokhn et al. (18) identified the MIC in 97.5% of the scans; Sahman et al. (150) examined CBCT scans from 243 patients from a Turkish population, and of the 486 hemimandibles the MIC was visible in 94.4% of the CBCT scans; Apostolakis and Brown (160) detected the MIC in 93% of 102 CBCT scans; Yovchev et al.

(161) detected the MIC in 92.9% of 140 CBCT scans; Kajan et al. (162) identified the MIC in 92.3% of 84 CBCT images of an Iranian population; Pires et al. (38), and Parnia et al. (163) identified MIC in 83% of CBCT cases; Raitz et al. (164) detected the MIC in 90.3% of 150 CBCT scans; and Ramesh et al. (67) detected the MIC in 71.66% from 120 CBCT scans of an Indian population, and they also mentioned that MIC may open on the lingual aspect of the mandible close to the genial tubercle.

In cadaver mandible studies, some authors have found high prevalence in MIC detection, such as: Obradovic et al. (165) who identified the MIC in 92% of 105 cadavers; and Mraiwa et al. (13) who identified the MIC in 96% of 50 cadaver mandibles. Whereas, other authors detected the MIC in all (100%) of the cadaver mandibles as in the following studies: in two studies by Uchida et al. (63, 166); by Tepper et al. (64) ; by Mardinger et al. (9) who identified the MIC in all 46 cadaver mandibles in which the neurovascular bundle was further described as follows: 21.7% with complete corticated MIC walls, 58.7% with partially corticated walls, and 19.6% with no corticated canal walls and the Mandibular Incisive Nerve (MIN) is enclosed in medullary space (159). Furthermore, De Andrada et al. (10) concluded that the MIN is a normal structure that typically extends closer to the mandibular midline, providing innervations to first premolar, canine, lateral and central incisors (167).

Many studies have investigated the MIC, yet its existence is still widely debated, especially because it is still considered as an anatomical variation in the interforaminal area (9, 11, 13, 14, 17, 38, 64, 163). One main explanation is that the identification of the MIC is very difficult in the central- lateral incisor region; as the closer it gets to the midline the thinner it becomes, until the neurovascular bundle emerges in the medullary space and the canal disappears (160). However, it was accepted that IAN from one side, infrequently, overlapped as far as the lateral incisor of the opposite side (168), yet in some cases, it terminates in the lateral incisor region on the same side (162). So, it is possible that the reason of the frequency variation in MIC detection, on radiographs, is because that the canal becomes thinner as it extends to the midline of the mandible (11, 46, 63, 151, 161, 163). Perhaps this is also the reason for the insignificant attention given to the MIC, while designing and placing dental implants (164). Another explanation for the different frequencies in detecting the MIC in this study compared with preceding imaging and anatomy studies can be attributed to the degree of MIC wall cortication; the MIC walls contain

less cortical bone than that of the MC (46), and so its identification in some imaging sections becomes difficult when compared to MC detection. Moreover, the less or the loss of wall cortication, means the less the possibility of accurate image detection (162). So, it can be argued that the fact that the level of MIC wall cortication is significant in image visualization and detection of the canal does not eliminate the fact that it is anatomically present (9, 10, 63, 64, 166). Other explanations can be attributed to the methodology, the make of CBCT machines used: as almost all the studies that detected MIC in 100% of the cases used iCAT CBCT units, as well as the ethnic group of the examined population (162,165).

MIC should be considered as a limiting factor while deciding the dental implant length, as trauma of the MIC can lead to sever bleeding. This fact is usually ignored, as MIC can be only detected in 2.7% of panoramic radiographs (156). Kütük et al. (65) reported sensory disturbances, ranging from mild paresthesia to complete anaesthesia, and\or neuropathic pain; burning, or tingling, or throbbing, depending on the degree of nerve injury. This may take place due to MIC perforation, while placing dental implants in the anterior mandible (65).

5.2. Mandibular Canal:

The mandibular canal is usually a single trunk on bilateral sides of the mandible, entering from the mandibular foramen, extending and giving off dental branches to supply the teeth. This main trunk ends by dividing into the mental and the incisive branches at the mental foramen level (61, 168). Studies proved the presence of a second and even a third mandibular canal (4, 69, 170-172). Furthermore, Wadhwani et al. (72), Claeys et al. (74), Lew et al. (173), and Murlimanju et al. (174) identified accessory mandibular foramina (AMF) in their studies. On dry mandibles, the later study (174) observed AMF in 11 mandibles; 6 equally unilateral, and bilateral in 5 (n=67). Needless to say, that the presence of AMF was usually associated with failure to obtain adequate local anaesthesia (95,173, 174). In the present study, the MC was single in 90.5% of the cases on the right side and 93% on the left, and the mandibular foramen was bilaterally single in 100% of the cases, and not affected by gender.

The presence of "double", or "duplicating", or "bifid" (52, 175), or "accessory" (53), or mandibular canal branches (176), was variably described in the available literature as: "rare" or "anomalies" (74, 177, 178), or "very rare" (52), "not a rare finding" (73), "occasionally present"

(60), "an unusual finding, but not rare"(175), "a variation" (179), "not an infrequent occurrence" or "a fairly common anomaly" (180), "an abnormality" or "an aberrancy" (181), or "an oddity" (52, 182). The TMC, on the other hand, is much rarer, and only few cases have reported it (70, 71, 79, 183). The detection of the BMC can only be confirmed by 3-D imaging (52, 53, 170, 176). Moreover, Fukami et al. (96) reported that the cross-section CBCT images of BMCs were consistent with the gross anatomical sections. The present study shows that the presence of BMC can be described as an unusual variation (16%), and TMC as a rare variation (1%) and their detection is irrefutable by CBCT imaging.

According to CT studies, and regardless of the type of classification used or adapted, wide variations of BMC prevalence rate were reported in different countries, ranging from 15.6% to 65%, with an average rate of 40.3% (176). In Turkey, Orhan et al. (82) reported 46.5% of 484 hemimandibels. In Belgium, De Oliveira-Santos et al. (66) reported 19%. In Taiwan, Fu et al. (80) reported 30.6%. In Spain, Muinelo-Lorenzo et al. (86) reported 36.8%, and in Japan, Naitoh et al. (19) reported 65%.

In Korea, Kang et al. (81) detected RMC in 5.38% of the CBCT images. In Italy, Lizio et al. (184) detected RMC in 14.6% of the CBCT images. In Turkey, Orhan et al. (82) observed the RMC in 28.10% and Dental type canal in 8.30%. In another study in Korea, Kawai et al. (101) detected RMC in 37% of CBCT scans.

In the present study, RMC imaging classification according to the course (Figure 2.10) was adapted from Von Arx et al. (89), who identified RMC in 25.6% of CBCT scans. In the same study, only 4 cases had bilateral RMC, and 5 had unilateral. Although women tended to have RMC more often than men in the same study, no statistical difference was found. Furthermore, the distribution of RMCs according to type was as follows: 41.9% type A1 (vertical course), 16.1% type A2 (vertical course with additional horizontal branch), 29% type B1 (curved course), 12.9% type B2 (curved course with additional horizontal branch), and 0% type C (horizontal course). The present study detected 19 (9.5%) RMC; 12 unilateral and 3 bilateral with one case having a RMC on the left side and a DMC on the right. Although women tended to have BMC and RMC more often than men on both right and left sides, no statistical difference was found in this study. According to RMC type: 36.8% were type A1, 0% type A2, 52.6% type B1, 5.3% type B2, and 5.3% type C. Sisman et al. (185) detected RMC in 26.7% of CBCT images

(28.46% type A1 and 26.09% type B1). In a Korean population (n=100), Park et al. (92) detected RMC in 23 (11.5%) of the 200 mandibular sides:type A1 in 37.3%, type B1 in 62.7%, and type C was not identified in any of the images. Han et al. (185), however, followed Ossenberg's (94) classification (Section 2.5.3), and detected RMC in 65%, and TCC in 0.90% of the CBCT scans, that belonged to males.

It is important to highlight that current knowledge of the RMC is mainly based on cadaver studies and case reports; most of which address Retromolar Foramen (RMF) rather than the canal (89). This study agrees with park et al. (92) that in the clinic, CBCT imaging is the superlative method for detecting RMC and other ambiguous associations between IANC and different mandibular anatomical landmarks. The results of the present study present practical information for surgical interventions that may protect patients from complications. The presence of RMC may alert clinicians regarding the possibility of inadequate anaesthesia or bleeding in the retromolar area (92, 93, 173).

Differences in RMC prevalence can be attributed to differences in methodology (89), differences in CBCT machines, and differences in various classification types adapted. For the reason that CBCT can provide high-resolution 3-D images, that can detect accessory canals or variations in any direction, CBCT was considered as an appropriate modality for comprehensive evaluation and detection of BMC (78), and other distinctive variations (52).

The present study detected only one TMC on the right side, Rashsuren et al. (20) detected 7 cases, Muinelo-Lorenzo et al. (86) detected none, Adisen et al. detected one on CBCT. Auluk et al (187) detected 3 TMCs, and in another study Auluck et al. (71) detected 4 TMC, also Mizbah et al. (79) detected 4 cases on CBCT. Rashsuren et al. (20) found BMC and TMC together in 22.6% of the images; (BMC 21.2% and TMC 1.4%), out of which 17.4% were RMC, 4.6% were Dental canals, 4.6% were Forward canals and 1% Buccolingual canal.

In the present study, BMC in general were detected in16% of the images; 9% on the right and 7% on the left, and there was one (0.5%) TMC on the right side (Table 4.1).Furthermore, out of the five types of BMC (Table 2. 1), only two types were detected; DMC (6.5%), and RMC (9.5%); type A1:36.8%, type B1:52.6%, type B2: 5.3% and type C 1: 5.3%.

Muinelo-Lorenzo et al. (86) detected RMC in 12% and DMC in 7.5% of the CBCT sections. Naitoh et al. (19) detected RMC in 29.8% and DMC in 7% of the CBCT sections. Han et al. (95) detected RMC in 8.5% of the cases, and as they adapted Ossemberg's classification in their study, RMC were as follows: 66.7% vertical, 20% horizontal and 13.3% independent from a separate foramen or TCC type. Thus, RMC prevalence in this study is almost consistent with that of Han et al. (95) and DMC is consistent with that of Muinelo-Lorenzo et al. (86) and Naitoh et al. (19).

In general, the prevalence of the retromandibular nerve ranged from 12-75% (93). In 136 cadavers from an Iranian population, Motamedi et al. (93) identified RM nerves in 40.4%. Accordingly, it can be suggested that the RMC is a normal anatomical variation of the IANC rather than an anomaly (93). This broad variation in frequencies can be due to differences in the sample size, the type of examination conducted (170), statistic analysis design; especially when each mandible is considered as a hemi section in the sample, and the type of classification followed and\or adapted. Furthermore, it can be attributed to different types of CBCT machines and accordingly; software facilities.

5.3. Mental Foramen:

One of the common complications affecting the mental nerve is injury at the time of flap reflection (188). In the present study, none of the BMC or TMC had connections with a distinct mental foaramen. According to the available literature, Rouas et al. (52) detected a BMC, where the two parts of the canal followed the same course under each other, and each one of them had a distinct mental foramen (52). Also, Berberi et al. (178), and Clayes et al. (74) identified BMC, using CT scans with two distinct mental foramina. Meoli et al. (177) also identified a case of "double foramen mentalis".

More than one mental foramen may be present (154). Sawyer et al. (189) examined the frequency of accessory mental foramina in skulls in four ethnic groups, and its prevalence was as follows: White Americans: 1.4%, African Americans: 5.7%, Asian Indians 1.5%, and Columbian Indians 9%. This study identified a single opening of the mental foramen in 95% of the cases, and an accessory mental foramen (two mental foramina in 10 cases (5%); 6 on the right side, and 4 on the left; 7 in females and 3 in males). Eshak et al. (15) detected 5 cases of

two mental foramina (1 female and 4 males). Miguel et al. (188) observed that the mental foramen had a single opening in 95.97% of the cases, two foramina in 14 of the cases 3.59%, which is almost consistent with the percentage in the present study, and three foramina in 2 cases (0.43%) with no correlation to gender. It is interesting to highlight that Senyurek (190) reported that multiple mental foramina were characteristic of prehistoric man and that evolution tended to reduce this number to one in contemporary man. Conversely, the absence of the mental foramen in cadaver mandibles, which is rarely observed, was reported by Matsuda (191), and also by De Freitas et al. (192) who detected the absence of the mental foramen twice on the right side (0.06%) and once on the left (0.03%) among 1435 dry human mandibles (193). Also, based on CBCT sections, the bilateral absence of the mental foramen was recently reported by Matsumoto et al. (194).

The present study identified two cases with vertical RMC having two mental foramina on the same side, but with no evidence of connection. Nonetheless, there was a statistically significant weak positive correlation between the number of the mandibular canals on the left side only and the number of mental foramina on the same side. In this regard, the present study is in agreement with Olivier (61); as he explained that an accessory mental foramen can only be a bony septum dividing the foramen into two openings (193), and accordingly, the bifid canal is not necessarily in contact with an accessory mental foramen. This also coincides with the classifications of Carter and Keen (69), Nortje (60), and Langlais (68) as mentioned earlier (Section 2.5.3), where none of the authors confirmed the presence of accessory mental foramina despite of the presence of BMC (74). It can be concluded that different patterns occurs, and it should not be always assumed that there is only one mental foramen on each side (154).

5.4. Mental Canal:

In the premolar area, the mental part of the IAN sometimes, after giving off the MIN branch, curves or loops back and upwards to exit through the MeF at the buccal aspect, and hence called: the Anterior Loop Nerve (ALN) (155, 195). Rothman (196) described its appearance on cross-sections as the figure eight "8", because the mandibular canal (lower) courses foreword and the mental canal or the AL (upper) courses backward.

During dental implant placement, the violation of the AL can lead to neurosensory disturbances in the area of the lower lip (140). The frequency of sensory disturbances varies according to many reasons: location of surgery, method of surgery, study design, sensitivity of assessment techniques, selection of outcome variables, terminology used to express sensory disturbances (154,197). Subsequent to dental implant insertion in the anterior mandible, the prevalence of transitory altered lip sensation was as the following: 8.5% in a study by Bartling et al. (198), 11% in a study by Wismeijer et al. (199), 24% in a study by Wolten (200), and Abarca et al. (201) reported neurosensory disturbance in 33% of the cases in the anterior region of the mandible after implant surgery with no statistical differences between the patients.

In this study, the results revealed that the mental canal length or the Anterior Loop Length (ALL) ranged between 2.40mm to 10.78mm (mean: 6.59mm), and the length for both right and left sides is affected by gender. Also, the mental canal angle of inclination, that traverses coronally, ranged from 0^0 to 83^0. Chen et al. (195) detected the ALL with maximum length of 8.41 mm, and a maximum angle of 81.79^0, which varied with gender and age. This ALL and angle are almost consistent with that in the present study, whereas Solar et al. (202) reported a slightly different angle of inclination that ranged from 11^0 to 77^0.

In the literature, there are different reports of ALL values, depending on the measurement technique used (155). Vujanovic-Eskenazi et al. (140) reported their maximum ALL as 4mm. Apostolakis and Brown (203) detected the maximum ALL as 5.70mm. Rothman (196) reported the ALL as 10mm. Neiva et al. (204) reported the longest ALL as 11mm. In these last two studies, the ALL is almost consistent with that in the present study. In addition, in the present study, only the mental canal length (MeCL, or ALL) on both sides was affected by gender, which may be attributed to the general discrepancy of mandible size between males and females (160). Moreover, increases in the degree of orientation of the mental canal on the right side were correlated with the increases in the degree of orientation of the mental canal orientation on the left side, and likewise.

Anatomical studies reported wide variations in ALL; the average length of the anterior loop based on direct measurements in cadaver samples ranged from 0.1 mm and 6.95 mm (137, 205-207). Uchida et al. (160) reported the ALL with maximum length of 9.00 mm, suggesting that the height of the individual and the gender influence the variations in ALL, whereas Benninger et

al. (208) attributed the variations to race. Moreover, the wide range of values in the literature may be due to high anatomical variability (140), ethnic differences, sample size, as well as different study techniques. Among the different techniques; the data obtained from cadavers are indeed the most accurate. However, CT and CBCT techniques gained acceptance as gold standard (155).

Considering the wide range of ALL, Uchida et al. (160), and Parnia et al. (162) concluded that it is risky to recommend any standard distance mesially from the mental foramen for dental implant placement in the mental foramen region (155), and at the time of dental implant treatment planning, this distance should be, routinely, measured for every patient individually.

5.5. Lateral Lingual Vascular Canals:

All of the detected LLVCs, in this study, were continuous with the IANC and MIC. It is accepted that the connection of LLVCs with either the IANC or the MIC supports collateral neural and vascular supply (37,128, 130). Detailed examination of anastomoses of posterior LLVCs demonstrated that canals originating in the premolar area mainly connect with the MIC, whereas those originating from the molar area connect with the IANC (130). The visible connection of the LLVCs with adjacent anatomic structures was reported by Von Arx et al. (130) as 100 %, and Sahman et al. (37) reported that almost all the LLVCs 98% had a connection with the MIC, and only 2% had it with the IANC, which are both consistent with the continuity fact in the present study. Nevertheless, Von Arx et al. (130) reported the connection between the LLVCs and MIC as 67%, and 33% with the IANC, and Patil et al. (132) reported 45.4% connectivity between LLVCs and IANC. The variations in frequency of LLVCs connectivity in the present study with other studies may be attributed to the study design and method. As in this study, in every single case on both right and left sides the IANC structure was detected, continuously and efficiently, from its beginning in the mandible; from the mandibular foramen to the midline. In this study, it is important to highlight that all the LLVCs started to appear in the image sections, either immediately, or after the mental foramen area (none were detected in the molar area), and are in direct connectivity with the MIC. Accordingly, it can be concluded that the LLVCs are located in the interforaminal vicinity.

In the present study, one lateral canal was detected on the right side of 42.5% of the images and in 40.5% on the left side. Two lateral canals were seen on the right side of 3% of the images, and in 4% on the left. Sahman et al. (37) demonstrated at least one LLVC in 25% of the CBCT cases. Tepper et al. (64) reported a LLVC frequency of 53% on CT sections. Katakami et al. (127) observed LLVCs in 40% of the cases, which is consistent with that in the present study. In other studies, the frequency of LLVCs ranged from 30-80% (69, 126). Kaufman et al. (53) suggested that LLVCs located on the lingual aspect are bilateral structures. In the present study, there was a total of 5 (2.5%) of the LLVCs opening on the labial aspect and a total of 92 (46%) opening on the lingual aspect. Furthermore, LLVCs types were detected both unilaterally and bilaterally; there was one unilateral canal in 54 (48.2%) of the cases, two unilateral canals in 5 (4.5%) of the cases; [2 canals in total; on one side], and there was one bilateral canal in 46 (41%) of the cases; [2 canals in total; one on each side], two bilateral canals in only one case (1%); [4 canals in total; 2 on each side], one canal on one side and two canals on the other side in 6 (5.3%) of the cases; [3 canals in total]. To our knowledge and according to the available literature, this is the first study to classify LLVCs types according to the number of canals unilaterally and bilaterally, detecting 4 LLVCs bilaterally.

Sahman et al. (37) reported unilateral LLVCs in 70% of the cases, bilateral in 30%, with two of the bilateral cases having 3 LLVCs collectively; two canals on one side and one canal on the other side, however; they did not specify the detailed types of LLVCs. Tagaya et al. (129) observed bilateral LLVCs in 55% of the cases. Furthermore, Przystanska and Bruska (209) reported that the occurrence of bilateral LLVCs was 36%, and Patil et al. (132) reported it as 34%. In accordance with these studies, the general occurrence of bilateral LLVCs in the current study was 47.35%, and unilateral in 52.7%.

The high frequency of LLVCs observed in anatomy studies, when compared to radiology studies, and the wide variation in different studies can be attributed to examination methods, sample size, study design, and racial differences (132).

In this study, and in regards to the location of lateral canals, the highest frequency of LLVCs was located between the canine and the first premolar 30% on the right side, 22.5% on

the left side at the same tooth range, and the lowest frequency was detected between the two lower central incisors. In regards to gender, in the present study, only the range of the lateral lingual vascular canals (when there was one canal) on the right side was statistically significant, yet it could not be correlated to any specific finding or reason.

Von Arx et al. (130) also reported the first premolar area with the highest frequency 27.5% of LLVCs. Similarly, Katakami et al. (127) observed the highest prevalence of LLVCs in the right second premolar site 39.7%. The present study detected the highest prevalence of LLVCs in the area between the canine and the first premolar on the right side: 30%, with the general range of LLVCs on the right side as statistically significant in regrds to gender. On the other hand, Sahman et al. (37) reported the lowest frequency of LLVCs: 2.3% at the first molar area. The present study detected no LLVCs in the molar region.

The orientation or direction of the first lateral canal (when there was one in number) was almost similar for both right and left sides, varying from 5-6% superior, 10.5-11.5% horizontal, and 28 -29% inferior. The orientation of the second lateral canal (when there were two canals) was near similar for both right and left sides, varying from 0.5-1% superior, 0.5-2% horizontal, and 1.5% inferior. According to the available literature, this is the first study to explain and detect the orientation of the LLVCs, indicating that the usual orientation of LLVCs is in the horizontal direction.

The mandibular bone height at which LLVCs were located (when there was one in number) was almost similar for both right and left sides, varying from 10% in the upper one third of the mandibular height at the level where the lateral lingual vascular canal was detected, 34-35% in the middle one third, and 0 -0.5% in the lower one third of the mandibular height. The height of the second lateral canal (when there were two canals) was also near similar for both right and left sides, varying from 1.5-2% in the upper one third, 1-2.5% in the middle one third, and none in the lower one third of the mandibular height. According to the available literature, this is the first study to explain and detect the height of the LLVCs according to the total height of the mandible, indicating that the middle one third of the mandible in the interforaminal area contains the highest frequency of LLVCs existence. At the very least, increases in the degree of orientation of

the lateral lingual canals (either if it is one or two in number) were correlated with increases in the height of the canals in regards to the overall alveolar bone height at the measurement site.

As it is impossible to visualize the LLVCs with conventional 2-D radiography, a CBCT evaluation is recommended prior to surgical intervention to avoid any complications (37, 131). Reported complications include: nerve disturbances (124), and hemorrhage or bleeding in the floor of the mouth during and after implant insertion (130, 131). In particular, while inserting long dental implants; 15mm or more in length, as the most common cause of uncontrolled heavy bleeding in the anterior mandible is lingual cortical bone perforation (210).

In an anatomy study, Tepper et al. (64) demonstrated a sublingual artery in relation to the LLVCs. Kawai et al. (128) found that branches of the submental artery communicate with the mandibular incisive branch of the inferior alveolar artery. Katakami et al. (127) reported that the LLVCs may contain a branch of either the submental artery, sublingual artery, or an anastomosis of these arteries. These neurovascular structures, entering the mandible through the LLVCs are at risk during surgical procedures (37,128). Vascular trauma may induce sever bleeding problems that can be difficult to control (111, 124), and massive bleeding may possibly lead to subsequent airway obstruction (109, 111). This can be lethal, and requires instant intervention of securing the airway and bleeding control (211). In order to avoid this uncommon, yet serious risk, it is advisable to use short implants (210), and more caution and awareness regarding this part of the mandible is, highly, recommended (37).

5.6. Nutrient Canals:

These canals are in continuation with the IANC, branching from the MIC, as they supply the lower anterior region of the mandible, coursing to the lingual surface of the alveolar crest. NCs can embrace a nerve and blood vessels, which may explain the complications of bleeding and neurosensory disturbances during and after dental implant insertion at that region (212).

In this study, the NCs were detected in 96% of the cases, indicating that NCs is an almost permanent finding on CBCT scans. As regarding the frequency of bilateral symmetrical NCs range between teeth: the minimum were detected between the lower first incisors 2 (1%), and the maximum between the lower canines 62 (32%). In addition, the NCs existence extended to the

level of the second premolar teeth: 14 (7.3%) within the interforaminal region. Ogawa et al. (212) detected NCs and their forameni only in the incisor teeth region in 17 (16.2%) of the images, as they suggested that NCs terminate in LF, otherwise they are not considered as true NCs. The present study is in agreement with Ogawa et al. (212) that the NCs arise and branch from the MIC. However, it is in disagreement in that the presence of NCs is limited to the existence of the LF. As Yildirim et al. (213) reported that 37% of the patients presented with LF located in the lateral incisor to the first premolar region, yet; these forameni may include, but not limited to NCs. Moreover, Wang et al. (214), based on anatomy studies, reported that NCs may terminate in forameni located at the interdental area on the labial or lingual aspects of the anterior mandible. According to the findings in the present study, it can be said that the NCs existence may extend to the second premolar area, and perhaps the fact that Ogawa et al. (212) detected NCs only in the incisor teeth area provides a justification of the incidence discrepancy between the two studies.

5.7. Lingual Canals:

Goaz and White (215) described Lingual Forameni (LF) and their associated canals (LC) as the termination of the incisive branch of the mandibular canal. To evade surgical complications at that area, it is important to consider the location of LF and LC (216). Gahleitner et al. (217) assumed that the diameter of the LC is directly proportional to the diameter of the entering artery. Even though an atery with a diameter less than 1mm in width is unlikely to cause major bleeding problems, those with a larger diameter should be described in the "Radiology Report", as they can present bleeding control difficulties. Babiuc et al. (218) reported that 31% of LC had a diameter of at least 1mm. Perhaps recognized as a weakness; the present study neither incorporated measurement of the LC diameter nor LC bony depth or height in its design.

In the present study, the number of LCs ranged between zero to 3 canals, and their incidences were as follows: 1.5% with no lingual canals 46% with one canal, 50% with two canals, and 2.5% with three canals. According to their location in relation to genial tubercles; 31.5% were above, 13.5% were below, 2.5% through, 38% were above and below, 2.5% were above, below and through, 7.5% were above and through, 2.5% were below and through, and 1.5% showed no lingual canals. Whereas, Babiuc et al. (218) reported the distribution of LC number in 36 CBCT images as followes: 1 canal in about 72% of the images, 2 in 9.4%, 3 in

15.6%, and 4 in 3% of the images. In relation to genial tubercles (GT), the canals were detected above G.T in 63.3% of the images, below in 13.34%, and above and below G.T (when there were many canals) in 23.3% of the images. Among the two studies, only the relation of LC below GT was consistent. This can be attributed to the differences in study design and to the sample size.

In other terms, and regardless of the total number of LC, the present study showed that there are 79.2% of the LC above GT, and 50% of the cases with 2 canals, which is almost equal with the number of cases having only one canal. That may indicate that the midline area of the anterior mandible is not a safe region. However, 97% of the LC, regardless of the number or relation to GT, opened on the lingual aspect of the mandible, only 1.5% opened on the labial aspect, and only the location of LC in relation to GT was affected by gender. This may be attributed to size differences of the mandibular bone between females and males. On the other hand, Aoun et al. (219) reported that the LF and LC were present in 93.33% of the CBCT cases, and the majority (76.64%) was located above GT, which is very close to the incidence in the present study, in the study by Sheikhi et al. (216), and in that by Babiuc et al. (218). However, in the same study by Aoun et al. (219) neither the number of LC nor the location of the LF were statistically significant in regards to gender.

In a previous study, Liang et al. (62) reported 72% of LC with a downwards course, running to the labial aspect, [or as described in the current study with a superior course, directing towards the lingual aspect] and 28% of them with an upward direction, running to the labial aspect [or as described in the current study with an inferior course, directing towards the lingual aspect]. Sheikhi et al. (216) reported 96% of the superior LC with a downwards course, 1% with an upward direction, and 3% with a horizontal course, wit them all running to the labial aspect. They reported that from the inferior LC running to the labial aspect; 21.47% with a downwards course, 77.8% with an upward direction, and 2.68% with a horizontal course, concluding that the majority of the superior LC were with a downwards course, running to the labial aspect, and most of the inferior LC were withan upward direction, running to the labial aspect. This is consistent with the findings in the study by Kawai et al. (220).

Within the limits of this study, it can be concluded that within this sample of Turkish patients, there was a considerable variability in the LF and LC anatomy and location. Therefore,

the 20 types or figures allocated in this particular study (Figure 4.7) are more reasonable in detecting the number in relation to the exact location and orientation of the lingual canals as one type may contain more than one canal, each with a different location and orientation or direction. Furtheremore, the number, location, orientation, and opening aspect of the lingual canals should be meticulously considered in CBCT images while planning for dental implant placement in the midline region of the anterior mandible.

5.8. Lingual Foramen:

This is a consistent foramen at the middle of the anterior mandible (221). The contents of LF are rather confusing; Ennis (222) described the contents as an artery that branches of the incisive artery, and anastomose with the lingual artery; McDonnell et al. (221) described the contents as a single artery that results from an anastomosis of sublingual arteries coming from right and left sides, joined to form a common artery, entering the LF, supplying the superior surface of the genioglossus muscle. The cross-sectional histology of the specimens in the same study by McDonnell et al. (221) confirmed this vessel to be an artery with a plexus of perivascular vessels and occasional very small nerves around the artery, with no evidence of a neurovascular bundle or a vein of compatible size to the artery.

In the present study, the lingual foramen was detected in 98.5% of the CBCT images, indicating that it is an almost constant finding. This prevalence is almost consistent with Babiuc et al. (218), Tepper et al. (64), Gahleitner et al. (217), and Sheikhi et al. (216) who detected the LF in all of the CBCT cases. Whereas, the prevalence in all of these studies, including the current study, is in disagreement with that of Vujanovic-Eskenazi et al. (140) who identified LF in only 49% of the CBCT cases. It is worth mentioning that Sheikhi et al. (216), Babiuc et al. (218), and Choi et al. (223) detected 4 LF in 2.9%, 3%, and 15% respectively. Moreover, Gahleitner et al. (217) detected 5 LF in their study.

Based on an anatomy study, McDonnell et al. (221) suggested that the LF is a consistent finding on the lingual aspect of the mandible at the midline, as it was present in 99.04% of the dried specimens examined. This incidence is consistent with the finding in the present study, and is higher than those previously reported by Shiller and Wiswell (224), and Sutton (126), who reported LF as 89% and 85% respectively.

5.9.**General Interpretation of the Findings**:

It is important to highlight that although there were discrepancies between gender for both right and left sides for: mandibular canal number, mental foramen number, mental canal location, mental canal orientation, visibility of mandibular incisive canal, lateral lingual vascular canals number, lateral lingual vascular canals orientation, lateral lingual vascular canals range between mandibular teeth on the left side, lateral lingual vascular canals height, lateral lingual vascular canals aspect, the number of lingual canals, aspect of lingual canals, the location of lingual canals, the number of lingual foramina, aspect of lingual foramina, and the location of lingual foramina, they were all statistically not significant, and thus not affected by gender. This may indicate that these anatomical features are normal findings in the human mandible and are not specific for a certain gender. The same result can be assumed for age: as it is statistically insignificant, and awareness is to be raised, in this regard, while considering the plan for dental implants and surgical interventions.

Furthermore, the results in this study in regards to correlation coefficient, surmised that there was no statistical significance between the visibility of the MIC on either side with the mental canal length, or with lateral lingual vascular canals number, or with lateral lingual vascular canals length on the left side, or with lingual canal number on the midline.

5.10. Applications of the Findings:

This is the first study, to our knowledge and according to the available literature, to propose a meticulous systematic method to investigate the CBCT (via iCAT) imaging anatomy of the entire IANC. It is systematic in the sense that it tracks the canal from both right and left mandibular foramina to the midline as a complete continuous entity, including all of its likely variations and associations in the same assessment for the same patient.

The results of the present study present practical information for surgical interventions, and may protect patients from complications. Knowledge of the IANC with its variations and associations are clinically important for surgical dental procedures that involve the mandible, and perhaps the main purpose of this study was to call attention to these variations and associations, as their presence may induce surgical or post-surgical complications, and anxiety in inexperienced practitioners.

The present study highly recommends a precise CBCT imaging guideline for placing dental implants in the mandible for each and every case at the allocated side(s). This CBCT imaging guideline includes detecting the following image parameters:

1.   Mandibular Foramen Number.

2.   Mandibular Canal Number.

3.   Mental Foramen Number.

4.   Mental Canal: Length- Location- Orientation-Angulation.

5.   Mandibular Incisive Canal visibility.

6.   Lateral Lingual Vascular Canals: Number in relation to side- Length- Orientation- Range-Height- Aspect.

7.   Nutrient Canals: Number and Range.

8.   Lingual Canal: Number- Aspect- Location- Type (classification).

9.   Lingual Foramen: Number- Aspect- Location.

Many of these image parameters can be correlated to certain classifications that already exist in the current CBCT imaging literature. However, the rest of these unrecognized and\or unorganized parameters; especially the novel ones, can be proposed by the present study as new classifications and sub-classifications.

5.10.1. Proposed Classifications and Sub-classifications:

With the discovery of new techniques and new prospective, scientific knowledge may transform. As a nature of science, researchers commonly debate new information, arriving at new understandings, and consequently new classifications. On those grounds and in accordance to the results of the present study; the following classifications can be recommended as a protocol for the "Radiology Report", while conducting CBCT image analysis, especially for dental implants placement.

5.10.1.1. Mental canal classification:

According to their distance and angulation of opening, Mental Canals (MeC) can be classified as two main classes: Symmetric and Asymmetric (Table 5.1). These can be further sub-classified in accordance to the angulation groups mentioned earlier (Table 4.4).

Table 5.1. Proposed Mental Canal Classification and sub-classification.

Class	Sub-class	Description
Symmetric	**A**	Symmetric with equel angles
	B	Symmetric and belong to the same angle group*
	C	Symmetric, but does not belong to the same angle group
Asymmetric	**A**	Asymmetric with equel angles
	B	Asymmetric and belong to the same angle group*
	C	Asymmetric, but does not belong to the same angle group
*Angle groups: Angle=0^0 (Horizontal) Angle above 0^0 and below 45^0 (Superior: 0^0-44^0) Angle above 45^0 and below 90^0 (Superior: 45^0-90^0)		

5.10.1.2. Mandibular Incisive Canal Classification:

According to their visibility, MIC can be mainly classified into two classes as Visible and Non visible (Table 5.2).

Table 5.2. Proposed Mandibular Incisive Canal Classification.

Class	Description
Class I	MIC Non visible
Class II	MIC Visible: • Visible and continuous • Visible, but not continuous.

5.10.1.3. Lateral Lingual Vascular Canals Classification:

According to their location on the right and\or left sides\side of the mandible, and according to their number in the interforaminal region, LLVCs can be mainly classified into three classes: No LLVCs, Unilateral LLVCs, and Bilateral LLVCs (Table 5.3).

Table 5.3. Proposed Lateral Lingual Vascular Canals Classification according to location.

Class	Description
Class 0	**No LLVC**
Class I	**Unilateral LLVCs:** • One canal at one side; right or left. • Two canals at one side; right or left.
Class II	**Bilateral LLVCs:** • One canal on both sides; right and left. • Two canals on both sides; right and left. • One canal on one side and two canals on the other side.

According to their location, LLVCs can be further sub-classified in accordance to: a. Range, and b. Height of the canals (Table 5.4).

Table 5.4. Proposed Lateral Lingual Vascular Canals sub-classification according to range and height.

Sub-class	Description
Range 1	Between the two central incisors: at the midline.
Range 2	Between central incisor and lateral incisor (at the same side).
Range 3	Between the lateral incisor and canine (at the same side).
Range 4	Between the canine and first premolar (at the same side).
Range 5	Between the first premolar and second premolar (at the same side).
Height 1	Upper one third of the bone height.
Height 2	Middle one third of the bone height.
Height 3	Lower one third of the bone height.

LLVCs can be further sub-classified, according to their: c. Orientation, and d. Aspect of opening in the interforaminal region (5.5).

Table 5.5. Proposed Lateral Lingual Vascular Canals sub-classification according to their orientation and aspect.

Sub-class	Description
Orientation 1	Superior direction
Orientation 2	Horizontal direction
Orientation 3	Inferior direction
Aspect 1	Lingual
Aspect 2	Labial

5.10.1.4. Lingual Canal Classification:

According to number and location in relation to Genial Tubercles (GT), LC can be classified into four classes, with each class assigned to LC figure number (Figure 4.7) in consideration to the LC number, orientation, and opening aspect (Table 5.6).

Table 5.6. Proposed Lingual Canal Classification according to number, orientation, figure and aspect.

Class	Description	LC Figure number
Class 0	**No Lingual Canals**	Fig. 7
Class I	**One LC:** • One LC above GT. • One LC through or at GT. • One LC below GT	Fig.3, Fig.6, and Fig.16. Fig.2 and Fig.11. Fig.8 and Fig.19.
Class II	**Two LCs:** • Two LCs; above and through or at GT. • Two LCs; above and below GT. • Two LCs; below and through or at GT. • Two LCs below GT.	Fig.5 and Fig.15. Fig.4, 9, 10, 12, 17 and Fig.18. Fig.13. Fig.14 and Fig. 20.
Class III	**Three LCs or more:** • Three LCs above, through, and below GT.	Fig.1.

5.11. The Limitations of the Study:

The procedure of following the steps in this proposed method can be tedious and protracted. In few cases, the process of selecting a lingual canal shape or figure from the 20 allocated figures was not easy, especially when there were more than one lingual canal and the canals were not aligned on the same cross-section. So, a very meticulous, continuous, and repetitive movement of the cursor is required.

In some cases, the measurement of LLVCs Height changed from one cross-section to another within millimetres, as the LLVC continued to exist in successive cross- sections, but in different heights. So, a numerical or a numbering system for each slice-thickness in every cross-section can be recommended to the software design manufacturer.

6. CONCLUSIONS

This study contains a CBCT imaging account of the intra-osseouse course of the IANC in the mandible. Accordingly, the following conclusions were made:

- The IANC is mainly constituted of the mandibular canal, which commences from the mandibular foramen and transmits the neurovascular bundle to the mental incisive region through the mental foramen and the mandibular inscisive canal. In general, this canal is a single structure with probable variations and associations.

- The MIC is a constant anatomical structure that can be detected in CBCT images, and should be considered in surgical treatment plans, especially dental implant.

- The presence of BMC can be described as an "unusual variation", the RMC as a "normal anatomical variation" rather than an anomaly, the NCs, LC and the LF at the midline as constant anatomical features and the TMC as a "rare variation". Nevertheless, their detection is irrefutable by CBCT imaging.

- The incidence of RMC emphasizes their clinical significance in surgical procedures involving the retromolar area, failure of inferior alveolar nerve block, and the possibility of bleeding.

- Different patterns occur, and it should not be always assumed that there is only one mental foramen on each side. Moreover, there is a great inconsistency of the ALL or mental canal length. Therefore, it is not safe to recommend any definite distance mesially from the mental foramen.

- LLVCs are located in the interforaminal vicinity with the highest frequency between the canine and the first premolar on both right and left sides in the middle one third of the mandibular bone height at the measurement site. At that region, their usual orientation is in the horizontal direction.

- The number, location, orientation, and opening aspect of the LC should be meticulously considered in CBCT images while planning for dental implant placement in the midline region. The incidence of LC above GT may indicate that the midline area of the anterior mandible is not a safe region. Accordingly, the use of short dental implants is adviced, and lingual canal or a

lateral lingual vascular canal with a diameter more than 1 mm in diameter has the potential to cause a major bleeding problem. Therefore it should be described in the "Radiology Report".

- Prior to the performance of surgical procedures in the vicinity of the IANC, it is crucial to conduct a meticulous evaluation method that involves a systematic radiographic examination, following a particular imging guidline, which considers not only the main structure of the canal, but also its variations and associations.

- Proposed classifications and sub-classifications can be recommended and integrated with the guidelines for the "Radiology Report", while conducting CBCT image analysis, especially for dental implant placement, namely conserning: the MeC, MIC, LLVCs, and LC.

- Currently, panoramic radiography might not be completely adequate. Therefore, CBCT imaging has been proved to be a gold standard among the various imaging modalities used in dental implant treatment planning, as cross-sectional CBCT images provide superlative evaluation of the IANC configuration and course, as well as comprehensive detection of distinctive variations and associations in the dental clinic.

7. REFERENCES

1. Topcu AO, Avcu N, Uysal S, Yamalik N. Presence, location and course of mandibular incisive canal and inter-examiner variation: A spiral CT scan study. *Clinical Dentistry and Research*. 2015; 39(2): 56-68.

2. Lindh C, Petersson A, Klinge B. Measurements of distances related to the mandibular canal in radiographs. *Clinical Oral Implants Research*. 1995; 6: 96–103.

3. Haribhakti VV. The dentate adult human mandible: An anatomic basis for surgical decision making. *Plastic and Reconstructive Surgery*.1996; 97: 536–543.

4. Wadu SG, Penhall B, Townsend GC. Morphological variability of the human inferior alveolar nerve. *Clinical Anatomy*. 1997; 10: 82–87.

5. Yang J, Cavalcanti MG, Ruprecht A, Vannier MW. 2-D and 3-D reconstructions of spiral computed tomography in localization of the inferior alveolar canal for dental implants. *Oral Surgery, Oral Medicine, Oral Pathology, Oral Radiology and Endodontology*. 1999; 87: 369–374.

6. Polland KE, Munro S, Reford G, Lockhart A, Logan G, Brocklebank L, McDonald SW. The mandibular canal of the edentulous jaw. *Clinical Anatomy*. 2001; 14: 445–452.

7. Serhal CB, Van Steenberghe D, Quirynen M, Jacobs R. Localisation of the mandibular canal using conventional spiral tomography: A human cadaver study. *Clinical Oral Implants Research*. 2001; 12: 230–236.

8. Serhal CB, Jacobs R, Flygare L, Quirynen M, Van Steenberghe D. Perioperative validation of localisation of the mental foramen. *Dentomaxillofacial Radiology*. 2002; 31: 39–43.

9. Mardinger O, Chaushu G, Arensburg B, Taicher S, Kaffe I. Anatomic and radiologic course of the mandibular incisive canal. *Surgical and Radiologic Anatomy*. 2000; 22: 157–161.

10. De Andrade E, Otomo-Corgel J, Pucher J, Ranganath KA, St George N Jr. The intraosseous course of the mandibular incisive nerve in the mandibular symphysis. *International Journal of Periodontics and Restorative Dentistry*. 2001; 21: 591–597.

11. Jacobs R, Mraiwa N, Van Steenberghe D, Gijbels F, Quirynen M. Appearance, location, course, and morphology of the mandibular incisive canal: An assessment on spiral CT scan. *Dentomaxillofacial Radiology*. 2002; 31: 322–327.

12. Jacobs R, Mraiwa N, Van Steenberghe D, Sanderink G, Quirynen M. Appearance of the mandibular incisive canal on panoramic radiographs. *Surgical and Radiologic Anatomy*. 2004; 26: 329–333.

13. Mraiwa N, Jacobs R, Moerman P, Lambrichts I, Van Steenberghe D, Quirynen M. Presence and course of the incisive canal in the human mandibular interforaminal region: Two dimensional imaging versus anatomical observations. *Surgical and Radiologic Anatomy*. 2003; 25: 416–423.

14. Makris N, Stamatakis H, Syriopoulos K, Tsiklakis K, Stelt PF. Evaluation of the visibility and the course of the mandibular incisive canal and the lingual foramen using cone-beam computed tomography. *Clin. Oral Impl Res*. 2010; 21: 766-771.

15. Eshak M, Brooks S, Abdel-Wahed N, Edwards PC. Con Beam CT evaluation of the presence of anatomic accessory canals in the jaws. *Dentomaxillofacial Radiology*. 2014; 43: 20130259.

16. Tadinada A, Schneider S, Yadav S. Evaluation of the diagnostic efficacy of two cone beam computed tomography protocols in reliably detecting the location of the inferior alveolar nerve canal. *Dentomaxillofacial Radiology*. 2017; 46 (5):20160389.

17. Patrícia P-M, Emerson T-S, Marcelo-Augusto O-S. The mandibular incisive canal and its anatomical relationships: A cone beam computed tomography study. *Med Oral Patol Oral Cir Bucal*. 2015; 1; 20 (6):723-278.

18. Sokhn S, Nasseh I, Noujeim M. Using cone beam computed tomography to determine safe regions for implant placement. *General Dentistry*. 2011; 59: 72-77.

19. Naitoh M, Hiraiwa Y, Aimiya H, Ariji E. Obsrevation of bifid mandibular canal using cone-beam computed tomography. *Int. J Oral Maxillofac Implants*. 2009; 24: 155-159.

20. Rashsuren O, Choi J-W, Han W-J, Kim E-K. Assessment of bifid and trifid mandibular canals using cone-beam computed tomography. *Imaging Science in Dentistry*. 2014; 44: 229-236.

21. Neves FS, Nascimento MC, Oliveira ML, Almeida SM, B´oscolo FN. Comparative analysis of mandibular anatomical variations between panoramic radiography and cone beam computed tomography. *Oral Maxillofac Surg*. 2014; 18: 419–24.

22. Haas LF, Dutra K, Porporatti AL, Mezzomo LA, Canto G, Flores-Mir C, Correa M. Anatomical variations of mandibular canal detected by panoramic radiography and CT: A systematic review and meta-analysis. *Dentomaxillofacial Radiology.* 2016; 45: 20150310.

23. Juodzbalys G, Wang HL, Sabalys G. Anatomy of mandibular vital structures. Part I mandibular canal and inferior alveolar neurovascular bundle in relation with dental implantology. *J Oral Maxillofac Res.* 2010; 1: e2.

24. Jacobs R, Lambrichts I, Liang X, Martens W, Mraiwa N, Adriaensens P, et al. Neurovascularization of the anterior jaw bones revisited using high-resolution magnetic resonance imaging. *Oral Surg Oral Med Oral Pathol Oral Radiol Endod.*2007; 103: 683–93.

25. Kalantar Motamedi MH, Navi F, Sarabi N. Bifid mandibular canals: prevalence and implications. *J Oral Maxillofac Surg.* 2015; 73: 387–390.

26. Angelopoulos C. Anatomy of the maxillofacial region in the three planes of section. *Dent Clin N Am.* 2014; 58(497-521).

27. White SC, Pharoah MJ. Oral Radiology: Principles and Interpretation. 7th ed.Elsevier, Mosby; 2014.

28. White SC, Pharoah MJ. Oral Radiology: Principles and Interpretation. 6[th]ed. Elsevier, Mosby; 2009.

29. Pauwels R, Araki K, Thongvigitmanee SS. Technical aspects of dental CBCT: State of art. *Dentomaxillofac Radiol.* 2015; 44: 20140224.

30. White SC, Pharoah MJ. The Evaluation and Application of Dental Maxillofacial Imaging Modalities. *Dent Clin N Am.* 2008; 52: 689-705.

31. Horner K, Islam M, Flygare L, Tsiklakis K, Whaites E. Basic principles for use of dental cone beam computed tomography: Consensus Guidelines of the European Academy of Dental and Maxillofacial Radiology. *Dentomaxillofac Radiol.* 2009; 38:187-195.

32. Scarfe WC, Farman AG. What is cone-beam ct and how does it work. *Dent Clin N Am.* 2008; 52: 707-730.

33. Alamri HM, Sadrameli M, Alshalhoob MA, Alshehri MA. Applications of CBCT in dental practice: a review of the literature. *Gen Dent.* 2012; 60: 390-400.

34. Koenig LJ, Tamimi D, Petrikowski CG, Harnsberger HR, Ruprecht A, Benson BW, Van Dis ML, Hatcher D, Perschbacher SE. Diagnostic Imaging: Oral and Maxillofacial. 1st ed. AMIRSYS, Inc; 2012.

35. SEDENTEXCT. Radiation Protection: Cone Beam CT for Dental and Maxiilofacial Radiology. Evidence based guidelines: A report prepared by the SEDENTEXCT project 2011: www.sedentexct.eu [Accessed on 16.03.2016].

36. European Commission. Radiation protection No. 172: Cone Beam CT for Dental and Maxillosacial Radiology. Evidence Based Guidelines. Luxembourg: Directorate-General for Energy; 2012.

37. Sahman H, Sekerci EA, Ertas ET. Lateral lingual vascular canals of the mandible: A CBCT study of 500 cases. *Surg Radiol Anat.* 2014; 36: 865-870.

38. Pires CA, Bissada NF, Becker JJ, Kanawati A, Landers MA. Mandibular incisive canal: cone beam computed tomographycid. *Clinical Implant Dentistry and Related Research.*2012; 14 (1): 228 67-73.

39. Matzen LH, Wenzel A. Efficacy of CBCT for assessment of impacted mandibular third molars: a review- based on hierarchical model of evidence. *Dentomaxillofac Radiol.* 2015; 44: 20140189.

40. Rana SS, Duggal R, Kharbanda OP. Area and volume of the pharyngeal airway in surgically treated unilateral cleft lip and palate patient: A cone beam computed tomography study. *Journal of Cleft Lip Palata and Craniofacial Anomalies*. 2015; 2(1): 27-33.

41. Tyndall DA, Brooks SL. Selection criteria for dental implant site imaging: a position paper of the American Academy of Oral and Maxillofacial Radiology. *Oral Surg Oral Med Oral Pathol Oral Radiol Endod.* 2000; 89:630–637.

42. Tal H, Moses O. A comparison of panoramic radiography and computed tomography in the planning of implant surgery. *Dentomaxillofac Radiol.* 1991; 20:40–42.

43. Casselman JW, Quirynen M, Lemahieu SF, Baert AL, Bonte J. Computed tomography in the determination of anatomical landmarks in the perspective of endosseous implant installation. *J Head Neck Pathol.* 1988; 7:255–264.

44. Schwarz MS, Rothman SLG, Rhodes ML, Chafetz N. Computed tomography: part 1. Preoperative assessment of the mandible for endosseous implant surgery. *Int J Oral Maxillofac Implants.*1987; 2:137–141.

45. Schwarz MS, Rothman SLG, Rhodes ML, Chafetz N. Computed tomography: part 2. Preoperative assessments of the mandible for endosseous implant surgery. *Int J Oral Maxillofac Implants.*1987; 2:142–145.

46. Rosa MB, Sotto-Maior BS, Machado VC, Francischone CE. Retrospective study of the anterior loop of the inferior alveolar nerve and the incisive canal using cone beam computed tomography. *The International Journal of Oral & Maxillofacial Implants*. 2013; 28:388-392.

47. Von Arx T, Häfliger J, Chappuis V. Neurosensory disturbances following bone harvesting in the symphysis: A prospective clinical study. *Clinical Oral Implants Research*. 2005; 16: 432-439.

48. Santos T, Gomes AA, Melo DG, Melo AR, Cavalcante JR, Araújo LG, et al. Evaluation of reliability and reproducibility of linear measurement of cone-beam-computed tomography. *Indian Journal of Dental Research.* 2012; 23:473-8.

49. Jeffcoat M, Jeffcoat RL, Reddy MS, Berland L. Planning interactive implant treatment with 3-D computed tomography. *J Am Dent Assoc.* 1991; 122:40–44.

50. Makins SR. Artifacts interfering with interpretation of cone beam computed tomography images. *Dent Clin North Am*. 2014; 58 (3): 485-495.

51. Tadinada A, Jalali E, Jadhav A, Schincaglia GP, Yadav S. Artifacts in cone beam computed tomography image volumes: An illustrative depiction. *J Mass Dent Soc*. 2015; 64 (1):12 15.

52. Rouas P, Nancy J, Bar D. Identification of double mandibular canals: literature review and three case reports with CT scans and cone bean CT. *Dentomaxillofacial Radiology*. 2007; 36:34-38.

53. Kaufman E, Serman NJ, Wang PD. Bilateral mandibular accessory foramina and canals: A case report and review of the literature. *Dentomaxillofacial Radiology*. 2000; 29:170-175.

54. Matzen LH, Christensen J, Hintze H, Schou S, Wenzel A. Diagnostic accuracy of panoramic radiography, stereo- scanography and cone beam CT for assessment of mandibular third molars before surgery.*Acta Odontol Scand.* 2013; 71: 1391-1398.

55. Tantanapornkul W, Okouchi K, Fujiwara Y, Yamashiro M, Marouka Y, Ohbayashi N, et al. A comparative study of CBCT and conventional panoramic radiography in assessing the topographic relationship between the mandibular canal and the impacted third molars. *Oral Surg Oral Med Oral Path Oral Radiol Endod.* 2007; 103: 253-259.

56. Naitoh M, Nakahara K, Suenaga Y, Gotoh K, Kondo S, Ariji E. Comparison between cone-beam and multislice computed tomography depicting mandibular neurovascular canal structures. *Oral Surg Oral Med Oral Pathol Oral Radiol Endod*. 2010; 109: 25–31.

57. Scarfe WC, Farman AG, Sukovic P. Clinical applications of conebeam computed tomography in dental practice. *J Can Dent Assoc.* 2006; 72: 75–80.

58. Babiuc I, Tarlungeanu I, Pauna M. Cone beam computed tomography observations of the lingual foramina and their bony canals in the median region of the mandible. *Rom J Morphol Embryol.* 2011; 52 (3): 872-829.

59. Kiersch TA, Jordan JE. Duplication of the mandibular canal. *Oral Surg Oral Med Oral Pathol.* 1973; 35: 133–4.

60. Nortje CJ, Farman AG, Grotepass FW. Variations in the normal anatomy of the inferior dental (mandibular) canal: A retrospective study of panoramic radiographs from 3612 routine dental patients. *Br J Oral Surg.* 1977; 15: 55–63.

61. Olivier, E. The inferior dental canal and its nerve in the adult. *British Dental Journal.* 1928; 49: 356–358.

62. Liang X, Jacobs R, Lambrichts I, Vandewalle G. Lingual foramina on the mandibular midline revisited: A macroanatomical study. *Clinical Anatomy.* 2007; 20:246-251.

63. Uchida Y, Noguchi N, Goto M, Yamashita Y, Hanihara T, Takamori H, et al. Measurement of anterior loop length for the mandibular canal and diameter of the mandibular incisive canal to avoid nerve damage when installing endosseous implants in the interforaminal region: Second attempt introducing cone beam computed tomography. *Journal of Oral and Maxillofacial Surgery.* 2009; 67:744-750.

64. Tepper G, Hofschneider UB, Gahleitner A, Ulm C. Computed tomographic diagnosis and localization of bone canals in the mandibular interforaminal regions for prevention of bleeding complications during implant surgery. *The International Journal of Oral & Maxillofacial Implants.* 2001; 16:68-72.

65. Kütük N, Demirbaz AE, Gönen ZB, Topan C, Kiliç E, Etö OA, et al. Anterior Mandibular Zone Safe for Implants. *The Journal of Craniofacial Surgery.* 2013; 24: 405-408.

66. Oliveira-Santos C, Souza PHC, Berti-Couto AS, Stinkens L, Moyaert K, Rubira-Bullen IRF, et al. Assessment of variations of the mandibular canal through cone beam computed tomography. *Clinical Oral Investigations.* 2012; 16: 387-393.

67. Ramesh AS, Rijesh K, Sharma A, Prakash R, Arun Kumar A, Karthik. The prevalence of mandibular incisive nerve canal and to evaluate its average location and dimension in Indian population. *J Pharm Bioallied Sci.* 2015; 7(2): 594–596.

68. Langlais RP, Broadus R, Glass BJ. Bifid mandibular canals in panoramic radiographs. *J Am Dent Assoc.* 1985; 110: 923-926.

69. Carter RB, Keen EN. The intra mandibular course of the inferior alveolar nerve. *J Anat.* 1971; 108: 433-40.

70. Bogdán S, Pataky L, Barabás J, Németh Z, Huszár T, Szabò G. Atypical courses of the mandibular canal: comparative examination of dry mandibles and x-rays. *J Craniofac Surg.* 2006; 17:487-91.

71. Auluck A, Pai KM, Mupparapu M. Multiple mandibular nerve canals: Radiographic observations and clinical relevance. Report of 6 cases. *Quintessence Int.* 2007; 38: 781-7.

72. Wadhwani P, Mathur RM, Kohli M, Sahu R. Mandibular canal variant: A case report. *J Oral Pathol Med.* 2008; 37: 122-124.

73. Grover PS, Lorton L. Bifid mandibular nerve as a possible cause of inadequate anesthesia in the mandible. *J Oral Maxillofac Surg.* 1983; 41: 177-179.

74. Claeys V, Wackens G. Bifid mandibular canal: Literature review and case report. *Dentomaxillofac Radiol.* 2005; 34: 55-8.

75. Naitoh M, Hiraiwa Y, Aimiya H, Gotoh M, Ariji Y, Izumi M, et al. Bifid mandibular canal in Japanese. *Implant Dent.* 2007; 16: 24-32.

76. Lee JS, Yoon SJ, Kang BC. Mandibular canal branches supplying the mandibular third molar observed on cone beam computed tomographic images: Reports of four cases. *Korean J Oral Maxillofac Radiol.* 2009; 39: 209-212.

77. Lee HW, Kim YG, Lee BS, Kwon YD, Choi BJ, Kim YR. Bifid mandibular canal: Radiographic observation and clinical relevance: A case report. *J Korean Dent Soc Anesthesiol.* 2009; 9: 24-29.

78. Kuribayashi A, Watanabe H, Imaizumi A, Tantanapornkul W, Katakami K, Kurabayashi T. Bifid mandibular canals: cone beam computed tomography evaluation. *Dentomaxillofac Radiol.* 2010; 39: 235-239.

79. Mizbah K, Gerlach N, Maal TJ, Bergé SJ, Meijer GJ. The clinical relevance of bifid and trifid mandibular canals. *Oral Maxillofac Surg.* 2012; 16: 147-51.

80. Fu E, Peng M, Chiang CY, Tu HP, Lin YS, Shen EC. Bifid mandibular canals and the factors associated with their presence: a medical computed tomography evaluation in a Taiwanese population. *Clin Oral Implants Res.* 2014; 25: 64-67.

81. Kang JH, Lee KS, Oh MG, Choi HY, Lee SR, Oh SH, et al. The incidence and configuration of the bifid mandibular canal in Koreans by using cone-beam computed tomography. *Imaging Sci Dent.* 2014; 44: 53-60.

82. Orhan K, Aksoy S, Bilecenoglu B, Sakul BU, Paksoy CS. Evaluation of bifid mandibular canals with cone-beam computed tomography in a Turkish adult population: a retrospective study. *Surg Radiol Anat.* 2011; 33: 501-507.

83. Chavez-lomeli MF, Mansilla Lory J, Pompa JA, Kjaer I. The human mandibular canal arises from three separate canales innervating different tooth groups. *J Dent Res* 1996; 75: 1540-1544.

84. Kim M-S, Yoon S-J, Park H-W, Kang J-H, Yang S-Y, Moon Y-H, Jung N-R, Yoo H-I, Oh W-M, Kim S-H. A false presence of bifid mandibular canals in panoramic radiographs. *Dentomaxillofacial Radiology.* 2011; 40, 434-438.

85. Orhan AI, Orhan K, Aksoy S, Ozgul O, Horasan S, Arslan A, et al. Evaluation of perimandibular neurovascularization with accessory mental foramina using cone-beam computed tomography in children. *J Craniofac Surg.* 2013; 24: 365–369.

86. Muinelo-Lorenzo J, Su´arez-Quintanilla JA, Fern´andez-Alonso A, Marsillas-Rascado S, Su´arez-Cunqueiro MM. Descriptive study of the bifid mandibular canals and retromolar foramina: cone beam CT vs panoramic radiography. *Dentomaxillofacial Radiology*. 2014; 43 (5) :20140090.

87. Patil S, Matsuda Y, Nakajima K, Araki K, Okano T. Retromolar canals as observed on cone-beam computed tomography: Their incidence, course, and characteristics. *Oral Surg Oral Med Oral Pathol Oral Radiol.* 2013; 115: 692-699.

88. Gamieldien MY, Van Schoor A. Retromolar foramen: An anatomical study with clinical considerations. *British Journal of Oral and Maxillofacial Surgery.* 2016. 54; 784–787.

89. Von Arx T, Hänni A, Sendi P, Buser D, Bornstein MM. Radiographic study of the mandibular retromolar canal: An anatomic structure with clinical importance. *J Endod.* 2011; 37 (12): 1630–1635.

90. Potu BK, Jagadeesan S, Bhat KM, Sirasanagandla SR. Retromolar foramen and canal: A comprehensive review on its anatomy and clinical applications. *Morphologie*. 2013; 97, (317): 31-37.

91. Von Arx T, Bornstein MM, Werder P, Bosshardt D. The retromolar canal (foramen retromolare). Overview and case report. *Schweiz Monatsschr Zahnmed*. 2011; 121 (9):821-34.

92. Park M-K, Jung W, Bae J-H, Kwak H-H. Anatomical and radiographic study of the mandibular retromolar canal. *Journal of Dental Sciences.* 2016; 11, 370-376.

93. Motamedi M H K, Gharedaghi J, Mehralizadeh S, Navi F, Badkoobeh A, Valaei N, Azizi T. Anthropomorphic assessment of the retromolar foramen and retromolar nerve: Anomaly or variation of normal anatomy?. *Int J Oral MaxillofacSurg*. 2016; 45: 241–244.

94. Ossenberg NS. Retromolar foramen of the human mandible. *Am J Phys Anthropol*. 1987; 73 (1):119-128.

95. Han S-S, Hwang Y-S. Cone beam CT finding of retromolar canals in a Korean population. *Surg Radiol Anat*. 2014; 36: 871-876.

96. Fukami K, Shiozaki K, Mishima A, Kuribayashi A, Hamada Y, Kobayashi K. Bifid mandibular canal: confirmation of limited cone beam CT findings by gross anatomical and histological investigations. *Dentomaxillofac Radiol.* 2012; 41: 460–465.

97. Silva FM, Cortez AL, Moreira RW, Mazzonetto R. Complications of intraoral donor site for bone grafting prior to implant placement. *Implant Dent.* 2006; 15: 420–6.

98. Renton T, Dawood A, Shah A, Searson L, Yilmaz Z. Postimplant neuropathy of the trigeminal nerve. A case series. *Br Dental J.* 2012; 212: e17.

99. Sanchis JM, Peñarrocha M, Soler F. Bifid mandibular canal. *J Oral Maxillofac Surg.* 2003; 61: 422–424.

100. Yeong-Hoon K, Hun-Mu Y. Conventional panoramic radiograph cannot identify the bifid mandibular canal. *J Craniofac Surg.* 2015; 26: 674–675.

101. Kawai T, Asaumi R, Sato I, Kumazawa Y, Youse T. Observation of the retromolar foramen and canal of the mandible: a CBCT and macroscopic study. *Oral Radiol.* 2012; 28:10–14.

102. Wyatt WM. Accessory mandibular canal: Literature review and presentation of an additional variant. *Quintessence Int.* 1996; 27:111–113.

103. Bilecenoglu B, Tuncer N. Clinical and anatomical study of retromolar foramen and canal. *J Oral Maxillofac Surg.* 2006; 64: 1493–1497.

104. Narayana K, Nayak UA, Ahmed WN, et al. The retromolar foramen in South Indian dry mandibles. *European Journal of Anatomy*. 2002; 6:141–146.

105. Singh S. Aberrant buccal nerve encountered at third molar surgery. *Oral Surg Oral Med Oral Pathol*. 1981; 52: 142-146.

106. Loubele M, Bogaerts R, Van Dijck E, Pauwels R, Vanheusden S, Suetens P, et al. Comparison between effective radiation dose of CBCT and MSCT scanners for dentomaxillofacial applications. *Eur J Radiol*. 2009; 71: 461–468.

107. Liang X, Jacobs R, Hassan B, Li L, Pauwels R, Corpas L, et al. A comparative evaluation of cone beam computed tomography (CBCT) and multi-slice CT (MSCT) Part I. On subjective image quality. *Eur J Radiol*. 2010; 75: 265–269.

108. Imada TN, Fernandes LP, Centurion BS, De Oliveira-Santos C, Honorio HM, Fischer IR, Rubira-Bullen IR. Accessory mental foramina: Prevalence, position and diameter assessed by cone-beam computed tomography and digital panoramic radiographs. *Clin Oral Implants Res*. 2014; 25: 94–99.

109. Givol N, Chaushu G, Halamish-Shani T, Taicher S. Emergency tracheostomy following life-threatening hemorrhage in the floor of the mouth during immediate implant placement in the mandibular canine region. *J Periodontol*. 2000; 71:1893–1895.

110. Mason ME, Triplett RG, Alfonso WF. Life-threatening hemorrhage from placement of a dental implant. *J Oral Maxillofac Surg*. 1990; 48:201–204.

111. Kalpidis CD, Setayesh RM. Hemorrhaging associated with endosseous implant placement in the anterior mandible: A review of the literature. *J Periodontol*. 2004; 75: 631–645.

112. Scaravilli MS, Mariniello M, Sammartino G. Mandibular lingual vascular canals (MLVC): Evaluation on dental CTs of a case series. *Eur J Radiol*. 2010; 76:173–176.

113. Brocklebank L. Dental radiology: Understanding the X-ray image. Oxford University Press: New York; 1997.

114. Goaz PW, White SC. Oral Radiology: Principles and Interpretation. 3rd ed. MosbyYear Book Inc: Toronto; 1994.

115. Kassle MJ. An Atlas of Dental Radiographic Anatomy. 3rd ed. W B Saunders: Toronto; 1989.

116. Mansong-Hing LR. Fundamentals of Dental Radiography. 3rd ed. Philadelphia: Lea and Febiger; 1990.

117. Langland OE, Langlais RP. Principles of Dental Imaging. Baltimore: Williams and Wilkins; 1997.

118. Last RJ. Anatomy, Regional and Applied. 7th ed. London: Churchill Livingstone, 1984.

119. Woodburne RT, Burkel WE. Essentials of Human Anatomy. 8thed. New York: Oxford University Press; 1988.

120. Williams PL, Warwick R, Dyson M, Bannister LH. Gray's Anatomy. 37thed. Edingburgh: Churchill Livingstone; 1989.

121. Agur AMR. Grant's Atlas of Anatomy. 9thed. Baltimore: Williams and Wilkins; 1991.

122. Moore K. Clinically Oriented Anatomy. 3rd ed. Baltimore: William and Wilkins, 1992.

123. Bodner L, Bar-Ziv J, Reichenthal E. Trigeminal neuropathy: Improved imaging with a dental computed tomography software program. *J Oral Maxillofac Surg*.1998; 56: 545 - 548.

124. Murlimanju BV, Prakash KG, Samiullah D, Prabhu LV, Pai MM, Vadgaonkar R, Rai R. Accessory neurovascular foramina on the lingual surface of mandible: Incidence, topography, and clinical implications. *Indian J Dent Res.* 2012; 23 (3): 433.

125. Oliveira-Santos C, Souza PHC, Berti-Couto SD, Stinkens L, Moyaert K, Van Assche N, Jacobs R. Characterisation of additional mental foramina through cone beam computed tomography. *J Oral Rehabil.* 2011; 38: 595–600.

126. Sutton RN. The practical significance of mandibular accessory foramina. *Aust Dent J.* 1974; 19: 167–173.

127. Katakami K, Mishima A, Kuribayashi A, Shimoda S, Hamada Y, Kobayashi K. Anatomical characteristics of the mandibular lingual foramina observed on limited cone-beam CT images. *Clin Oral Implants Res.* 2009; 20: 386–390.

128. Kawai T, Sato I, Yosue T, Takamori H, Sunohara M. Anastomosis between the inferior alveolar artery branches and submental artery in human mandible. *Surg Radiol Anat* 2006. 28:308–310.

129. Tagaya A, Matsuda Y, Nakajima K, Seki K, Okano T. Assessment of the blood supply to the lingual surface of the mandible for reduction of bleeding during implant surgery. *Clin Oral Implants Res.* 2009; 20: 351–355.

130. Von Arx T, Matter D, Buser D, Bornstein MM. Evaluation of location and dimensions of lingual foramina using limited cone-beam computed tomography. *J Oral Maxillofac Surg.* 2011; 69: 2777–2785.

131. Kilic E, Doganay S, Ulu M, Celebi N, Yikilmaz A, Alkan A. Determination of lingual vascular canals in the interforaminal region before implant surgery to prevent life threatening bleeding complications. *Clin Oral Implants Res.* 2014; 25: 90-93.

132. Patil S, Matsuda Y, Okano T. Accessory mandibular foramina: a CT study of 300 cases. *Surg Radiol Anat.* 2013; 35:323–330.

133. Yu S-K, Lee M-H, Jeon YH, Chung YY, Kim HJ. Anatomical configuration of the inferior alveolar neurovascular bundle: A histomorphometric analysis. *Surg Radiol Anat*. 2016; 38 (2): 195-201.

134. Hwang K, Lee WJ, Song YB, Chung IH. Vulnerability of the inferior alveolar nerve and mental nerve during genioplasty: An anatomic study. *J Craniofac Surg.* 2005; 16: 10–14.

135. Kim ST, Hu KS, Song WC, Kang MK, Park HD, Kim HJ. Location of the mandibular canal and the topography of its neurovascular structures. *J Craniofac Surg.* 2009; 20: 936–939.

136. De Oliveira Ju´nior MR, Saud AL, Fonseca DR, De-Ary-Pires B, Pires-Neto MA, de Ary-Pires R. Morphometrical analysis of the human mandibular canal: A CT investigation. *Surg Radiol Anat.* 2011; 33 (4): 345–352.

137. Bavitz JB, Harn SD, Hansen CA, Lang M. An anatomical study of mental neurovascular bundle-implant relationships. *Int J Oral Maxillofac Implants* 1993; 8:563–567.

138. Juodzbalys G, Wang H-L, Sabalys G. Injury of the inferior alveolar nerve during implant placement: A literature review. *J Oral Maxillofacial Res.* 2011; 2 (1): 1-19.

139. Scarfe W, Farman A. Soft tissue calcifications in the neck: Maxillofacial CBCT presentation and significance. *AADRT Newsletter.* 2010; 2 (2): 3-15.

140. Vujanovic-Eskenazi A, Valero-James JM, Sánchez-Garcés MA, Gay-Escoda C. A retrospective radiographic evaluation of the anterior loop of the mental nerve: Comparison between panoramic radiography and cone beam computerized tomography. *Med Oral Patol Oral CirBucal*. 2015; 20 (2): 239–245.

141.   Benavides E, Rios HF, Ganz SD, An CH, Resnik R, Reardon GT, et al. Use of cone beam computed tomography in implant dentistry: The International Congress of Oral Implantologists consensus report. *Implant Dent*. 2012; 21:78-86.

142.   İlgüy D, İlgüy M, Ersan N, Dölekoğlu S, Fişekçioğlu E. Measurements of the Foramen Magnum and Mandible in Relation to Sex Using CBCT. *Journal of Forensic Sciences.* 2014; 59: (3): 601–605.

143.   Mischkowski RA, Pulsfort R, Ritter L, Neugebauer J, Brochhagen HG, Keeve E, et al. Geometric accuracy of a newly developed cone-beam device for maxillofacial imaging. *Oral Surg Oral Med Oral Pathol Oral Radiol Endod.* 2007; 104 : (4): 551–559.

144.   Watanabe H, Honda E, Kurabayashi T. Modulation transfer function evaluation of cone beam computed tomography for dental use with the oversampling method. *Dentomaxillofac Radiol.* 2010; 39 : (1): 28–32.

145.   Kamburoglu K, Kilic C, Ozen T, Pehlivan S. Measurments of mandibular canal region obtained by cone beam computed tomography: A cadaveric study. *Oral Surg Oral Med Oral Pathol Oral Radiol Endod.* 2009; 107: 34-42.

146.   Statistics_help_for_students.com\How_do_I_report_independent_samples_T_test_data_i n_APA_style.htm [Accessed on 20.07.2017].

147.   Statistics_help_for_students.com\How_do_I_report_Pearsons_r_and_scatterplots_in _APA_style.htm [Accessed on 25.07.2017].

148.   Zografos J, Kolokoudias M, Papadakis E. The types of the mandibular canal. *Hell Period Stomat Gnathopathoprosopike Cheir*. 1990; 5: 17-20.

149.   Sweet APS. A statistical analysis of the incidence of nutrient channels and foramina in 500 periapical full-mouth radiodontic examinations. *Am J Orthod Oral Surg.* 1942; 28: 427-442.

150.   Sahman H. Sekerci AE, Sisman Y, Payveren M. Assessment of the visibility and characteristics of the mandibular incisive canal: Cone beam computed tomography versus panoramic radiography. *The International Journal of Oral and Maxillofacial Implants*. 2014; 29 (1): 71-78.

151.   Romanose GE, Greenstein G. The incisive canal: Considerations during implant placement: Case report and literature review. *The International Journal of Oral and maxillofacial Implants*. 2009; 24 (4): 740-745.

152. Cantekin K, Sekerci AE, Miloglu O, Buyuk SK. Identification of the mandibular landmarks in a pediatric population. *Medicina Oral, Patolologia Oral y Cirugia Bucal*. 2013; 19: 136-141.

153. Sonick M, Abraham J, Faiella RA. A comparison of the accuracy of periapical, panoramic, and computerized tomographic radiographs in locating the mandibular canal. *Int J Oral maxillofac Implants.* 1994; 9: 455-460.

154. Greenstein G, Tarnow D. The mental foramen and nerve: Clinical and anatomical factors related to dental implant placement: A literature review. *J Periodontal*. 2006; 77:1933-1943.

155. Sahman H, Sisman Y. Anterior loop of the the inferior alveolar canal: A cone beam computerized tomography study of 494 cases. *Journel of Oral Implantology*. 2016; XLII (4): 333-336.

156. Kusum CK, Mody PV, Indrajeet, Nooji D, Rao SK, Wankhade BG. Interforaminal haemorrhage during anterior mandibular implant placement: An overview. *Dental Research Journal.* 2015; 12 (4): 291-300.

157. Angelopoulos C, Thomas SL, Hechler S, Parissis N, Hlavacek M. Comparison between digital panoramic radiography and cone-beam computed tomography for the identification of the mandibular canal as part of presurgical dental implant assessment. *J Oral maxillofac Surg*. 2008; 66: 2130-2135.

158. Al-Ani O, Nambiar P, Ha KO, Ngeow WC. Safe zone for bone harvesting from the interforaminal region of the mandible. *Clin Oral Implants Res*. 2013; 24 (100): 115-121.

159. Leite GMF, Lana JP, Machado VDC, Manzi FR, Souza PEA, Horta MCR. Anatomic variations and lesions of the mandibular canal detected by cone beam computed tomography. *Surg Radiol Anat*. 2014; 36: 795-804.

160. Apostolakis D, Brown JE. The dimensions of the mandibular incisive canal and its spatial relationship to various anatomical landmarks of the mandible: A study using cone beam computed tomography. *Int J Oral Maxillofac Implants*. 2013; 28 (1): 117-124.

161. Yovchev D, Deliverska E, Indjova J, Zhelyazkova M. Mandibular incisive canal: A cone beam computed tomography study.*Biotechnology and Biotechnological Equipment*. 2013; 27 (3): 3848-3851.

162. Kajan ZD, Salari A. Presence and course of the mandibular incisive canal and presence of the anterior loop in cone beam computed tomography images of an Iranian population. *Oral Radiol.* 2012; 28: 55-61.

163. Parnia F, Moslehifard E, hafezeqoran A. Mahbub F, Mojaver- Kahnamoui. Characteristics of anatomical landmarks in the mandibular interforaminal region: A cone beam computed tomography study. *Medicina Oral, Patologia Oral Y Cirugia Bucal*. 2012; 17 (3): 420-425.

164. Raitz R, Shimura E, Chilvarquer I, Fenyo-Pereira M. Assessment of the mandibular incisive canal by panoramic radiograph and cone beam computed tomography. *International Journal of Dentistry*. 2014 (2014): 1-6.

165. Oradovic O, Todorovic L, Pesic V, Pejkovic B, Vitanovic V. Morphometric analysis of mandibular canal: Clinical aspects. *Bull Group Int Rech Sci Stomatol Odontol*. 1993; 36 (3-4): 109-113.

166. Uchida Y, Yamashita Y, Goto M, Hanihara T. Measurement of anterior loop length for the mandibular canal and diameter of the mandibular incisive canal to avoid nerve damage when installing endosseous implants in the interforaminal region. *J Oral Maxillofac Surg*. 2007; 65 (17): 72-79.

167. Juodzbalys G, Wang H-L, Sabalys G. Anatomy of mandibular vital structures. Part II: mandibular incisive canal, mental foramen and associated neurovascular bundles in relation with dental implantology. *J Oral Maxillofac Res.* 2010; 1 (1): e3.

168. Starkie C, Stewart D. The intra-mandibular course of the inferior dental nerve. *J Anat*. 1931; 65: 319-323.

169. Stewart D, Wilson SL. Regional anaesthesia and innervations of the teeth. *Lancet.*1928; 2, 809-811.

170. Correr GM, Iwanko D, Leonardi DP, Ulbrich LM, De Araújo MR, Deliberador TM. Classification of bifid mandibular canals using cone beam computed tomography. *Braz. Oral Res.* 2013; 27 (6): 510-516.

171. Moiseiwitsch JRD. Position of the mental foramen in a North American, white population. *Oral Surg Oral Med Oral Pathol Oral Radiol Endod*. 1998; 85 (4): 457-460.

172. Nikzad S, Azari A, Sabouri S. Double mandibular foramina and canal: Report a case with interactive CT-based planning software. *Iran J Radiol*. 2008; 5 (2): 83-86.

173.   Lew K, Townsen G. Failure to obtain adequate anaesthesia associated with bifid mandibular canal: A case report. *Aust Dent J.* 2006; 51: 86-90.

174.   Murlimanju BV, Prabhu LV, Prameela MD, Ashraf CM, Krishnamurthy A, Kumar CG. Accessory mandibular foramina: Prevalence, emberyological basis and surgical implications. *Journal of Clinical and Diagnostic Research*. 2011; 5 (5): 1137-1139.

175.   Bhateja S, Arora G, Bhasin M. Bifid mandibular canal: Case report and review of literature. *Journel of Health Research & Reviews*. 2014; 1 (1): 25-26.

176.   Castro MAA, Lagravere-Vich MO, Amaral TMP, Abreu MHG, Mesquita RA. Classifications of mandibular canal branching: A review of literature. *World J Radiol*. 2015; 28: 7 (12): 531–537.

177.   Meoli S, Fucci G, Vaia E. Un raro caso di doppio foro mentoniero. Imaging con tomografia computerizzata. *Radiol Med* 1993; 85: 854–857.

178.   Berberi A, Mani J, Nasseh I. Duplicated mandibular canal: Report of a case. *Quintessence Int.* 1994; 25: 277–281.

179.   Nortjé CJ, Farman AG, De V Joubert JJ. The radiographic appearance of the inferior dental canal: An additional variation. *Br J Oral Surg.* 1977; 15: 171–172.

180.   Durst JH, Snow JE. Multiple mandibular canals: Oddities or fairly common anomalies? *Oral Surg Oral Med Oral Pathol.* 1980; 49: 272–273.

181.   Strider JW. Anomaly of the mandibular canal. *Oral Surg Oral Med Oral Pathol.* 1988; 65: 376–377.

182.   Mader CL, Konzelman JL. Branching mandibular canal. *Oral Surg Oral Med Oral Pathol.* 1981; 51: 332.

183.   Adisen MZ, Misirlioglu M, Yilmaz S. Trifid mandibular nerve canal. *Journal of Oral and Maxillofacial Radiology*. 2013; 1 (2): 67-69.

184.   Lizio G, Pelliccioni, Ghigi G, Fanelli A, Marchetti C. Radiographic assessment of the mandibular retromolar canal using cone beam computed tompgraphy. *Acta Odontologica Scandinavica*. 2013; 24 (4): 365-369.

185.   Sisman Y, Ercan-Sekerci A, Payveren-Arikan M, shaman H. Diagnostic accuracy of cone-beam CT compared with panoramic images in predicting retromolar canal during extraction of impacted mandibular third molars. *Medicina Oral Patologia Oral Y Cirugia Bucal*. 2015; 20 (1): 74-81.

186. Han S-S, Hwang J-J, Park C-S. The anomalous canal between two accessory foramina on the mandibular ramus: The temporal crest canal. *Dentomaxillofacial Radiology*. 2014; 43, 20140115.

187. Auluck A, Ahsan A, Pai KM, Shetty C. Anatomical variations in developing mandibular nerve canal: A report of three cases. *Neuroanatomy.* 2005; 4: 28–30.

188. Miguel V-T, Miguel P-M, Gustavo A-O, Raul G-D, Andres C, Pablo G-M. Inferior alveolar nerve trajectory, mental foramen location and incidence of mental nerve anterior loop. *Med Oral Patol Oral Cir Bucal*. 2017; 1: 22 (5): 630-635.

189. Sawyer DR, Kiely ML, Pyle MA. The frequency of accessory mental foramina in four ethnic groups. *Arch Oral Biol*. 1998; 43: 417-420.

190. Senyurek MS. Multiplemental foramina. *Nature.* 1946; 157: 792-793.

191. Matsuda Y. Future observations on the mental foramen in the human mandibles. *Am Dent Surg*. 1929; 49: 445-452.

192. De Freitas V, Maderia MC, Toledo Filho JL, Chagas CF. Absence of the mental foramen in dry human mandibles. *Acta Anat (Basel).* 1979; 104: 353-355.

193. Anderson LC, Kosinski TF. Mentag PJ. A review of the intraosseeous course of the nerves of the mandible. *Journal of Oral Implantology*. 1991; XVII (4): 394-403.

194. Matsumoto K, Araki M, Honda K. Bilateral absence of the mentl foramen detected by cone-beam computed tomography. *Oral Radiol.* 2013; 29: 198-201.

195. Chen Z, Chen D, Tang L, Wang F. Relationship between the position of the mental foramen and the anterior loop of the inferior alveolar nerve as determined by cone beam computed tomography combined with mimics. *Journal of Computer Assisted Tomography*. 2015; 39 (1): 86–93.

196. Rothman SLG. Dental applications of computerized tomography. Chicago: *Quintessence*. 1998: 42-45.

197. Dao TT, Mellor A. Sensory disturbances associated with implant surgery. *Int J Prosthodont.* 1998; 11: 462-469.

198. Bartling R, Freeman K, Kraut RA. The incidence of altered sensation of the mental nerve after mandibular implant placement. *J Oral Maxillofac Surg*. 1999; 57: 1408-1412.

199. Wismeijer D, Van Wass MA, Vermeeren JI, kalk W. Patients' perception of sensory disturbances of the mental nerve before and after implant surgery. A prospective study of 110 patients. *Br J Oral Maxillofac Surg*. 1997; 35: 254-259.

200. Wolten JN. Altered sensation associated with implants in the anterior mandible: A prospective study. *J Prosthet Dent*. 2000; 83: 443-449.

201. Abarca M, Van Steenberghe D, Malevez C, De Ridder J, Jacobs R. Neurosensory disturbances after immediate loading of implants in the anterior mandible: An initial questionnaire approach followed by a psychophysical assessment. *Clinical Oral Investigations*. 2006; 10: 4: 269-277.

202. Solar P, Ulm C, Frey G, Matejka M. A classification of the intra osseous paths of the mental nerve. *Int J Oral Maxillofac Implants*.1994; 9: 339-344.

203. Apostolakis D, Brown JE. The anterior loop of the inferior alveolar nerve prevalence, measurement of its length and a recommendation for interforaminal implant instillation based on cone beam CT imaging. *Clin Oral Implants Res*. 2012; 23: 1022-1030.

204. Neiva RF, gapski R, wang HL. Morphometric analysis of implant related anatomy in Caucasian skulls. *J Periodontol*. 2004; 75 (8): 1061-1067.

205. Kuzmanovic DV, Payne AG, Kieser JA, Dias GJ. Anterior loop of the mental nerve: A morphological and radiographic study. *Clin Oral Implants Res*. 2003; 14: 464–471.

206. Arzouman MJ, Otis L, Kipnis V, Levine D. Observations of the anterior loop of the inferior alveolar canal. *Int J Oral Maxillofac Implants*. 1993; 8: 295–300.

207. Meijer HJ, Steen WH, Bosman F. A comparison of methods to asses marginal bone height around endosseous implants. *J Clin Periodontol.* 1993; 20: 250–253.

208. Benninger B, Miller D, Maharathi A, et al. Dental implant placement investigation: is the anterior loop of the mental canal clinically relevant? *J Oral Maxillofac Surg*. 2011; 69: 182-185.

209. Przystanska A, Bruska M. Anatomical classification of accessory foramina in human mandibles of adults, infants, and fetuses. *Anat Sci Int*. 2012; 87: 141–149.

210. Balaguer-Martí J-C, Peñarrocha-Oltra D, Balaguer-Martínez J, Miguel Peñarrocha-Diago M. Immediate bleeding complications in dental implants: A systematic review.*Med Oral Patol Oral Cir Bucal*. 2015; 1:20 (2): 231-238.

211. Chan H-L, Brooks SL, Fu J-H, Yeh C-Y, Rudek I, Wang H-L. Cross-sectional analysis of the mandibular lingual concavity using cone beam computed tomography. *Clinical Oral Implants Research.* 2010; 22: 2: 201–206.

212. Ogawa A, Fukuta Y, Nakasato H, Nakasato S. Cone beam computed tomographic evaluation of nutrient canals and foramina in the anterior region of the mandible. *Surg Radiol Anat.* 2016 DOI 10. 1007\s00276-016-1664-3.

213. Yildirim YD, Güncü GM, Galindo-Moreno P, Velasco- Torres M, Juodzbalys G, Kubilius M, Gervickad A, Al-Hezaimi K, Al-Sadhan R, Yilmaz HG, Asar NV, Karabulut F, Wang HL, Tözüm TF. Evaluation of mandibular lingular foramina related to dental implant treatment with computerized tomography: A multicenter clinical study. *Implant Dent.* 2014; 23: 57-63.

214. Wang PD, Serman NJ, Kaufman E. Continuous radiographic visualization of the mandibular nutrient canals. Stereographic assessments of mandibular canal in relation to the roots of impacted lower third molar using multiprojection narrow beam radiography. *Dent Maxillfac Radiol.* 2001; 30: 131-132.

215. Goaz PW, White SC. Oral Radiology; Principles and Interpretation, 2nd ed. Toronto: C. V. Mosby; 1987.

216. Sheikhi M, Mosavat F, Ahmadi A. Assessing the anatomical variations of lingual foramen and its bony canals with CBCT taken from 102 patients in Isfahan. *Dent Res J (Isfahan).* 2012; 9 (1): 45–51.

217. Gahleitner A, Hofschneider U, Tepper G, Pretterklieber M, Schick S, Zauza K, Watzek G, Lingual vascular canals of the mandible: Evaluation with dental CT. *Radiology.* 2001, 220 (1): 186–189.

218. Babiuc I, Tărlungeanu I, Păuna M. Cone beam computed tomography observations of the lingual foramina and their bony canals in the median region of the mandible. *Rom J Morphol Embryol.* 2011, 52 (3): 827–829.

219. Aoun G, Nasseh I, Sokhn S, Rifai M. Lingual foramina and canals of the mandible: Anatomic variations in a Lebanese population. *J Clin Imaging Sci.* 2017; 7: 16.

220. Kawai T, Asaumi R, Sato I, Yoshida S, Yosue T. Classification of the lingual foramina and their bony canals in the median region of the mandible: Cone beam computed tomography observations of dry Japanese mandibles. *Oral Radiol.* 2007; 23: 42–48.

221. McDonnell D, Nouri MR, Todd ME. The mandibular lingual foramen: A consistent arterial foramen in the middle of the mandible. *J. Anat*. 1994; 184: 363-369.

222. Ennis LM. Roentgenographic variations of the maxillary sinus and the nutrient canals of the maxilla and mandible. *International Journal of Orthodontics and Oral Surgery*. 1937; 23, 173-193.

223. Choi DY, Woo YJ, Won SY, Kim DH, Kim HJ, Hu KS. Topography of the lingual foramen using micro-computed tomography for improving safety during implant placement of anterior mandibular region. *J Craniofac Surg*. 2013; 24: 1403–1407.

224. Shiller WR, Wiswell OB. Lingual foramina of the mandible. *Anatomical Record*. 1954; 119, 387-390.

8. APPENDICES

8.2. Appendix1: General Consent Form

Hastalarınızla aranızda doğacak sorunların önüne geçilmesi açısından da büyük önem taşıyan form Yeditepe Üniversitesi Dişhekimliği Fakültesi tarafından hazırlanmıştır. Katkılarıdan dolayı Yeditepe Üniversitesi Diş Hekimliği Fakültesine teşekkür ederiz. İstanbul Diş Hekimleri Odası Yönetim Kurulu.

GENEL BİLGİLENDİRME VE GENEL ONAM FORMU

Sayın Hastamız,

Aşağıda size verilen bilgileri okuyunuz. Bu bilgileri okuyup imzalayarak size ya da çocuğunuza uygulanacak tedaviler hakkında bilgi sahibi olacaksınız. Tedaviplanlamasının fayda ve risklerini öğrenmek sizin tedavi sonunda memnun olmanızı sağlayacaktır. Sağlıklı ve mutlu bir yaşam dileğiyle.

Tedaviler esnasında ağrı kontrolünü sağlamak amacıyla sınırlı uyuşturmauygulanmaktadır. Gerekli hallerde öncelikle topikal anestezik madde(sprey) ile dişeti veya yanağın iç kısmı uyuşturulur. Bölge uyuştuğunda anestezik sıvı enjektör ile enjekte edilerek, diş ve bulunduğu bölge bir süreliğine hissizleştirilir. Lokal anestezi uygulaması sonrası nadir de olsa hastalarda alerjik reaksiyonlar, his kaybı, kanama, geçici kas spazmları, geçici yüz felci görülebilir. Lokal anestezi uygulaması, bölgede anatomic farklılıklar veya akut enfeksiyonlar olmadığı sürece başarılı bir uygulamadır. Lokal anestezi uygulanan bölge yaklaşık 2–4 saat boyunca hissizdir. Bu nedenle, ısırmaya bağlı yanak içi ve dudakta yara oluşmaması için hissizlik geçene kadar yeme içme önerilmez. 2–4 saat sonrasında anestezinin etkisi ortadan kalkar.

Tedavileriniz esnasında ileri tetkik için biyopsi alınması gerekebilir.

Sağlık kuruluşumuzun, düzeninin ve tedavi programının aksamaması için randevularınıza sadık olmaya ve zamanında gelmeye özen gösteriniz. Gelmeniz mümkün olmadığında, randevunuzu 24 saat öncesinden iptal ettiriniz.

Hasta veya Hastanın Yasal Temsilcisi* - Yakınlık Derecesi

Adı-Soyadı: ………………………………………………………………………

T.C. Kimlik No'su: ………………………………………………………………….

Adresi: …………………………………………………………………………….

Telefon:………………………………………………………………………………

İmza

GENEL ONAM FORMU

Aşağıda imzası olan ben/hastanın vasisi/hastanın velisi, dişhekimi tarafından hastalığın teşhisi, tedavi planı ve alternatif tedaviler hakkında bilgilendirildim. Bana önerilen tedavileri kabul ettim.

Şüpheli tedavilerde planlamanın değişebileceği anlatıldı, anladım ve kabul ettim. Tedavilerimle ya da çocuğumun/………………….. tedavisi hakkında merak ettiğim tüm sorulara cevap verildi.

Yapılacak tedavilerin başarısının bana da bağlı olduğu, evde üzerime düşen ağız temizliği ve diyet önerilerine uymam gerektiği anlatıldı, kabul ettim.

Benim/çocuğumun/……………….. vazgeçmemiz gereken zararlı alışkanlıklarla ilgili önerileri yerine getirmem ve bana/çocuğuma/…………….. yazılacak reçetelerdeki ilaçları tarife uygun doz ve sürelerde kullanmam gerekliliği anlatıldı ve kabul ettim.

Bana/çocuğuma/……………………… uygulanacak tedavilerin uzun süreli garantiedilemeyeceği anlatıldı, anladım ve kabul ettim.

Tedaviyi kabul ettikten sonra bana/çocuğuma/……………………….. ait bilgi, radyografi, fotoğraf, video ve diğer dokümanların eğitim ve/veya bilimsel amaçlı çalışmalarda kullanılmasını kabul edip izin verdim.

Tedavim sırasında kişisel eşyalarımın(para, mücevher, takı, giyecek, cep telefonu vb.) sorumluluğu ve güvenliğinin bana ait olduğu bildirildi, anladım ve kabul ettim.

Yukarıda belirtildiği gibi tedavi planlaması sırasında bana/çocuğuma/………………anlatılan ve benim tarafımdan kabul edilen diş tedavilerini onayladım ve kabul ettim.

Hasta haklarıyla ilgili olarak bilgilendirildi.

Hasta veya Hastanın Yasal Temsilcisi* - Yakınlık Derecesi

Adı-Soyadı : ....

T.C. Kimlik No'su : ....

Adresi : ....

Telefon : ....

İmza : ....

Hekimin

Adı-Soyadı : ....

Tarih : ....

İmza : ....

* Yasal Temsilci: Vesayet altındakiler için vasi, reşit olmayanlar için anne- baba, bunların bulunmadığı durumlarda 1. derece kanuni mirasçılardır.(Hasta yakınının isminin yanında yakınlık derecesini belirtiniz.

8.2. Appendix 2:

1. Mandibular Foramen Number (MaFN) for both Rand L sides: (MaFN R) and (MaFN L)

   No foramen=0

   One foramen=1

   Two foramina=2

2. Mandibular Canal Number (MaCN); For R and L: (MaCNR) and (MaCNL)

   No canal=0

   Single canal=1

   Bifid canals=2

   Trifid canals=3

   Retromolar canal=4

3. Mental Foramen Number (MeFN); For R and L :(MeFN R) and (MeFNL)

   None=0

   One foramen=1

   Two foramina=2

4. Mental Canal Length in mm (MeC Le); For R and L: (MeCLe R) and (MeCLe L)

5. Mental Canal location (MeCl); For R and L: (MeCl R) and (MeCl L)

   Symmetrical=1

   Mesial=2

   Distal=3

6. Mental Canal Orientation (MeCO); For R and L:(MeCOR) and (MeCOL)

   Superior direction=1

   Horizontal direction =2

   Inferior direction =3

7. Mental Canal Angulations' (MeCA); for R and L:MeCAR) and (MeCAL)

   The angle between a horizontal line and the upper border of the mental canal opening was measured in degrees.

8. Mandibular Incisive Canal visibility (MIC); For Rand L: (MIC R) and (MIC L)

   Good visibility (canal is visible and continues) =1

   Moderate visibility (canal is visible but not continues) =2

   Not visible=0

9. Lateral Lingual Vascular Canals' Number (LLVCN)For R and L: (LLVCNR) and (LLVCNL)

   None=0

   One canal=1

   Two canals=2

10. Lateral Lingual Vascular Canals' Length in mm (LLVC Le)For R and L: (LLVC Le R) and (LLVC Le L) if present.

    None=0

11. Lateral Lingual Vascular Canals' Orientation (LLVC O)For R and L: (LLVC O R) and (LLVC O L) if present:

    Superior direction=1

    Horizontal direction =2

    Inferior direction =3

    None=0

12. Lateral Lingual Vascular Canals' range between teeth (LLVCr) For R and L :(LLVCr R) and (LLVCr L) if present:

    Between 41 and 31 =11

    Between 31and 32 or 41 and 42 =1

    Between 32and 33 or 42 and 43 =2

    Between 33 and 34 or 43 and 44=3

Between 34 and 35 or 44 and 45 =4

Between 35and 36 or 45 and 46 =5

None=0

13. Lateral Lingual Vascular Canals' Height (LLVCH)); For R and L: (LLVCHR) and (LLVCHL):
    The canal's height in mm was measured from the highest point of the canal's upper border to the
    lower border of the mandible in proportion to the total height of the mandibular bone, where the
    canal was detected, divided by 3:
    Height in the upper one- third = 1
    Height in the middle one- third = 2
    Height in the lower one-third = 3
    None=0

14. Lateral Lingual Vascular Canals Aspect (LLVCA)For R and L :(LLVCA R) and (LLVCA L):
    Lingual=1
    Labial=2
    Both lingual and labial=3
    None=0

15. Nutrient Canals Number (NCsN)

16. Nutrient Canals Range (NCsR)

17. Lingual Canal Number at the midline (LCN):
    None=0
    One canal=1
    Two canals=2
    Three canals=3

18. Lingual Canal Aspect (LCA):
    Lingual=1

Labial=2

Both=3

None=0

19. Lingual Canal location (LCl)

Midline=1

Right=2

Left=3

None=0

20. Lingual Canal in relation to Genial Tubercles (GT) (LCGT):

Above GT=1

Below GT=2

Through GT=3

Above and below GT=4

Above, below and through GT=5

Above and through GT=6

Below and through GT=7

None=0

21. Lingual Canal type resembling figure number (LCfig):

There are almost 20 types or forms or figures of LC.These were detected by the first observer, while selecting the images for this study. Moreover,these figures were regrouped into 8 classes (see Lingual Canal Classification LC Class, section 23), according to their relation with GT (see Lingual Canal in relation to Genial Tubercles LCGT, section 18).

22. Lingual Foramen Number (LFN):

None=0

One foramen=1

Two foramina=2

Three foramina=3

Four foramina=4

23. Lingual Foramen Aspect (LFA):

Lingual=1

Labial=2

Both=3

None=0

24. Lingual Foramen location (LFl)

Midline=1

Right=2

Left=3

None=0

25. Lingual Canal Classification (LC Class)

LC figure number	LC Class
Fig.7	1
Fig.3, Fig.6, Fig.16	2
Fig.8, Fig.14, Fig. 19, Fig. 20.	3
Fig.2, Fig.11	4
Fig.4, Fig.9, Fig.10, Fig.12, Fig.17, Fig.18	5
Fig.1	6
Fig.5, Fig.15	7
Fig.13	8

Sayı : 37068608-6100-15-1317   **13/04/2017**
Konu: Klinik Araştırmalar
       Etik kurul Başvurusu hk.

İlgili Makama (Erdoğan Fişekçioğlu)

Yeditepe Üniversitesi Diş Hekimliği Fakültesi Ağız – Diş ve Çene Radyolojisi Anabilim Dalında görevli Dt. Mervet Elzuki'nin sorumlu olduğu **"İnferior Alveolar Kanalın Konik Işınlı Bilgisayarlı Tomografi ile Metodolojik Analizi: Retrospektif Çalışma"** isimli araştırma projesine ait Klinik Araştırmalar Etik Kurulu (KAEK) Başvuru Dosyası (**1305** kayıt Numaralı KAEK Başvuru Dosyası), Yeditepe Üniversitesi Klinik Araştırmalar Etik Kurulu tarafından **12.04.2017** tarihli toplantıda incelenmiştir.

Kurul tarafından yapılan inceleme sonucu, yukarıdaki isimi belirtilen çalışmanın yapılmasının etik ve bilimsel açıdan uygun olduğuna karar verilmiştir (**KAEK Karar No: 701**).

Ancak, "İlaç ve Biyolojik Ürünlerin Klinik Araştırmaları" hakkında yönetmelik gereği dosyanızda yer alan araştırma için" Türkiye İlaç ve Tıbbi Cihaz Kurumu'nca da onaylanması / uygun görülmesi gerekmektedir. Bu nedenle, Araştırma Dosyanız TİTCK başkanlığına sunulmuştur. İlgili kurumdan araştırma dosyanızı takip edebilirsiniz.

Prof. Dr. Turgay ÇELİK
Yeditepe Üniversitesi
Klinik Araştırmalar Etik Kurulu Başkanı

Yeditepe Üniversitesi 26 Ağustos Yerleşimi, İnönü Mahallesi Kayışdağı Caddesi 34755 Ataşehir / İstanbul
T. 0216 578 00 00   www.yeditepe.edu.tr   F. 0216 578 02 99

142

T.C
SAĞLIK BAKANLIĞI
Türkiye İlaç ve Tıbbi Cihaz Kurumu

NORMAL

Sayı : 71146310-511.06-
Konu : 2017-082

Sayın Doç Dr. Erdoğan FİŞEKÇİOĞLU
Yeditepe Üniversitesi Diş Hekimliği Fakültesi
Ağız Diş ve Çene Anabilim Dalı
Caddebostan mah. Bağdat caddesi Kadıköy İstanbul

İlgi: 29.05.2017 tarihli ve E.148084 sayılı başvurunuz.

Sorumlu araştırmacısı olduğunuz "İnferior Alveolar Kanalın Konik Işınlı Bilgisayarlı Tomografi ile Metodolojik Analizi: Retrospektif Çalışma " isimli klinik araştırma başvurunuz değerlendirilmiştir.

Bilindiği üzere 3359 sayılı Sağlık Hizmetleri Temel Kanunu Ek Madde 10'da, "Herhangi bir tedavi yöntemi veya araçlarının veyahut ruhsat veya izin alınmış olsa dahi ilaç ve terkiplerinin, tıbbi ve biyolojik ürünler, bitkisel ürünler, kozmetik ürünler ve hammaddeleri ile tıbbi cihazların bilimsel araştırma amacıyla insanlar üzerinde kullanılabilmesi için Sağlık Bakanlığı veya bağlı kuruluşlarından izin alınmasının yanında;" ifadesi yer almaktadır. Bu doğrultuda ilgili çalışmanın Sağlık Hizmetleri Temel Kanunu Ek Madde 10 hükümlerine göre Kurumumuzdan izin alınması gereken çalışmalar kapsamına girmemesi nedeni ile çalışmanın sadece ilgili etik kurul kararı doğrultusunda yürütülmesi tarafımızca uygun bulunmuştur.

Bu bağlamda gönüllülerden bilgilendirilmiş gönüllü olur formu alınması, çalışma konusu ile ilgili ödemelerin, çalışma boyunca yapılacak olan eş zamanlı tedavi ve kurtarma tedavilerinin gönüllüye ödettirilmemesi ve yazımızın bir örneğinin ilgili etik kurula iletilmesi hususunda;

Bilgilerinizi ve gereğini rica ederim.

Dr. Asım HOCAOĞLU
Kurum Başkanı a.
Daire Başkanı

Söğütözü Mahallesi, 2176.Sokak No:5 06520 Çankaya/ANKARA
Tel: (0 312) 218 30 00– Fax : (0 312) 218 34 60 www.titck.gov.tr

Bilgi İçin: Eda TÜRKÖZ
Unvan: Mühendis

143

CURRICULUM VITAE

PERSONAL INFORMATION

First Name	Mervet	Last name	El-Zuki
Place of Birth	U.S.A	Date of Birth	18.06.1970
Nationality	Libya	T.C ID No.	99103495684
Email	mervetaz02@yahoo.com mervet.a.elzuki@gmail.com	Tel.	++905444808222

EDUCATION QUALIFICATIONS

Degree	Place	Name of Graduated Institution	Graduation Year
Doctorate	Istanbul- Turkey	University of Yeditepe	2018
M.Phil	Manchester- UK	University of Manchester	2005
Bachelor of Dental Surgery (B.D.S)	Benghazi- Libya	University of Benghazi	1993
High school	Benghazi- Libya	Al -Alweia Al- Khadra School	1988

ENGLISH LANGUAGE

Exam	Score
IELTS	(7.5) December 2005 (6.5) Jan 2013
TOEFL	(607) October 2012 (580) May 2013

PROFESSIONAL EXPERIENCE

[Over 20 years of professional experience]

Task	Institution	Duration
Internship	Faculty of Dentistry, University of Benghazi	**1993-1994**
Full-timeGeneral Dental Practitioner (GDP)	Benghazi Dental Centre	**1995**
Part-time GDP	The Libyan Red-Crescent	**1996-1998**
GDP	The Ministry of Health; Rass- Obada Polyclinic Centre	**1996-1998**
Part-time GDP	Benghazi Dental Centre	**1999-2003**
Demonstrator	Faculty of Dentistry, University of Benghazi	**1999-2003**
Course instructor and tutor for Dental Nurses	Faculty of Dentistry, University of Benghazi	**2001**
Staff member and Oral Radiology Unit Director	Faculty of Dentistry, University of Benghazi	**2006-2013**
Member of the Quality Assurance Department	Faculty of Dentistry, University of Benghazi	**2010**
Head of the Quality Assurance Department and Dental Institutions Auditor.	Faculty of Dentistry, University of Benghazi	**2011-2013**
Part-time staff member;	Faculty of Dentistry, The Libyan International Medical University (LIMU)	**2009-2013**
Full-time PhD student,	Faculty of Dentistry, University of Yeditepe	**2014-2017**

COMPUTINGSKILLS

Program	Usage
Microsoft Office: Word, Power Point, and Excel.	Very good
Adobe Photo Element	Good
EMAGO and Win TAS	Good
InVivoDental5 Version 5.2 Anatomage software for iCATunits.	Very good
IBM SPSS Advanced Statistics 20	Good

ACADEMIC PUPLICATIONS

1. **El-Zuki M**. Survey of radiation protection measures to the patients in Benghazi dental clinics. *Cairo Dental Journal* 2011; 27-3.

2. Mahfoud S, **El-Zuki M**. Screening of 200 digital panoramic images randomly selected from Oral Diagnosis and Radiology Department for periodontal diseases; in a Libyan population sample. *Cairo Dental Journal* 2013; 29-2.

3. **El-Zuki M**, Omami G, Horner K. Assessment of trabecular bone changes around endosseous implants using image analysis techniques: A preliminary study. *Imaging Science in Dentistry* 2014 (June); 44-2.

4. Fişekçioğlu E, **El-Zuki M**. Manyetik rezonans görüntülemede paranazal sinüs patolojileri: Paranasal sinuse pathology in Magnetic Resonance Imaging. *Türkiye Klinikleri: Ağız Diş ve ÇeneRadyolojisi* 2015, 1-1.

CONFERENCES AND SCIENTIFIC MEETINGS

2005: **The Spring Scientific Meeting of the British Society of Dental and Maxillofacial Radiology** on the 29th April 2005, University of Manchester, UK; (**Attendee**).

2007: **The 3rd Libyan Dental Congress and 4th Exhibition** (10-12th April) Benghazi, Libya; (**Presenter**: Assessment of trabecular bone changes with time around endosseous implants using image analysis techniques).

2009: **The 2nd Conference of the Post-graduates** (March the 31st to April the 2nd 2009) Al Arab Medical University. Benghazi, Libya; (**Attendee**).

2010: **The 1st Scientific Day** (17th of April), Faculty of Dentistry, University of Garyounis; Benghazi, Libya (**Poster**: In the shades of grey: Digital imaging).

2012: **The 2nd Scientific Day** (15-16th of May), Faculty of Dentistry, University of Benghazi;

(**Presenter**: Screening of 200 digital panoramic images randomly selected from Oral Diagnosis and Radiology Department for periodontal diseases).

AWARDS AND RECOGNITIONS

2003: Scholarship for Master Degree: Ministry of Higher Education and Scientific Research, Libyan Government.
2009: Scholarship for PhD Degree: Ministry of Higher Education and Scientific Research, Libyan Government.
2015: High performance in oral Diagnosis and Dentomaxillofacial Department Faculty of Dentistry, Yditepe University. Istanbul, Turkey.

OTHER CERTIFICATS AND SKILLS

2013: Quality Management System Diploma. Horizons learning; London, UK, and Dar Noon for Training and Consultation, Benghazi, Libya. Trainer: Dr. Ali Al-Zubaidi.
2015: Basic Life Supporting Course: Faculty of Dentistry, University of Yeditepe, Turkey.
2015: Cross Infection Control Course: Faculty of Dentistry, University of Yeditepe, Turkey.
2005: Basic Life Supporting Course: School of Dentistry, University of Manchester, UK.
2006- 2017: Skilful lecturer and presenter.
2009-2017: Problem Based Learning and Evidence Based Dentistry teaching skills.